safecoast

keeping our feet dry in the north sea lowlands

# COMPARISON BETWEEN DIFFERENT FLOOD RISK METHODOLOGIES

## ACTION 3B REPORT

April 2008

## Disclaimer

The ideas described in this report are the personal interpretation of the researchers themselves and not of their National Agencies (in case Flanders Hydraulics Research) nor of the Interreg IIIb North Sea Secretariat. The information in the report is checked by a follow up committee installed for this project and related projects about risk and coastal safety going on in Flanders. Mistakes are however the responsibility of only the authors.

# Foreword

Nowadays, more and more damage and risk calculations are executed in addition to hydraulic simulations. However, calculating damage and risk is not an aim in itself. Interpretation of the results by experts and/or stakeholders is necessary to derive useful information. In this way, damage and risk calculations can be a part of e.g. a multi criteria analysis. Risk maps can help in a decision support process but they are not a decision criterion on their own as in most cases only the tangible effects are (partly) taken into account. Risk calculations allow to compare scenarios. Most importantly risk calculations take a broad view dealing with not only hazards but also vulnerabilities. Besides tangible risk, the water manager and decision maker needs information about the number of affected people, the natural and historical values in the area… Although risk is not a total and complete indicator, the authors see it as a useful means to evaluate management scenarios for protection against flooding.

The structure of this report wants to guide the reader through a description and comparison of different European methodologies with reference to the Flemish methodology. After the introduction you will find a short overview of the Flemish methodology in chapter 2. In chapter 3 the SAFECoast time horizon, the year 2050, is incorporated in the risk methodology. Chapter 4 describes the similarities and differences between different vulnerability methods. Chapter 5 reports on sensitivity calculations for the risks in the case study area of the Belgian eastern coastal zone. In chapter 6 a general uncertainty analysis is elaborated, which leads to the conclusions.

# Contents

# 1. Introduction

The Interreg IIIB project SAFECoast considers the question "How to manage our North Sea coasts in 2050?' and focuses on the consequences of climate change and spatial developments with respect to safety from coastal flooding. Therefore, a team of coastal managers from the Netherlands, Germany, Belgium, Denmark and the UK are continuing their cooperation in SAFECoast which aims to build on each other's experiences in, and understanding of coastal risk management.

Flanders Hydraulics Research (FHR, located in Borgerhout, Belgium) has proposed a flood risk methodology in the past which makes it possible to compare different areas and different situations with a view to damage and risk calculations. In the past years, the methodology has been extended and improved, and meanwhile it is used in several studies in Flanders.

This report is the contribution of Flanders Hydraulics Research to the SAFECoast project (action 3b). The goal is to compare basic parameters of the existing coastal risk methodologies and make an inventory of the strong and weak points of the different approaches. It is neither possible nor desirable to make a ranking of them. Because of data availability and case specific parameters and constraints, each methodology generally fits the best for the area they are made for. However we want to learn from them and incorporate good ideas to improve the existing methodologies.

To improve coastal risk methodology means to make its results less uncertain, or more complete. In this study all the different sources of uncertainty are analysed and compared so it becomes possible to identify the weak links in the calculation chain.

# 2. A risk based methodology: a short overview of the Flemish methodology

In the past, the Flemish approach to flood management had a strong focus on heightening and strengthening the water defences. In recent years it has become clear that these measures can be supplemented by other types of management options. The Flemish government came with a new approach in the nineties of the past century. This new approach is based on following ideas:

- offering protection against flood damage,
- avoiding casualty risks,
- reducing safety risks.

The new approach has the ambition of restricting the floods to places where the effects caused by the water are limited, or even positive. This is the case, for example, in some nature conservation zones. The opposite is true for densely populated areas or zones with important industrial installations. In those areas extra efforts have to be taken to avoid flooding.

## 2.1 Purpose of a risk based methodology

The new approach of the Flemish Government focuses on minimizing the consequences of flooding instead of avoiding floods. Therefore, knowledge has to be acquired about the value of land use in Flanders.

A risk based methodology has been set up to estimate the risk on flood damage, based on land use properties and socio-economical information. The technique has multiple objectives:

- calculation of risk for the whole of Flanders based on uniform input data,
- studying changes in risk as a consequence of changes in land use and new infrastructures for water management (e.g. heightening of dikes, land use or demographic changes, climate change),

A risk based approach means not only to take into account the hazard of extreme weather events, but also the consequences of these events. In this way, risk is defined as the product of probability of occurrence and consequence. So, for each return period (which stands for the chance of an extreme event) a damage calculation is executed, after which these can be summed up to obtain the risk.

In the next sections, several phases are considered which are necessary for the calculation of damage and risk. First, these two important concepts are discussed in detail.

## 2.2 Definitions for damage and risk

Damage can be defined in multiple ways. From a financial point of view, one can split up damage in monetary damage and non-monetary damage, sometimes referred to as emotional damage. In the present risk based methodology, only the monetary damage is taken into account. A second classification can be made between internal and

external damage. Internal damage is defined as the damage caused in the inundated zone itself, external damage occurs at places outside the inundated area. An example of the latter is production loss due to economic dependence on customers and/or suppliers which are located in the flooded area. External damage is not taken into account in the present methodology. A third difference is made between direct and indirect damage. While the first refers to the damage affecting buildings, furniture, stocks, crops... the second refers to other economic consequences (in the inundated zone) such as production losses and clean up costs. Direct damage and to some extent indirect damage are taken into account in the damage and risk calculations.

Summarizing, the present risk based methodology defines monetary, internal damage, direct and to some extent indirect.

Risk expresses the average potential damage (in euros) over one year for a specific area. The value is set up by different inundations, each with a different chance on appearance (return period) in accordance to different water depths varying along the study area.

## 2.3 Calculation of damage and risk

Step 1: defining probability and extend of flooding

*Risk = probability x vulnerability* implies knowledge about the probability that a particular area will be flooded. What will be the extent of flooding? And what will be the water depth in these areas?

*Calculating return periods.* Through statistical analysis of levels and flow rates in the past, coastal researchers calculate the average period of time in which a particular maximum water level may reoccur. The higher the water level, the longer it will take on average before it occurs.

*Producing flood maps.* Once the highest water levels for a particular recurrence period are known, computer models are used to produce different types of flood maps of the coastal zone for different return periods.

- a flood map showing the maximum water level. This map shows precisely which area was affected by a certain flood.

- a flood map showing the maximum current velocities. This map indicates where current velocity is high, and possibly causes extra damage due to e.g. collapse.

- a flood map showing the maximum speed at which the water will rise. When the water rises quickly there may be more casualties.

The calculation of a damage map implies the need for flood maps of which each one represents a certain return period. These flood maps can be obtained by using characteristic storm surges as boundary conditions in the hydraulic model. Basically, each random chosen return period has a corresponding flood map. In real terms, this is impossible. One can only calculate a limited number of return periods and thus provide a limited number of flood maps. However, this is not a problem through the fact that two nearby return periods have rather small differences in water depth (e.g. 98 years and 100 years). Logically, the corresponding damage will be small in that case.

Step 2: determining the damage

What is the possible number of casualties in a particular area? What is the material damage? How can this be answered using standard methodology?

*Determining land use*. The first step is to determine the land use in the flooded area. There is a large variety of land us maps available, based on topographic maps, satellite imagery, orthophotograph interpretation, Europe-wide initiatives as CORINE Land Cover, etc. Different types of land use are distinguished: built-up areas, agricultural land, industrial sites, woodland etc.

*Calculating the economic damage*. For the calculation of damage, the replacement value of goods is used, not the original value of purchase. The replacement value of the different goods is variable in space and time. This explains the use of average values for the smallest surface area for which data is available in a homogeneous way.

Different land use categories are defined, for example agriculture, residential areas, infrastructure, industry... For each category, a maximum damage is computed by unit of length or surface. Between maximum damage and water depth, a relation exists, which isn't linear and which differs in land use category. This relation is made visually by a damage function (Figure 1).

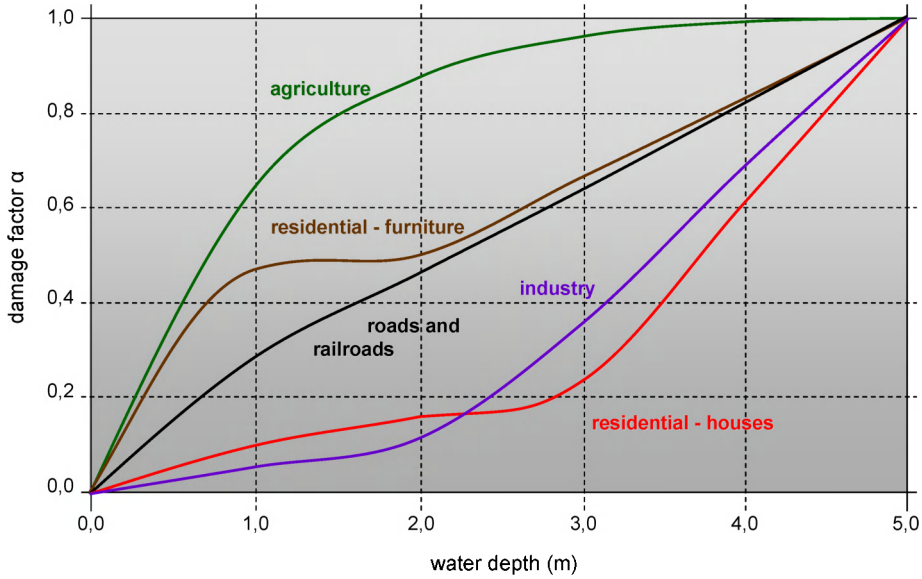


Figure 1 Expected damage (α) as a function of water depth

The real damage inside an inundated area is calculated by multiplying the maximum damage of each land use category with the corresponding α-factors and by subsequently summarizing these with all different land use categories of a certain area. It is taken into account that salt water flooding results in higher damage compared to fresh water flooding (for the same water depth).

Step 3: Defining the risk

Finally, the damage maps are combined into one risk map, based on the *probability x vulnerability* formula, which indicates the expected average annual damage for a given area. The chain of computations is presented schematically in Figure 2.

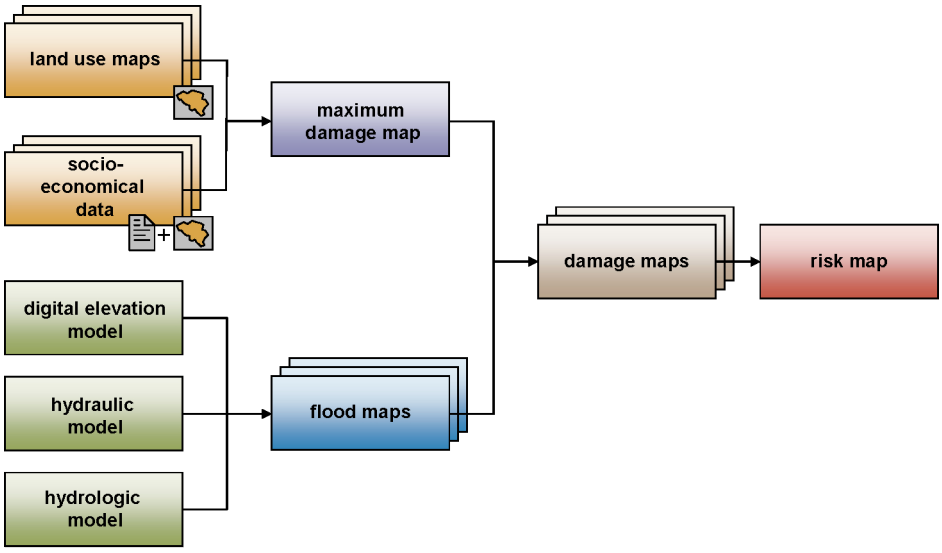


Figure 2 Derivation scheme of risk mapping

# 3. Incorporating the 2050 time horizon in the risk methodology

## 3.1 Description of the subject

Different values are to be adopted for the different system characteristics evolving over time (time horizon of several decades e.g. 2010-2050) with regard to the rate at which they evolve (assumed constant both in time and place, i.e., equal for the whole time scale that is looked at and the whole coastal zone).

The following three evolving system parameters are extremely important:

1. evolution of the economic value (~the maximum damage in the coastal zone)
2. evolution of the sea level (relative rise in average high water in relation to the sea wall)
3. the discount rate

It can be accepted that these are viewed as external factors for the coastal risk manager. They are external factors which evolve slowly but surely over the years, and which will have a big impact over the complete time scale that is being considered (e.g. 2010-2050).

The question is how these three changing system parameters can be taken into account in carrying out the risk assessments with a time scale up to the time horizon considered (e.g. 2010-2050).

This is a methodological question which arises for every risk assessment that takes a time horizon of several decades or more.

Optimum coastal risk management would ensure that the protection measures “grow” at the same rate as the increasing economic value in the costal zone and with the rising sea level.

The discount rate at which future costs have to be actualised is taken into consideration in order to assess whether it would not be financially more efficient to postpone investments. This aspect is included in view of the analogy with taking into account the growth of the economic value and the rise in sea level. This gives a picture of the relative impact on the risk of the increase in the economic values and rise in sea level, on the one hand, and of the discount rate, on the other hand.

## 3.2 The rate factor

The traditional risk formula does not take into account these system parameters changing over time. The expected value of the annual damage E(S) is calculated as:

$$E(S) = \sum P_i \cdot S_i$$

which is an addition of representative storms (its probability of occurrence times its associated damage).

The adaptation of the risk formula to include for system parameters changing slowly over time, but at a constant growth rate, consists of multiplying it with the so-called "rate factor". The formula is then:

$$E(S) = \sum P_i \cdot S_i \cdot \frac{(1+r)^T - 1}{rT}$$

in which T [years] is the time scale and r [% per year] is the relative rate at which the system parameter(s) under consideration increase either the chances of flooding (P) or the damage (S) at the rate of a constant annual growth.

The rate factor is therefore by definition:

$$ratefactor = \frac{(1+r)^T - 1}{rT}$$

This formula can be used if several system parameters cause a slow constant increase (or decrease) at the same time, either of the chances (Pi) or of the consequences (Si). In fact, this means the following formula has to be used then in order to calculate a total net r [%/year]:

$$(1+r) = \prod (1+r_j)$$

in which the product is calculated for all the system parameters "j"

This formula can be simplified to

$r = \sum r_j$ because for all $r_j$ , $r_j$ <<1

N.B. : The formula for the "rate factor" is mathematically deduced by using the formula for the sum of the terms of a geometrical series.

It is now a matter of demonstrating for each of the three system parameters slowly changing over time that they each result in a slow but constant growth over time, of either the chances (Pi) or the consequences (Si).

1. evolution of the economic values (=the maximum damage in the coastal zone).

The evolution of the economic values in the coastal zone results in the same evolution of $S_{max}$ and therefore also for the same evolution of the consequences (Si); it has no effect on the chances (Pi). The evolution of the economic values in the coastal zone can be placed on a scale with macro-economic indicators, in particular especially the GNP (Gross National Product) [van der Klis et al, 2005, which refers to the publications of the Dutch Central Planning Bureau and the Dutch Central Bureau for Statistics]. Therefore the extent of the relative evolution of the economic values in the coastal zone can be made equivalent to the economic growth of the region around it, the GNP of Belgium or the gross regional product of Flanders or Europe… The economic growth is gradual, but constant over time. Over a time scale of several decades, it is possible

to average out economic fluctuations. However, corrections must be made for inflation (which is standard practice in macro economics).

2. evolution of the sea level (relative rise of average high water in relation to the sea wall)

This relative rise of the sea level is a system parameter which results in a slow but constant increase in the chances (Pi); there is no effect on the consequences (Si). The relative rise in high water in relation to the sea walls can be expressed in a translation of the extrapolated curve for extreme water levels (storm surges). The reason for this is that at present no significant change is expected in the climate of storms/winds on the North Sea (although further scientific research on this topic is needed), so that the distribution of chances with regard to storms/winds remains relatively constant over time. The extrapolated curve for extreme water levels is (virtually) straight on a logarithmic scale (Figure 3).

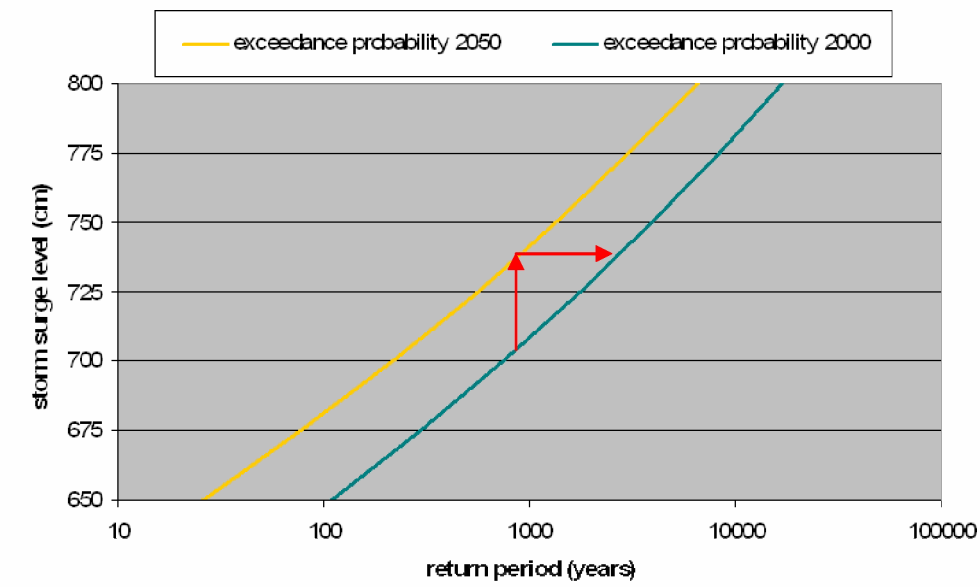


Figure 3 Effect of sea level rise on exceedance probabilities of storm surge levels

An increase in water level $\Delta w$ [m] (vertical red arrow) therefore corresponds to a (almost) constant relative increase in probabilities $\Delta p$ [%] (horizontal red arrow). A sea level position increasing over time in a linear fashion (constant rise in sea level) therefore results in a constant growth of the chances (Pi).

3. the discount rate

In our western capitalist economies the discount rate shows the rate at which money makes money. If the government postpones investments, it can make savings so that the capital increases over time. Therefore future costs and liabilities must be up to date and must be divided by a factor taking into account the principle of compound interest, which is identical to the formula for the rate factor. Therefore this complies with the criterion put forward for slow constant growth in the risks of flooding ($P_i.S_i$),

although in this case this is a negative growth. The calculation of the discount rate must make corrections for inflation (which is standard practice in macro economics).

## 3.3 Application for Belgian coastal zone for time horizon 2050

1. evolution of the economic values (~maximum damage in the coastal zone)

The question which arises is how big the average economic growth in the region will be up to 2050.

The study reports of planning bureaus are consulted to estimate this.

In the first report [Federal Planning Bureau, 2007] the historical growth is studied for the period from the 1970s up to now. This shows a clear declining trend in the economic growth over a time scale of decades. It states that this sort of decline has also been observed in our neighbouring countries, and that within the European Union. See the figures below from the report referred to (Figure 4).

**Figure 10** GDP **growth**
*average annual growth rate in percent*

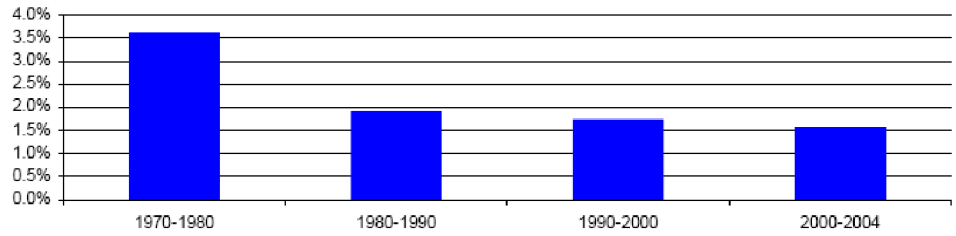


**Figure 1** GDP **per capita**
*annual growth rate in percent*

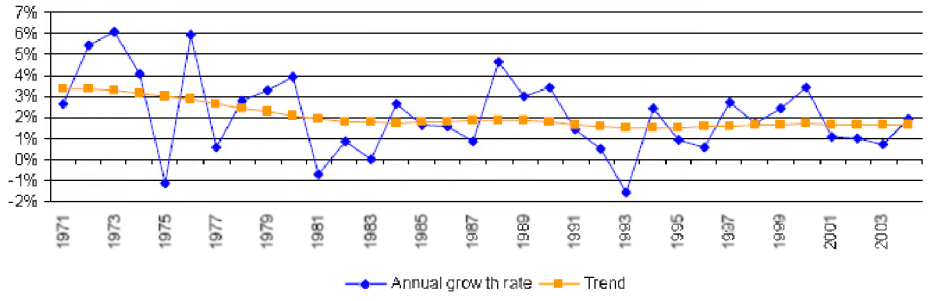


Figure 4 Historical economic growth rate for Belgium [Federal Planning Bureau, 2007]

The second report [Federal Planning Bureau, 2006] provides prognoses for the economic growth up to 2020. This reveals an expected constant growth of 2,0 % (corrected for inflation), i.e., a slightly stronger growth than in previous decades. See the figure below in the report referred to.

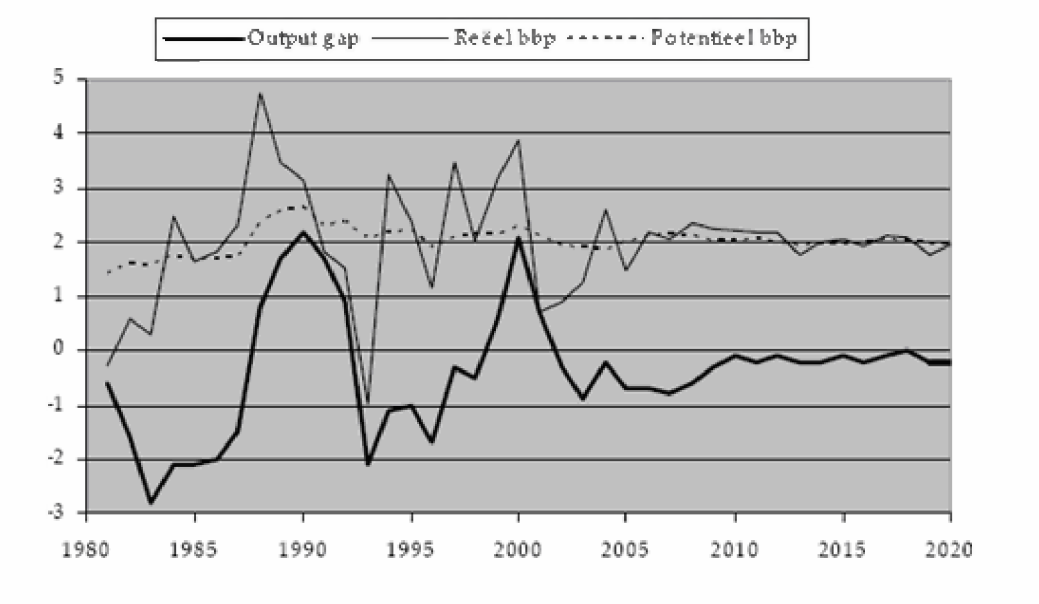


Figure 5 Projected economic growth rate for Belgium [Federal Planning Bureau, 2006]

The third report, "Prosperity and Environment" [CPB, NMP, CBS, 2004] gives different prognoses for the economic growth for the Netherlands up to 2040, looking at four different realistic scenarios in terms of the general societal evolution, which are possible combinations of two basic evolutions as key uncertainties, viz., in the first place, the extent to which countries operate internationally, and the extent to which the government acts (cf. leaving individuals free to act / private initiative). The rate of economic growth is estimated for these four scenarios up to 2040. The growth of the GNP is between 0,7 and 2,6% per year on average. In all four scenarios the growth up to 2040 is higher than that in the period afterwards. See the figures below from the report referred to above.

Tabel 3.1 Belangrijkste uitkomsten van de vier scenario's.

| | | Global Economy | Strong Europe | Transatlantic Market | Regional Communities |
|---|---|---|---|---|---|
| | 1971-2001 | 2002-2040 | 2002-2040 | 2002-2040 | 2002-2040 |
| | Mutaties per jaar in % | | | | |
| Bevolking | 0,7 | 0,5 | 0,4 | 0,2 | 0,0 |
| Arbeidsaanbod | 1,1 | 0,4 | 0,1 | 0,0 | - 0,4 |
| Werkgelegenheid | 0,9 | 0,4 | 0,1 | 0,0 | - 0,5 |
| Arbeidsproductiviteit | 1,9 | 2,1 | 1,5 | 1,9 | 1,2 |
| Volume BBP (marktprijzen) | 2,6 | 2,6 | 1,6 | 1,9 | 0,7 |
| BBP per hoofd | 1,9 | 2,1 | 1,2 | 1,7 | 0,7 |

Figure 6 Projected economic growth rate for the Netherlands [CPB, NMP, CBS, 2004]

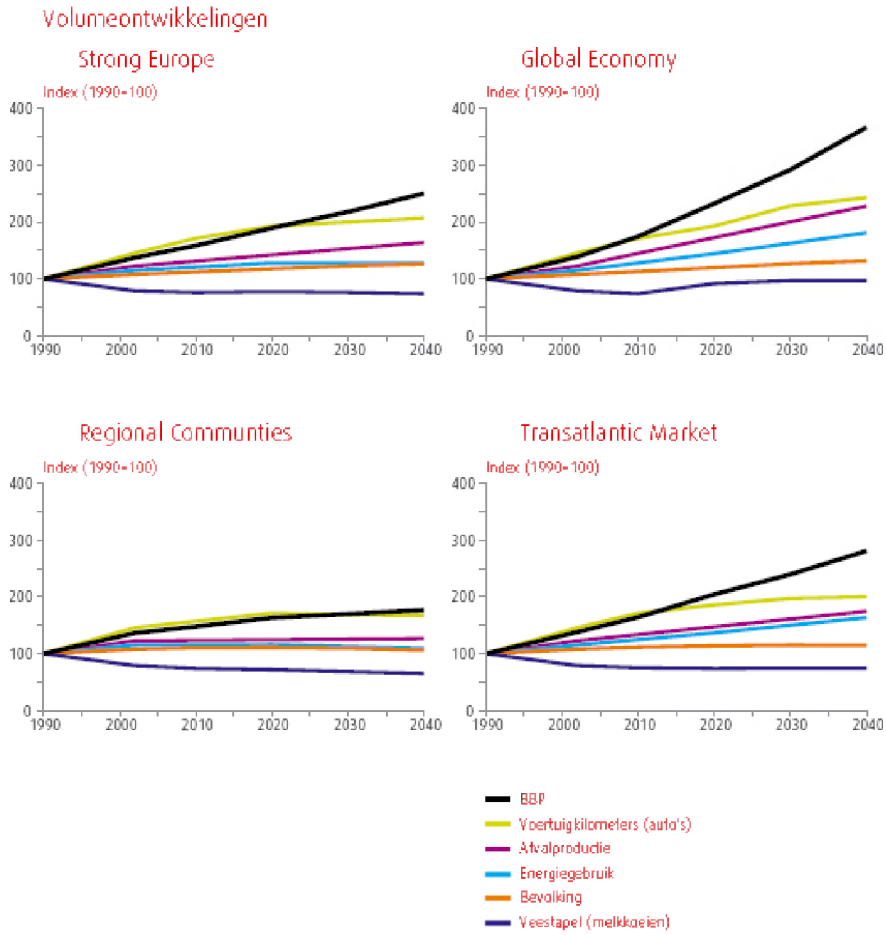


Figure 6-bis Projected economic growth rate for the Netherlands [CPB, NMP, CBS, 2004]

In conclusion the average of the growth figures for these four scenarios - 1,7% - is seen as the best estimate for the economic growth in the region up to 2050, and therefore also for the increase in the economic values in the coastal zone.

2. evolution of the sea level (relative rise in the average high water in relation to the sea wall)

The expected rise in the high water during the period 2000-2050 in relation to the level of the sea wall is estimated in [Viaene P., 2000] and [IMDC, 2005-a] as 30 cm, i.e., on average, 6 mm/year. On the other hand, there is the present, observed sea level rise of 1,8 mm/year in our coast, based on recent maregraph observations [Verwaest en Verstraeten, 2005].

In recent years different extrapolated curves for extreme water levels have been drawn up on the basis of the data set of the maregraph measurements in Ostend, The results from [Technum-IMDC-Alkyon, 2002], [Probabilitas, 1999] and [Verwaest, 1999] are shown together on the graph below.

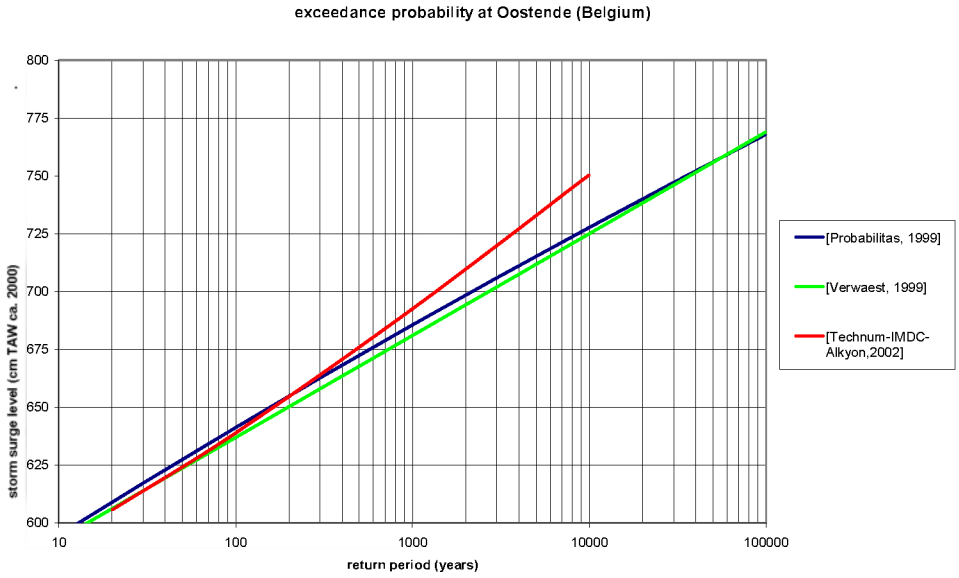


Figure 7 Different curves giving the exceedance probabilities of storm surge levels at Oostende (Belgium)

The difference in storm surge level of the extrapolated curves between the return periods of 1000 and 10000 years is on average 50 cm.

In that case a rise in sea level of 6 mm/year corresponds to an increase in the extrapolated chances of 2,8 % per year ( 1,028 = 106/500 ).

3. the discount rate

In the MKBA updated Sigmaplan [Gauderis et al, 2005] the value to be used for this discount rate is determined at 4 %. Because this figure is sufficiently smaller than 1, this can be calculated as a negative growth of approximately -4 % (more precisely calculated as: 1/(1+4%)-1 = -3,8%).

The net growth up to 2050 is: + 0,5% per year because:

Effect of the increase in economic values in the coastal zone + 1,7 % per year

Effect of the rise in sea level (high waters) in relation to the sea defence + 2,8 % per year

Effect of discount rate - 4 % per year

TOTAL, NET GROWTH + 0,5 % per year.

The rate factor to be applied with which the risk (euro/year) must be multiplied in order to take into account these changing system parameters in the course of the period up to 2050 is then calculated as 1,13, i.e., an increase of 13 %. ( 1,13 = (1,00550-1)/(50 * 0,005) )

This is a small net increase which is the result of the large gross increase resulting from the increase in economic values and rising sea level (+4,5 % - rate factor approximately. 3,5) and a large gross reduction resulting from the discount rate (- 4 % - rate factor approximately. 1/2,5).

## 3.4 Estimate of uncertainties

There is a margin of uncertainty regarding the best estimate found for the rate factor, viz. 1,13. This margin of uncertainty can be estimated by separately quantifying the uncertainties which exist for the three different trends (increase in economic values, rise in sea level and discount rate) and then translating these on to the effect on the rate factor.

1. evolution of the economic values (-the maximum damage in the coastal zone)

In terms of size, the uncertainty with regard to the future economic growth up to 2050 can be estimated by looking at the variability of the growth figures for the different scenarios looked at in the "Prosperity and Environment" report quoted above [CPB, NMP, CBS, 2004]. In that case it is explicitly presumed that each of the four scenarios has the same chance of becoming the reality. The report shows that this was actually the aim of working out the four scenarios. In that case the standard deviation with regard to the average of 1,7 % per year (calculated for this) is calculated as a $\sigma = 0{,}8$ % per year.

2. evolution of the sea level (relative rise of average high water in relation to the sea wall)

The uncertainty regarding the future rise in sea level up to 2050 is caused above all by the uncertainty regarding the impact of worldwide climate evolution. Depending on the worldwide climate policy (emission scenarios), the IPCC has worked out scenarios which all indicate a different acceleration in the current rise in sea level. The most recent IPCC report (4th assessment) quantified the uncertainties regarding the future worldwide rise in sea level more clearly (in comparison with the previous report, the third assessment). It is possible to estimate the variability on the basis of the published synthesis report of the WG 1 [IPCC, 2007]. Figures are given only up to 2100; these can be used as a good approximation for up to 2050. The figures are:

**Table SPM-3.** Projected globally averaged surface warming and sea level rise at the end of the 21st century. {10.5, 10.6, Table 10.7}

| Case | Temperature Change (°C at 2090-2099 relative to 1980-1999) [a] | | Sea Level Rise (m at 2090-2099 relative to 1980-1999) |
|---|---|---|---|
| | Best estimate | *Likely* range | Model-based range excluding future rapid dynamical changes in ice flow |
| Constant Year 2000 concentrations [b] | 0.6 | 0.3 – 0.9 | NA |
| B1 scenario | 1.8 | 1.1 – 2.9 | 0.18 – 0.38 |
| A1T scenario | 2.4 | 1.4 – 3.8 | 0.20 – 0.45 |
| B2 scenario | 2.4 | 1.4 – 3.8 | 0.20 – 0.43 |
| A1B scenario | 2.8 | 1.7 – 4.4 | 0.21 – 0.48 |
| A2 scenario | 3.4 | 2.0 – 5.4 | 0.23 – 0.51 |
| A1FI scenario | 4.0 | 2.4 – 6.4 | 0.26 – 0.59 |

Table notes:

[a] These estimates are assessed from a hierarchy of models that encompass a simple climate model, several Earth Models of Intermediate Complexity (EMICs), and a large number of Atmosphere-Ocean Global Circulation Models (AOGCMs).

[b] Year 2000 constant composition is derived from AOGCMs only.

Figure 8 Variability of projected sea level rise in 21st century [IPCC, 2007]

Therefore there is a variability resulting from the possible emission scenarios (six scenarios considered equally probable) and a variability resulting from the fact that it is not possible to predict the consequences of an emission scenarios 100%. This is characterised by a spread $\sigma$ of 1,2 mm/year (average for the six scenarios). The variability between the scenarios has a $\sigma$ of 0,5 mm/year. A combination of these gives a total variability with a $\sigma$ of 1,4 mm/year. This translates into a standard deviation for the growth of the risks from a rise in sea level, viz, a $\sigma$ = 0,7 % per year.

3. the discount rate

The discount rate to be used can be theoretically determined as the return which the government can earn per year by postponing an investment. Corrections must be made for inflation. Obviously this return will vary over time, depending on the economic evolution in the region and the whole world (continuing globalization of the economy). Furthermore there are different perspectives about how a discount rate can be theoretically determined. However, there are regulations with regard to the discount rate to be used for government investments. A summary is provided by the working group on “updating the discount rate” currently active in the Netherlands [Working group on updating the discount rate, January 2007].

The discount rates prescribed to be used for the evaluation of government investments:

- the Netherlands : until recently 4% per year, now 2,5 % per year
- Germany : 3 % per year
- UK : 3,5 % per year
- France : 4 % per year
- Belgium: railway investments: 4 % per year
- Belgium - Wallonia - road investments: 6,5 % per year
- The European Commission requires 5 % per year as a starting point for projects which require investment subsidies, while 3% per year is proposed in European harmonisation projects as a standard discount rate for the EU.

Recently (March 2007) it was decided to reduce the discount rate in the Netherlands from 4 % per year to 2,5 % per year, in view of the fall in the risk-free capital market interest. Furthermore, additional research is carried out to see whether the discount rate should be further reduced when the investments concerned focus on problems which are fundamentally irreversible, such as long-term problems like adaptation to climate change.

The variability of the prescribed discount rates given here has a $\sigma$ = 1,2 % per year.

The three trends result in a variability in the total net growth with a $\sigma$ = 1,6 % per year. This figure was achieved as the quadratic average of the three different distribution values (because the normal distributions are independent from each other).

Translating this variability to the rate factor then produces the following results (for T = 50 years):

| | | RATE FACTOR |
|---|---|---|
| (~ - 2 sigma) | r = -2,7 % | 0,55 |
| (~ - sigma) | r = -1,1 % | 0,77 |
| | r = 0 % | 1 |
| (~ median ) | r = 0,5 % | 1,13 |
| (~ + sigma) | r = 2,1 % | 1,74 |
| (~ + 2 sigma) | r = 3,7 % | 2,78 |

The variability for the rate factor can be modelled as a lognormal distribution with a sigma factor of 1,5. By way of illustration, see the figure below.

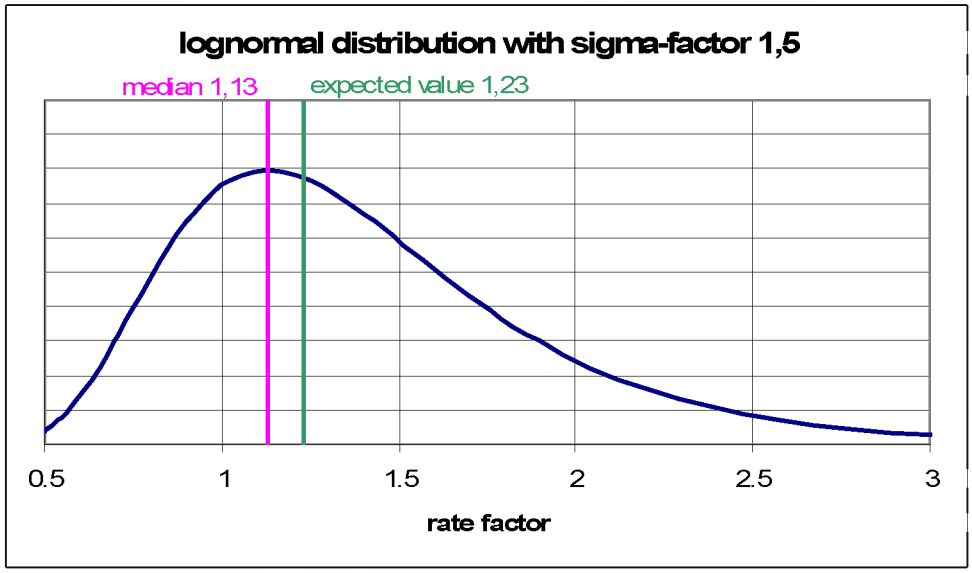


Figure 9 Lognormal distribution with a sigma factor of 1,5

Because the lognormal distribution is asymmetrical (the figures higher than the median have greater weight than the figures lower than the median), the expected value for the rate factor is higher than the median value. However, because of the relative small sigma factor of 1,5 this effect is small, viz., an increase of 9%. The expected value for the rate factor is then 1,13 x 1,09 = 1,23.

## 3.5 Conclusion

In order to take into account the trends expected up to a certain time horizon of several decades into the future (e.g. 2010-2050) in terms of the increase in economic values in the coastal zone and in terms of the relative rise in sea level with regard to high waters, and the discount rate, the damage-risk (euro/year) that is calculated using the data for the current situation (~ the first decade of the 21st century) must be multiplied by a rate factor.

In the example for the Belgian coastal zone with a time horizon to 2050 the rate factor has an expected value of 1,23. Therefore there is a 23 % increase as a result of the time scale that was looked at up to 2050 in relation to the risk for purely the current situation.

Applying this methodology in the optimum way means making the best estimates of the evolution of the three system parameters referred to, as well as the uncertainty related to this.

In this respect the figures mentioned above for the Belgian coastal zone are the start values. By means of an additional study of the literature it should be possible to make better, more widely applicable estimates, viz., in particular:

- a broader consultation of the reports of planning agencies on macro-economic expectations will allow for an even better estimate of the evolution of the economic values in the coastal zone;
- using regional climate scenarios which will be based on the 4th assessment report of the IPCC, it will be possible to make a better estimate on this basis with regard to the evolution of the rise in sea level;

- better information will become available on the discount rate to be applied when the results are available for the Dutch working group currently focusing on the possible reduction in the discount rate for investments in climate adaptation; it is also necessary to follow up whether any regulations apply or will apply which impose the use of a compulsory discount rate.

# 4. Flood modelling for risk evaluation - methodological improvements

## 4.1 Calibration of a breach growth model

**Breach formation and breach growth**

In the COMRisk case study (Vlaanderen/Zeeuws-Vlaanderen' (IMDC, 2005-b) breach growth was modelled by means of time series, which were in turn based on simple assumptions regarding growth velocities in depth and width. In this study, one aimed at and examined a more advanced approach in modelling breach growth.

Breach formation/initiation and growth in sandy dikes caused by wave overtopping or overflow passes through five stages (Visser, 2002):

1. increase of landside slope
2. regressive erosion
3. lowering of crest
4. (super)critical flow
5. subcritical flow

The course of the first three stages is shown in Figure 10.

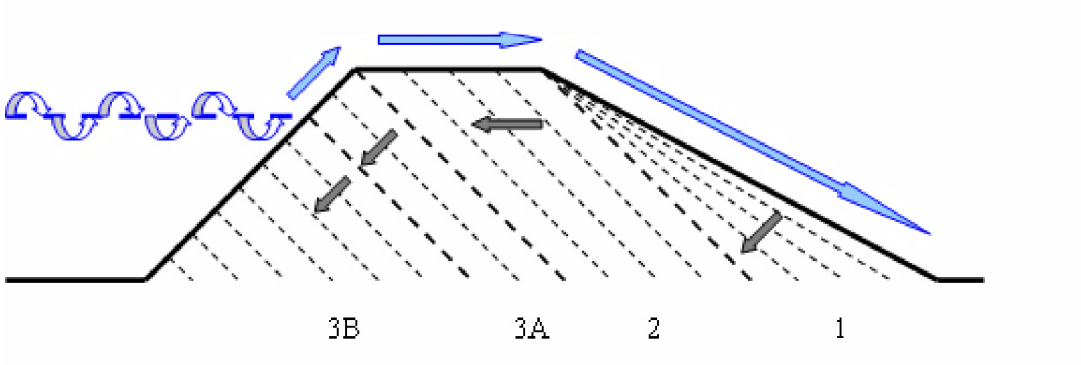


Figure 10 Breach growth in a sandy dike (Visser, 2002)

Breach formation, i.e. as long as the crest level of the dike exceeds the mean water level (no wave action), is described by stages 1, 2 and 3A. However, stages 3B, 4 and 5 represent the actual breach growth. During stage 3, mainly growth in width takes place. Stage 4 and 5 account primarily for growth in depth.

Breach formation is studied when analysing failure behaviour of the sea defence (determination of residual strength), while breach growth is a part of the hydraulic analysis. Hence, the process of breach growth, modelled within the hydraulic model should not start from the original (trapezoidal) dike profile, but should only take the residual profile at the beginning of stage 3B into account. This residual profile is triangular and has a crest height as high as the mean water level at the moment of breaching.

**Breach growth described by Verheij-vanderKnaap**

The equation of Verheij-vanderKnaap divides breach growth into two phases: first vertical growth, followed by horizontal growth. Growth in depth is considered to be a function of time, while growth in width is in addition also function of water level and dike properties.

Growth in depth: $t \leq t_0$

$$B(t) = B_0$$

$$Z(t) = Z_o - (Z_o - Z_{\min}) * (\frac{t}{t_0})$$

Growth in width: $t > t_0$

$$B(t) = B_0 + \frac{f_1 g^{0.5} (h_{up} - h_{down})^{1.5}}{u_c} \log\left(1 + \frac{f_2 g}{u_c}(t - t_o)\right)$$

$$Z(t) = Z_{\min}$$

where:

$B_o$ = initial breach width (m)

B(t) = breach width at time t (m)

$Z_o$ = initial breach crest level (m AD)

$Z_{min}$ = lowest breach crest level (m AD)

Z(t) = breach crest level at time t (m AD)

$t_o$ = duration of phase with only vertical breach growth (s)

$h_{up}$ = upstream water level (m AD)

$h_{down}$ = downstream water level (m AD)

g = gravity ($m/s^2$)

$f_1$ = coefficient (-)

$f_2$ = coefficient (-)

$u_c$ = critical erosion velocity (m/s)

The flow through the breach is in SOBEK1D2D (Delft Hydraulics) modelled as weir flow using the following equations:

$$Q(t) = cB(t)(2/3)(h_{up} - Z(t))\sqrt{(2/3)g(h_{up} - Z(t))} \qquad \text{(free flow)}$$

$$Q(t) = cB(t)(h_{up} - Z(t))\sqrt{2g(h_{up} - h_{down})} \qquad \text{(drowned flow)}$$

with:

Q(t) = flow through the breach ($m^3/s$)

c = discharge coefficient (-)

For calibration purposes, the equation of Verheij-vanderKnaap was implemented into a spreadsheet. Not only the discretisation used in SOBEK1D2D, also the SOBEK1D2D flow formulae were built in into the spreadsheet.

**Erosion-based breach growth described by the sediment transport equation from Engelund-Hansen**

The erosion-based breach growth model of MIKE 11 (DHI) accounts simultaneously for growth in depth and width. Vertical growth is a function of the dike properties as well as the amount of sediment transported through the breach. Growth in width is set to a fixed proportion of growth in depth. Sediment transport itself is calculated by means of the equation of Engelund-Hansen.

Growth in depth:

$$\frac{dZ}{dt} = \frac{q_t}{L\,(1-\varepsilon)}$$

Growth in width:

$$\frac{dB}{dZ} = 2\,SEI$$

with:

Z = breach crest level (m AD)

B = breach width (m)

L = breach length in the direction of the flow (m)

$q_t$ = sediment transport per unit width ($m^2/s$)

ε = porosity (-)

SEI = side erosion index (-)

Calculating the length of the breach in the direction of the flow requires knowledge of the dike geometry (crest level, crest width and inner/outer slope). Sediment transport calculations, however, demand in addition knowledge of the sediment characteristics (grain size, density and critical shear stress for erosion).

The flow through the breach is in MIKE modelled using the general flow equations for a structure:

$$Q(t) = c\sqrt{\frac{2g(h_{up} - Z(t))}{\frac{1+\zeta}{A_s^2} - \frac{1}{A_{up}^2}}}$$ (free flow)

$$Q(t) = c\sqrt{\frac{2g(h_{up} - h_{down})}{\frac{\zeta}{A_s^2} - \frac{1}{A_{up}^2} + \frac{1}{A_{down}^2}}}$$ (drowned flow)

where:

Q(t) = flow through the breach ($m^3/s$)

$\zeta$ = energy loss coefficient (-)

$A_s$ = structure cross section ($m^2$)

$A_{up}$ = upstream cross section ($m^2$)

$A_{down}$ = downstream cross section ($m^2$)

c = critical/free flow coefficient (-)

The above mentioned equations are available in the basic version of MIKE 11. These equations were evaluated using a simple test case model.

**Calibrating erosion-based breach growth on Verheij-vanderKnaap**

The equation of Verheij-vanderKnaap contains two parameters ($f_1$, $f_2$) which were obtained based on a number of laboratory experiments and historical breaching events. A third parameter ($u_c$) is set to be function of the soil type and can be obtained from a table. In this study, the equation of Verheij-vanderKnaap was applied with standard values for $f_1$, $f_2$ and $u_c$ for a typical sandy dike, which is considered to allow for a fair representation of breach growth in an average sandy dike.

As mentioned before, MIKE 11 models erosion-based breach growth as a sediment transport process through the use of the equation of Engelund-Hansen. Given the fact that the Engelund-Hansen equation is strictly-speaking not valid for flow through a breach (rapidly varied flow, supercritical), calibration is necessary.

Most of the parameters of the erosion-based breach growth model of MIKE 11 have physical meanings, so rough estimates can be obtained. Next, the rough estimates were iteratively adjusted in order to obtain maximum compliance between breach growth (crest level, width) predicted by Verheij-vanderKnaap and by Engelund-Hansen.

A perfect match between both models is impossible because of the following two conceptual differences:

Within Verheij-vanderKnaap breach growth in width starts only after growth in depth has been completed. Within the erosion-based breach growth model of MIKE 11, both processes act simultaneously (and proportional to each other);

Breach growth is assumed to be a function of dike characteristics, water level and time by Verheij-vanderKnaap, whereas it is only a function of the first two by erosion-based breach growth model of MIKE 11.

It is not clear if the time-dependency in the equation of Verheij-vanderKnaap accounts for periods in which breach growth is paused due to a drop of the (mean) water level below the breach crest. Hence, two alternatives were considered, namely one based on the total elapsed time since breaching and a second one where only the time of actual flow through the breach is used. The latter results in slightly larger breach widths, although Mr. Verheij recommends the first approach (personal communication, Delft Hydraulics).

The calibration exercise was performed using a very simplified1D MIKE 11 test case under free flow conditions at the land side of the breach. In total four situations were looked at: a high (8 m AD) and a low (6,5 m AD) water level together with a small (10 m) and a large (200 m) initial breach width. Maximum compliance between both models was aimed at, especially during the first tidal cycle. As a consequence, breach growth by the erosion-based Engelund-Hansen model will always be higher for the next

tidal cycle as compared to Verheij-vanderKnaap. Within the latter, the velocity of breach growth decreases in time, where this is not the case in the former.

Finally, the results of both breach growth models were compared with the approach where breach growth is determined by a time series, following the assumptions used within the COMRisk-study. The flow through the breach was calculated using the flow equations implemented within SOBEK1D2D.

**Results**

Calculations are based on the following assumptions:

General:

- Failure at maximum water level
- Maximum breach width = 300 m
- Free flow at landward side

Time series (COMRisk):

- Initial breach depth = 0 m
- Growth in depth takes 2 hours (depth > 2 m)
- Growth in width = 30 m/h

Verheij-vanderKnaap (SOBEK1D12):

- Initial breach depth = 0 m
- Growth in depth = 4 m/h
- Growth in width = determined by default values of f1 (1,3) and f2 (0,04)
- Critical erosion velocity uc = 0,2 m/s (sand)

Calibrated erosion-based breach growth (MIKE 11):

- Initial breach depth = 0,2 m
- Crest level = mean water level at breach formation (m AD)
- Crest width = 0 m
- Slope = 3H:1V
- Grain size = 250 micrometer
- Specific density = 2,6
- Porosity = 0,4
- Critical shear stress (Shields) = 0,03
- Side erosion index (SEI) = 2

  Initially, based on the time series used within the COMRisk study, a SEI of 15 was estimated. During calibration the SEI was adjusted to a value of 2.

The following graphs show a comparison of the breach crest level (Z) and according breach width (B) based on time series (tijdreeks), two alternatives of implementing the equation of Verheij-vanderKnaap (V-vdK and V-vdK', resp. accounting for the total elapsed time or only accounting for periods with flow through the breach) and finally the calibrated version of the erosion-based breach growth model of MIKE 11 (erosie). In

addition, the upstream water level ($H_{opw}$) is presented. A second series of graphs are showing the corresponding discharges (bresdebiet) trough the simulated breaches.

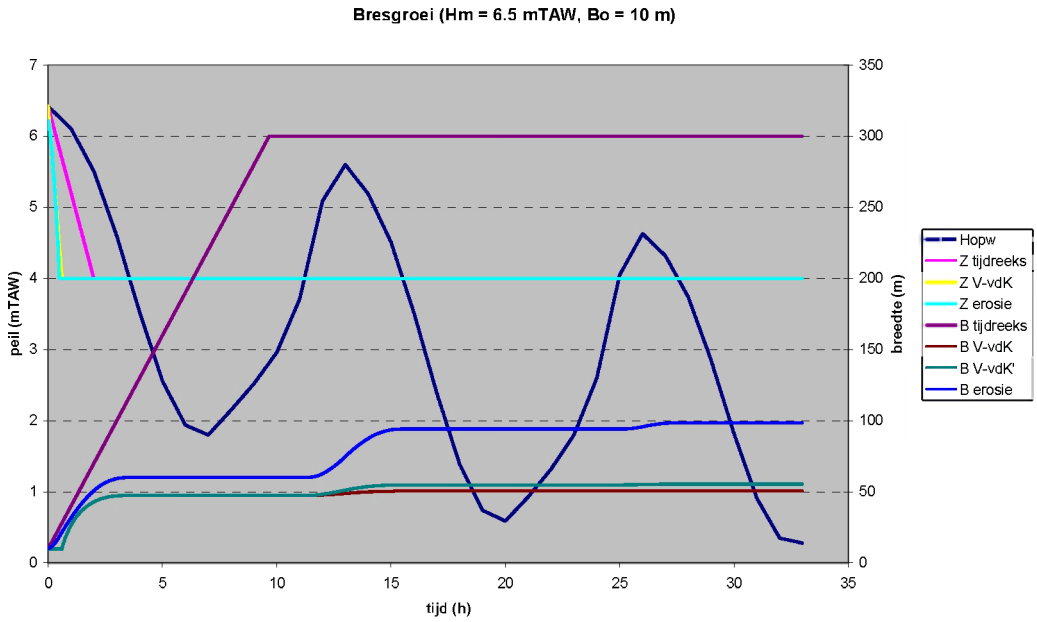


Figure 11 low water level (6,5 m AD) and small initial breach width (10 m)

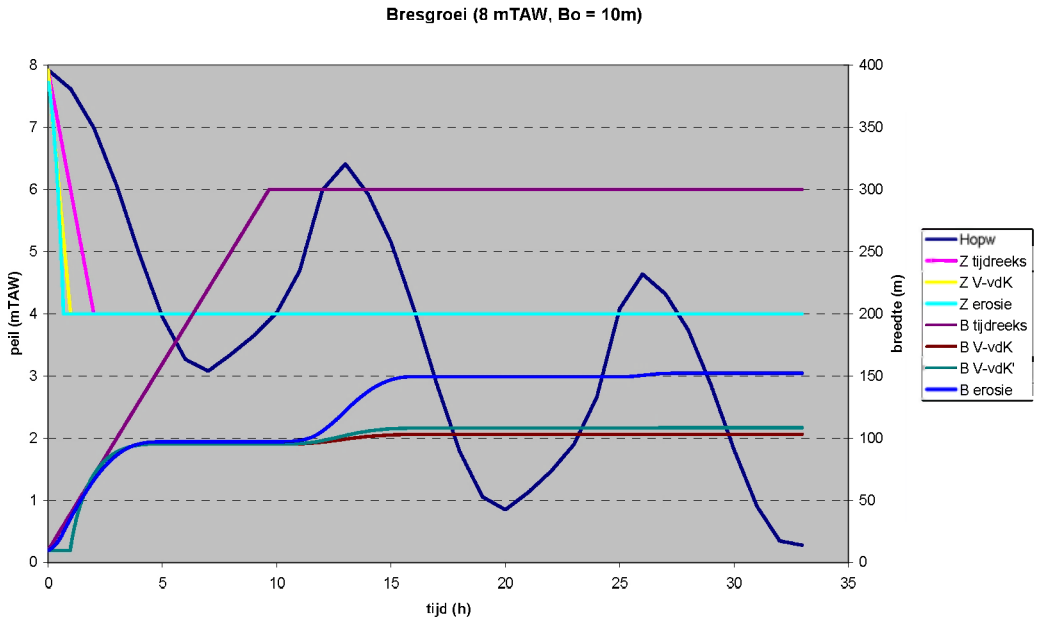


Figure 12 high water level (8 m AD) and small initial breach width (10 m)

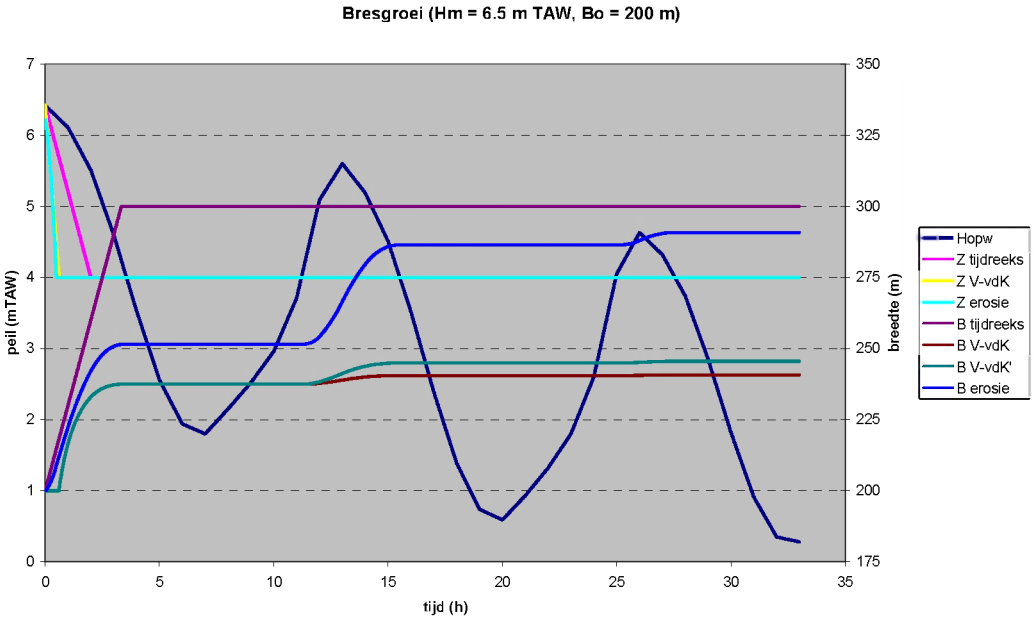


Figure 13 low water level (6,5 m AD) and large initial breach width (200 m)

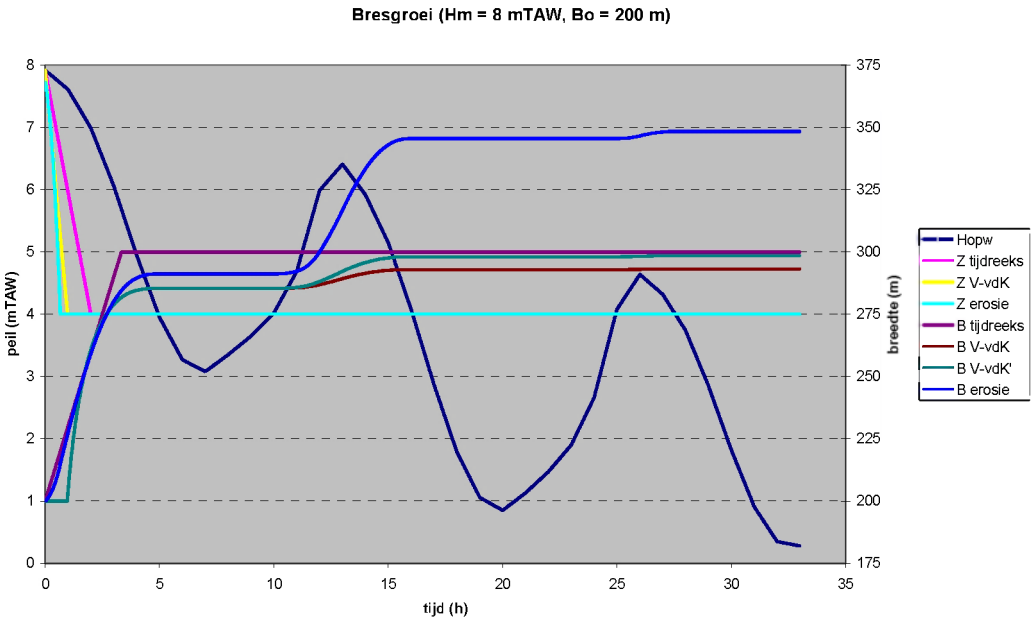


Figure 14 high water level (8 m AD) and large initial breach width (200 m)

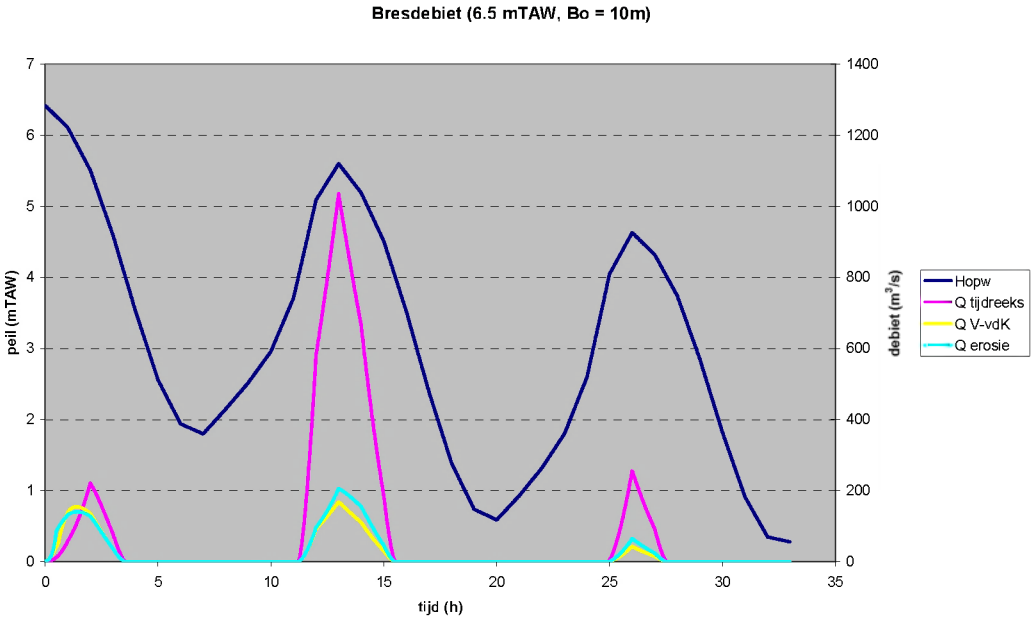


Figure 11-bis low water level (6,5 m AD) and small initial breach width (10 m)

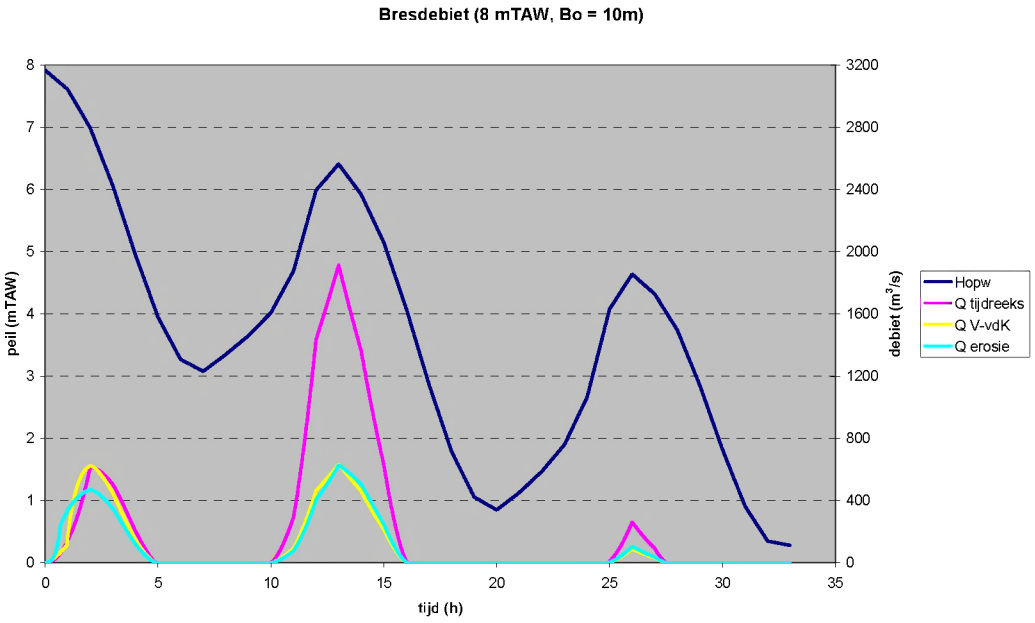


Figure 12-bis high water level (8 m AD) and small initial breach width (10 m)

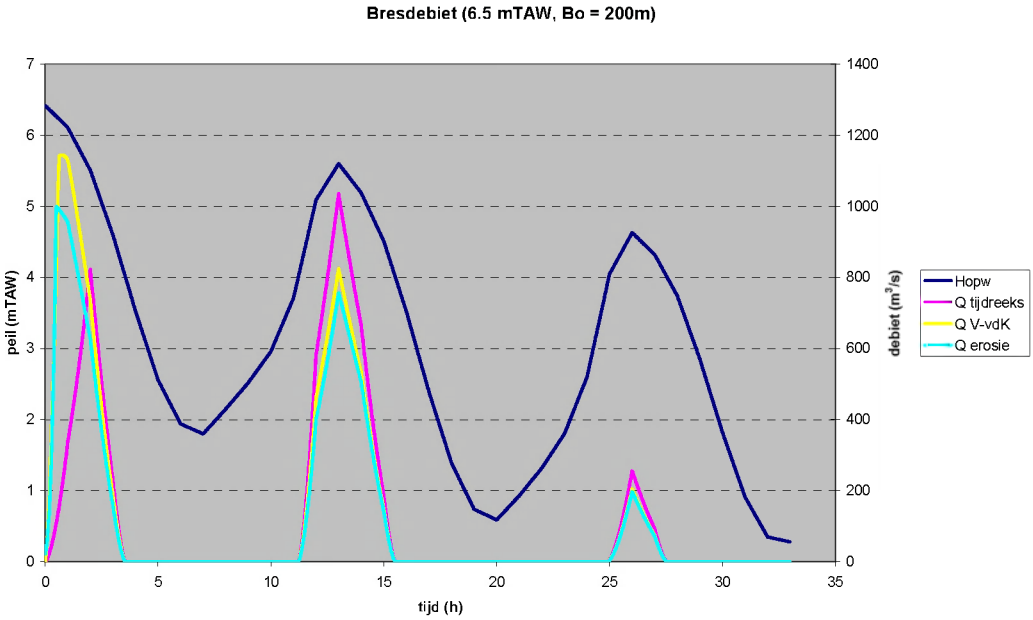


Figure 13-bis low water level (6,5 m AD) and large initial breach width (200 m)

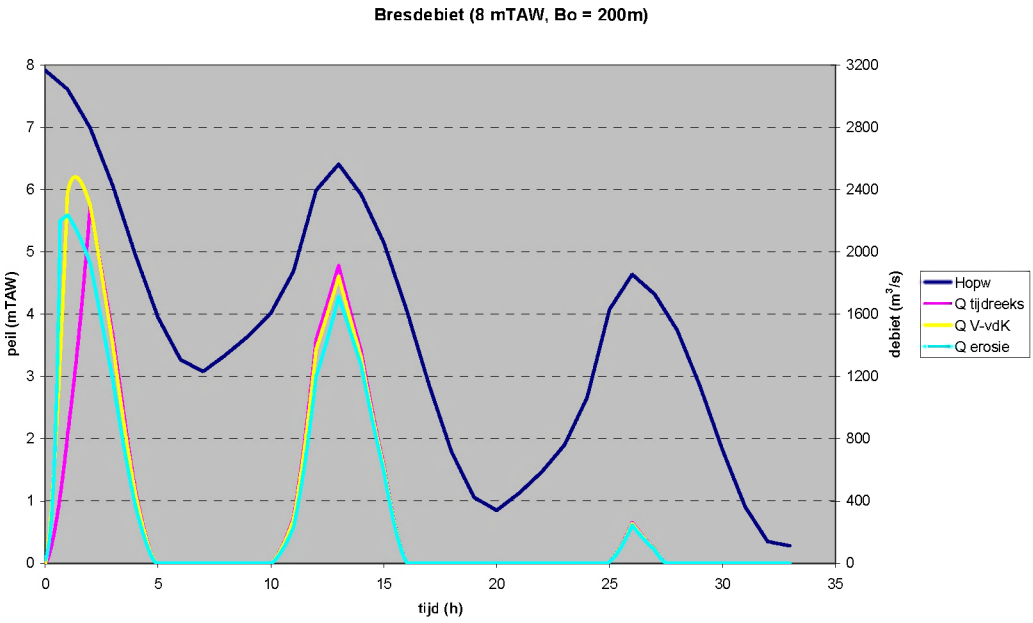


Figure 14-bis high water level (8 m AD) and large initial breach width (200 m)

Immediately after breach formation started, the breach width obtained with the erosion-based growth model is lager than those calculated by Verheij-vanderKnaap. According to the latter, growth in width starts only after growth in depth is completed, while in the former both processes occur simultaneously. During he first tidal cycle, good compliance between Verheij-vanderKnaap and the erosion-based model is obtained, with a small overrating. For the next tidal cycles, the erosion-based model always results in larger breach dimensions than those obtained with Verheij-vanderKnaap. In the latter breach growth decreases as a function of time. In some cases maximum breach widths according to Verheij-vanderKnaap as well as the erosion-based model do differ significantly from those obtained with the (COMRisk) time series. In the case of Verheij-vanderKnaap and the erosion-based model, maximum breach width is function of the initial breach width and the water level. Depending on the circumstances, maximum breach width ranges from about 50 m to about 350 m. In the case of time series, the final breach dimensions are defined in advance.

The graphs also illustrate clearly the conceptual advantage of erosion-based breach growth models as compared to a time series based model. Between 5 and 10 hours after breach formation, the water level tends to drop below the breach crest and hence in reality breach growth is interrupted, while breach growth in the time series based model still continues …

The flow hydrographs obtained with Verheij-vanderKnaap and with calibrated Engelund-Hansen modelled breaches are much alike. The initial differences during the first tidal cycle can be assigned to the conceptual differences between both approaches. Other deviations can be ascribed to different flow equations (discharge coefficient or energy losses). Nevertheless, differences between Verheij-vanderKnaap and erosion-based Engelund-Hansen are small compared to the flow hydrographs of the time series based model.

**Conclusion**

The erosion-based breach growth model of MIKE 11 can be calibrated in such a way that the calculated breach dimensions (crest level and width) are in good agreement with breach growth as described by the Verheij-vanderKnaap equation. Differences between both breach growth models are of a conceptual nature (parallel or serial breach growth in depth and width, reduction of growth in time).

Flow hydrographs obtained with the Verheij-vanderKnaap equation and according SOBEK1D2D flow formulae do correspond well with those obtained within MIKE 11 (calibrated Engelund-Hansen and according MIKE 11 flow formulae). Again, differences between the flow hydrographs are of a conceptual nature, not only between both breach growth models, but also between the applied flow formulae (discharge coefficient and energy losses).

Breach growth calculated by the calibrated erosion-based breach growth model of MIKE 11 represents a more realistic course than the one predicted by the (COMRisk) time series with the assumption of a steady growth velocity. Hence, the calibrated erosion-based breach growth model of MIKE 11 is recommended as a good alternative for the time series based approach (used within COMRisk).

## 4.2 Construction of a DEM for flood modelling

### Introduction

Test simulations starting from the digital elevation model (DEM) constructed for the COMRisk case study 'Vlaanderen/Zeeuws-Vlaanderen' (IMDC, 2005-b) indicate a major reliance of the inundation calculation on the chosen grid resolution of the DEM. A coarser grid is likely to smooth down the topography in general, but also to flatten out small line-shaped obstructions (like dikes, roadsides railway sides, …) in particular. On the other hand, computational limits and increasing demands on calculation speed often make it necessary to use coarser grid DEM's. In order to prevent unrealistic flow patterns when using a coarser grid size, a procedure for incorporating small line-shaped obstructions in a semi-automated manner was developed.

### Study area

The procedure was developed and tested on the Flemish East coast. The study area is shown in Figure 15 and contains the coastal plain between Zeebrugge and the Dutch border. While the western limits are determined by the presence of the Leopolds canal, the southern and eastern limits are set by the Damme-Sluis canal and the Dutch border respectively.

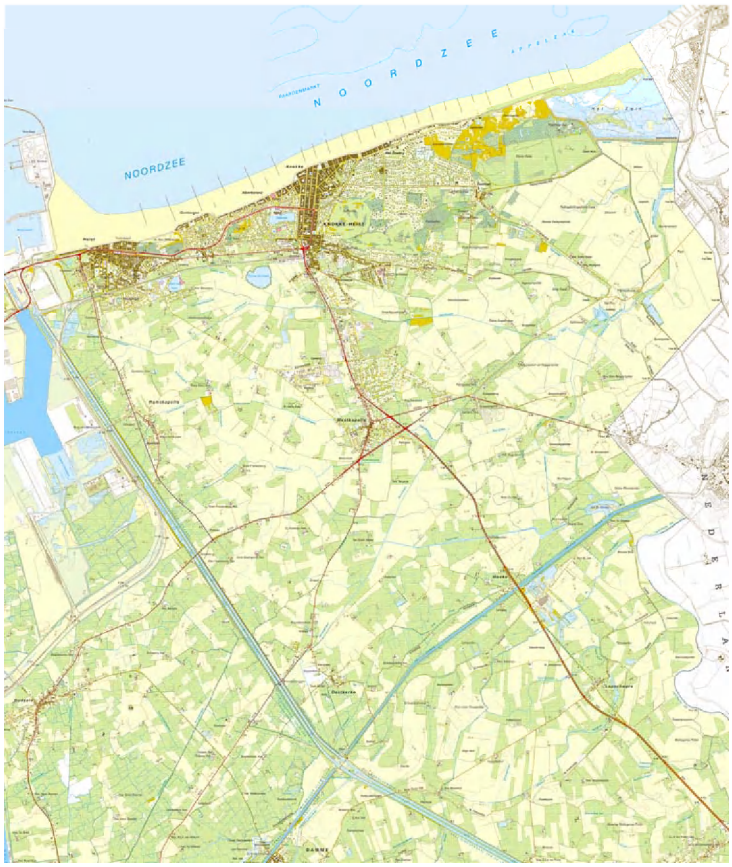


Figure 15 Study area (source NGI)

The coastal floodplain contains numerous line-shaped elements (old Zwin dikes, canal dikes, roads, railways, …) which have a potential water obstructing function. Figure 16 shows the major line-shaped obstructions.

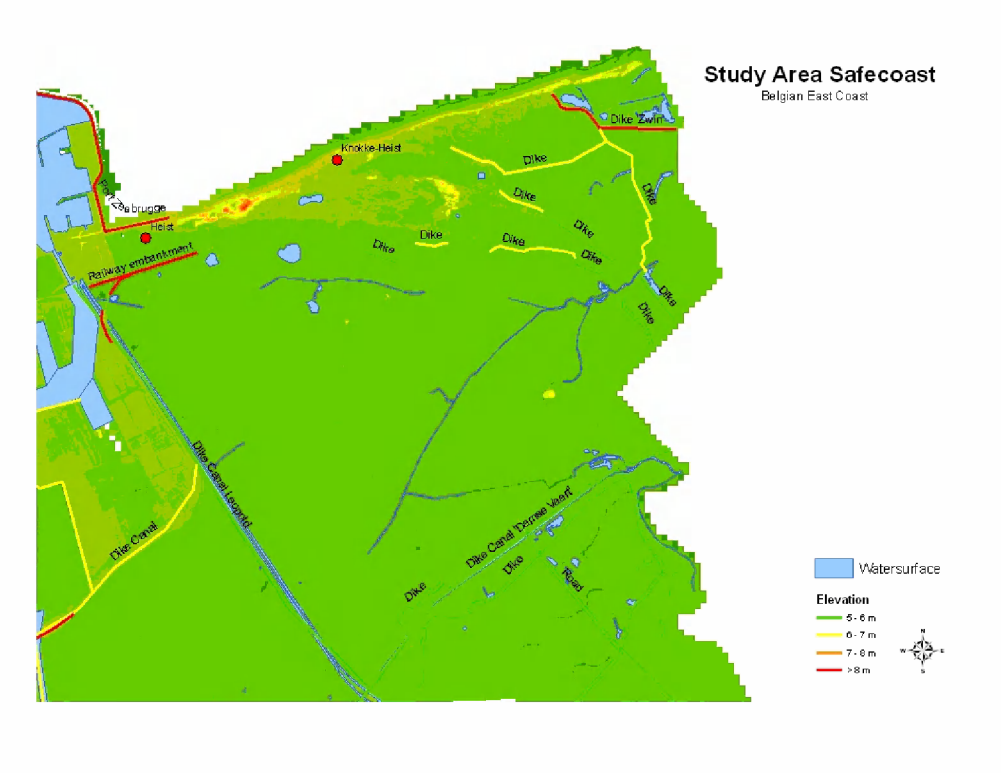


Figure 16 DEM and presence of line-shaped obstructions

**Resolution issues**

Through aggregation two elevation models were derived from DEM Flanders (grid size 5 m): a fine (grid size 20m) and a coarse (grid size 40m). Aggregation was based on averaging the elevation of 4 resp. 16 underlying points of DEM Flanders. Although this procedure is very easy to apply, narrow line-shaped elements smaller than 20 or 40 m are unfortunately smoothened out.

**Small line-shaped obstruction**

Small line-shaped elements with a potential water obstructing function were identified using DEM Flanders and the vectorial digital topographic map of Flanders.

Based on DEM Flanders, the elevation and surface slope were visualised. Next, the following line-shaped structures were selected:

hydrography: sea defence, quay, jetty with slopes on both sides

railways: all structures with slopes on both sides

roads: all structures with slopes on both sides

topography: slopes, banks, dikes, walls, …

Line-shaped structures are assumed to be potentially water blocking when their length exceeds 300 m and surface slope has a positive inclination larger than 6°.

The potential water blocking structures are converted from vector into raster formats. Due to fact that the location of the original line-shaped structures not necessarily matches the location of the crest within DEM Flanders, first a 10m-buffer around every line-shaped element was defined. This buffer was then transformed from vector into raster format with the same grid resolution as DEM Flanders (5m). Finally, the corresponding elevation from DEM Flanders was assigned to each grid cell.

Aggregating the rastered buffer resulted in a fine and coarse grid containing line-shaped structures with resolution 20 m and 40 m. To each aggregated cell the maximum elevation of the contributing cells was assigned. In this way, the elevation of each grid cell of line-shaped elements corresponds with the maximum of the elevation of the underlying points of DEM Flanders. Unless the buffer was not drawn wide enough, the assigned elevation corresponds to the crest level of the line-shaped structure.

All selected line structures were added to the elevation model by combining both grids and giving a higher ranking to the values within the line-shaped structure grid. In this way, small line-shaped obstructions were added to the fine and coarse elevation model for use in 2D flood modelling.

The exact shape of the line-shaped structure depends on the applied grid size. On the other hand, the crest elevation is no function of the chosen grid size, but is set equal to the highest and nearest elevation point from DEM Flanders. Obviously, structures which are not well represented by the original DEM (i.e. because the dimensions are smaller then the original grid size) can not be represented well in the derived elevation models.

Figure 17 shows the different versions of DEM's used for 2D flood modelling.

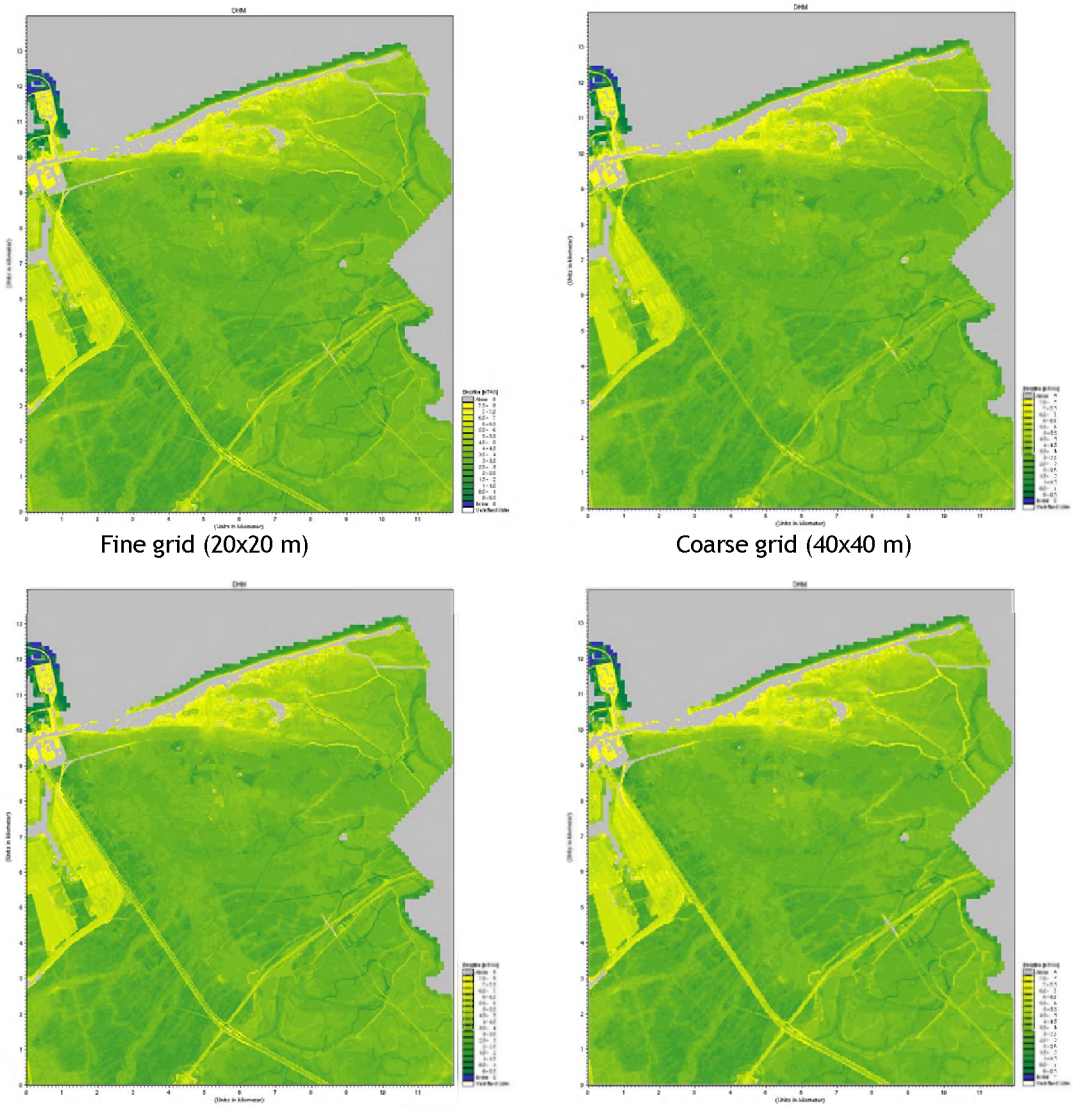

Fine grid (20x20 m)

Coarse grid (40x40 m)

Fine grid with line-shaped structures

Coarse grid with line-shaped structures

Figure 17 Digital elevation model

with and without small line-shaped elements taken into account

**Conclusion**

Small line-shaped potentially water blocking structures can be incorporated in a coarse(r) elevation models using simple, semi-automated procedures.

An analysis of the use of different elevation models on the flood results and in terms of damage and casualties will be discussed in the case study in chapter 6.

# 5. Comparison of vulnerability methodologies

## 5.1 Different methods used in the North Sea region

### Introduction

The focus here is on the valuation analysis and the calculation of damage and risk. Hydraulic boundary conditions, failure mechanisms and other related important elements are not taken into account.

Four methodologies (Flemish, Danish, German and English) will be compared, together with other useful methodologies out of the partner countries and outside. The comparison in this document is based on the end reports of COMRisk and combined with extra information available on the internet and received during interviews.

### Flood Maps and return periods

In the Danish and German methodology one return period (or probability of flooding) is considered to calculate the corresponding inundation and risk. In Germany an annual probability of $1 \times 10^{-4}$ is chosen, in Denmark $2{,}5 \times 10^{-4}$.

In the U.K. and in Flanders a range of return periods is used, each with is own consequences. In the U.K. (Lincolnshire case) 5 return periodsare chosen: T = 1, 20, 50, 200 and 500 years. The flood of 1953 is used for calibration. A fixed set of 7 return periods is used for the navigable waterways in Flanders: T = 1, 2, 5, 10, 25, 50 and 100 years. For the tidal area of the river Scheldt return periods until 1 000 years are added. This series of return periods makes little sense in the Flemish coastal area, were return periods of 1000, 4000 and 10 000 years are relevant.

In Denmark, Germany and Flanders a regular grid is defined to delineate the flooded area and to calculate the water depth. The German Digital Elevation Model (DEM) has a grid size of 2 x 2 meters. For the whole of Flanders a DEM of 5 x 5 meters is available but due to practical reasons (such as calculation times, computer storage capacity …) calculations were usually done on a 10 x 10 meter grid. Since the end of COMRisk computer storage and calculation capacity has increased seriously and a 5 x 5 meters grid is used for the SAFECoast calculations. A grid of 25 x 25 meters is used in Denmark. These grid sizes are different from those used for the final presentation of damage and risks.

The calculated water levels (adapted from hydrodynamic models or geographic information systems (GIS)) are reclassed in the methodologies. In Denmark and Germany depth classes of 0,5 meter are used, working with the average. A water depth between one and fifty centimetres is reclassed to a value of 25 centimetres. The Flemish methodology works with water depth classes of 25 centimetres using a conservative reclassification. This means that every water depth is reclassed to the next multiple of 25. All values between 26 and 50 centimetres are reclassed to 50 centimetres. The Lincolnshire methodology does not use one of these concepts because

only the maximum damage (also called potential damage, see below) is taken into account.

Table 1 Flood maps and return periods

| | Flanders (COMRisk) | Flanders (SAFECoast) | Denmark | Germany | U.K. |
|---|---|---|---|---|---|
| Return Period | $1 \times 10^{-3}$, $2{,}5 \times 10^{-4}$, $1 \times 10^{-4}$ | | $2{,}5 \times 10^{-4}$ | $1 \times 10^{-4}$ | $1{,}5 \times 10^{-2}$, $2 \times 10^{-2}$, $5 \times 10^{-3}$, $2 \times 10^{-3}$ |
| DEM Grid Size | 10 x 10 m | | 25 x 25 m | 2 x 2 m | n.a. |
| Water Depth Classes | 25 cm | | 50 cm | 50 cm | n.a. |

**Definition of damage**

The main focus of all methodologies is direct monetary valuable damage and victims (direct non monetary). Every methodology takes some extras into account. Description of direct monetary valuable damage is worked out in detail in chapter 4.

In Germany several classes of direct monetary valuable damage classes are taken into account. Added value is an indirect monetary valuable damage class. Direct non monetary valuated classes are tourist beds, jobs and residents.

Besides the direct monetary valuable damage, inhabitants and vehicles[1] are taken into account as direct non monetary valuable damage. Tourism and jobs is seen as indirect non monetary valuable damage in the Danish approach.

The U.K. methodology for Lincolnshire deals with six risk calculations. The described approach below is the one where the consequences for damage and victims are taken into account. The methodology has some classes for direct monetary valuable damage and victims as direct non monetary valuable damage class.

The Flemish methodology has his main focus on the direct monetary valuable damage. Indirect monetary valuable damage is taken into account in a conceptual way using rise factors (as done in the economic approach of cost benefit analysis) for housing, industry and agriculture. Inhabitants are the only direct intangible class taken into account.

[1] Due to the specific situation of car insurance in Denmark

**Damage categories and damage functions**

A text describing in detail all different damage classes, the spatial distribution in the study area, the valuation analysis and damage functions is available in Dutch. In this comparison only the most important elements are described. The outcome for the definitions can be found in the tables in the appendix.

Little information was found about the Lincolnshire case (U.K.). This explains the regular absence of this case study in this comparison.

Buildings (residential)

When combining the damage per surface and the total affected area damage to buildings is a very important part of the total damage for all case studies in COMRisk.

In the U.K. case only a number of affected residential buildings and a total possible damage is calculated. Caravans are seen as a separate class here. The other methodologies make a distinction between the building and the furniture (see further).

The total number of houses is divided over the surface. The exact location is known in the Langeoog case, the parcel of a building is located in the Ribe case but the exact position of the building on the parcel is unknown. Because topography is not changing a lot in one parcel, it is not increasing the uncertainty. The Flemish methodology knows the number of houses in one statistical sector and divides them over the residential surface on the land use map in that sector using a distribution code. This distribution code makes the density in areas with a land use code 'continuous urban fabric' 3 times higher then in 'open urban fabric'. In the transition zone between both the densities are 2 times higher then in open urban fabric. Because statistical sectors are small and chosen to be more or less homogeneous this simplification does not influence the results significantly.

Valuation of residential housing is based on average selling prices in Flanders, on data in a public register in Denmark and on construction guideline prices in Germany. In Flanders and Denmark the price of the land is included, in Germany this value is in the real estate class of residential areas.

The Flanders methodology for valuation is based on average selling prices, based on several areas with more or less homogenous characteristics. These areas contain usually one or more municipalities.

Danish researchers use a public register for the valuation of property. One damage function is defined for all buildings, which takes also indirect costs into account such as cleaning costs, repainting etc.

For the German method, field work has been done to know the structure of the building, the number and the use of storeys, the existence of an attic or a basement, and the age and the general equipment of the building. The valuation of buildings is performed based on the height of each storey, the ground surface (land register) and

the age. Several correction factors are taken into account, because of the significant regional differences in construction costs. Four different damage functions are defined, each for a different type of building (Table 2).

Table 2 Different damage functions for residential buildings, according to German methodology (MERK)

| Type | Number of storeys | Basement (Y/N) | Damage function |
|---|---|---|---|
| #1 | 2 | N | y = 5x |
| #2 | 2 | Y | y = 5x + 3 |
| #3 | 4 | N | y = 3x |
| #4 | 4 | Y | y = 3x + 3 |

All methodologies use a depth-damage relationship, however it seems in Denmark there is no strong correlation between water depth and damage under €8000.

Furniture

In all methodologies furniture is linked to (residential) buildings, but the valuation of these goods are different.

In Langeoog case, price setting is done based on assurances, where 700 euro per $m^2$ is the standard. However, in case of low quality buildings or extensions to buildings, a lower value is chosen. Damage functions are defined for each storey of a building, and according to the potential level of flooding (specific location). Attention is given to possible replacements within the building if the water level is not too high.

In Denmark, damage to furniture is derived from compensation payments. The method is identical to this of buildings.

In Flanders, valuation of furniture is defined as 50% of the average selling price of (residential) buildings. This percentage is based on the Belgian professional union of enterprise assurances (Assuralia) and fits within price settings of assurance companies for (residential) buildings and furniture.

Inhabitants

The number of inhabitants is defined in a different way for all the methodologies but always taken as direct intangible damage. The way of defining inhabitants in the Lincolnshire methodology is not known at the moment. In Germany the number of inhabitants in every house is known for the study area and also inhabitants of second residences are included. An average number of 2,3 people per house is used in Denmark. The Flemish methodology uses the total number of inhabitants in a statistic sector (more or less homogeneous sub area of a community) and divides them over the total area with land use housing.

In Germany a flood can only cause victims when there is no dry floor in a house left. In Flanders victims are possible when the coefficients for water depth and rising velocity are greater then zero. In Denmark and the U.K. only the number of inhabitants in the study area is indicated.

Industry

In the Danish methodology, the category industry is integrated as separate classifications within "buildings". Difference is made between farm, workplace, buildings for public water and energy supplies and other buildings for agriculture or industry. These classifications are combined into one group: agricultural and industrial constructions. Damage calculation is then performed with damage functions, analogous to those for residential buildings.

For the Langeoog case, German researchers have created a classification "fixed capital", which comprises buildings for economical purposes (industry, transport, services...) Like damage calculation for residential buildings, several damage functions are defined for fixed capital (Table 3). Furthermore, the damage is calculated separately for each storey and depends on the economical sector the buildings belong to. Loss of goods is taken into account in the German methodology. Annual reports from companies provide the possibility to determine stock supplies. Furthermore, attention is given to added value of production goods. In this way, an estimation can be made of possible production losses as a consequence of flooding. This is done by a damage function with respect of time: the length of production interruption is defined as the sum of flood and reparation duration.

Flanders has developed a methodology for the category industry, which is based on two different calculations methods. On the hand, damage calculation is done based on the area of the industrial sites, on the other hand calculations are performed using the number of employees for each company as key reference. For the latter a distribution code is developed to become twice employees in workplaces and factories as on car parks and stocks. Indirect damage (cleaning costs, production losses etc.) is estimated as a variable percentage of direct tangible damage.

Table 3 Damage functions for industrial buildings, according to German methodology (MERK)

| Sector | higher storeys | basement | hall |
|---|---|---|---|
| trade and administration | y = 57Vx + 5 | y = 68Vx - 6 | -- |
| production | y = 20x | y = 28x | y = 28x |

Jobs (employees)

This category is only taken into account in the German and Danish methodology. In both methods, the number of employees working in the study area (not where they pay social security or the total economic active population) is divided over the industrial / commercial surface

In Flanders, the number of employees is used as key reference for damage calculation of industry (see above), but is not used as input for victim calculations.

### Infrastructure

According to the Flemish methodology, "infrastructure" contains buildings located in foreign areas, such as sports centre in recreational area, halls on shunting-yards, parts of port infrastructure, etc. Flanders has chosen to use the same valuation for infrastructure as for industry, namely € 100/m². No indirect damage is taken into account.

The other case studies (Ribe, Langeoog and Lincolnshire) don't define infrastructure as a separate classicification. However, they do often incorporate such building types (if they exist in the study area). In that case, they are classified in "buildings".

### Airport / Airfield

Airport and airfields only occur in the Flemish and German case studies. In Langeoog is worked with a fixed cleaning and repairing cost. In Flanders, a distinction is made between the larger airports - Zaventem (Brussels), Antwerp and Ostend - and smaller airfields for private planes. The large airports are seen as distinct point elements in landscape and their valuation is done individually based on insurance data and information of the airport. For smaller airfields is worked with a maximum damage identical to this of industry when worked with damage per surface (see further). This value is only given to sheds and airstrips. All other areas related to the airfield (grassland, herbage …) and approaching routes have no economic damage.

The Flemish method uses a depth-damage relationship, identical to the function for industry (surface approach). There a no indirect damages calculated for this land cover.

### Recreation

In Flanders and Germany, recreation is defined as tangible damage to sports fields, camping sites, playgrounds, golf courses, etc. In Flanders, the maximal damage to recreation areas is rather small, because of its definition. Buildings and infrastructure on recreational areas belong to "infrastructure" as mentioned above. The damage to recreation is merely determined by cleaning and reparation costs (€ 0,03/m²).

For Germany, damage function is also determined by cleaning and reparation, but the costs are set higher: € 1/m².

Denmark and U.K. don't have a clear methodology for dealing with recreation. Danish researchers take into account recreational buildings, but don't mention sports fields and suchlike. In Lincolnshire case, recreation is defined by caravans, of which the number and value is known. It is unclear if more recreational elements are taken into account.

### Tourism

Tourism is only taken into account in the German and Danish methodology. In both methods it is seen as indirect intangible damage. The number of affected guest beds is

used in Germany. In Denmark the number of visitors for the 6 most important tourist places is used. There is a strong seasonal variance in the number of visitors.

Cars

Cars are seen as tangible in the Flemish and German methodology. In Langeoog (German case study in COMRisk) there are only a few electric cars and some commercial vehicles (firemen, ambulance, …). Valuation is based on expertise for them. In Flanders FEBIAC and Federauto (automotive sector) give data about the number of cars of a specific age and the average new price in a year. They also divide tables with prices for second hand cars over time. Combination of all these data gives a function to calculate the average price of a car. The number of cars is known per statistical sector but aggregated to community level (cars move a lot during the day, the week, the year). They are divided over all residential, industrial and infrastructure surfaces, not taken into account a density function (see further in paragraph Housing). Both German and Flemish methodology use a depth-damage function to calculate the damage. In Germany the maximum damage is 60% of the replacement value, in Flanders 100%. The Flemish methodology takes a evacuation factor into account of 70%, in Germany it is 80% (when replacement is possible, otherwise it is 0%).

In Denmark the average number of cars per household is calculated as 1,3. Division over surface is done in relationship to buildings (see further). There is an average value for cars available but it is hardly comparable with the values in other countries due to a specific taxing system. So cars are seen as direct intangible damage.

Agriculture

Agricultural areas are an important surface in landscape but their damage per surface unit is rather small. All methodologies take agricultural damage as direct and tangible. More details about the U.K. method for Lincolnshire are not available. Agriculture is not that important in the German case, because there are no crop fields. In the MERK methodology can be found how to deal with these damage for other study areas. For the occurring grasslands is only a maximum value available.

The Danish methodology starts from detailed cadastral maps grouped to homogeneous cultures. A maximum damage per surface is defined for different crops and grassland. In Flanders the methodology starts with dividing the area into zones based on agricultural areas and catchment borders. For every zone a detailed analysis is made of all occurring crops on the fields on a specific moment (wheat, vegetables, maize …). Grassland is taken out of the analysis. Based on the surface every crop has in the area, the average yield per surface and the average wholesaler's price and a maximum damage per surface is calculated. For salt water an extra damage value is added because of the need to spread chalk and because the yield will be lower in the next year too.

In the Danish methodology a time-damage function is created for every crop type and for every period of the year. The Flemish methodology works with a dept-damage relationship for fresh and salt water.

Table 4 Average damage to agriculture according to flood duration and time period (damage in DKK/ha) (COMRisk, Ribe case study)

| | Oct | Nov | Dec | Jan | Feb | Mar |
|---|---|---|---|---|---|---|
| 5 days | 170 | 232 | 425 | 557 | 775 | 1097 |
| 14 days | 303 | 411 | 595 | 823 | 1020 | 1337 |
| 28 days | 1013 | 1281 | 1617 | 1952 | 2120 | 3030 |

Livestock

Livestock is taken into account in the German and Danish methodology. Valuation in the Lincolnshire methodology is maybe done but not known. The Flemish methodology does not take into account death of livestock.

Both German and Danish methods use wholesaler's prices for the valuation. In the German methodology is worked with evacuation factors and fixed percentages for death, in the Danish methodology a threshold value for different species is used. If the water value is above the threshold the animal is considered to be death. The fact that animals die from stress is also taken into account in Denmark.

In the Danish methods the animals are placed in the farm of the owner, in the German case is worked with terrain controls and official statistics. It is not totally clear where the animals are placed exactly but it seems that they are coupled to their farm too. The Danish methodology also takes some extra direct and indirect damages into account. The most important ones are the productivity loss of the animals (e.g. the milk of cows that can be sold) is direct damage; loss of production capacity until the farm can use all capacity again is seen as indirect damage.

Forestry

Denmark and U.K. do not mention nature or forestry in their methodology. Flanders and Germany have a similar approach for this type of land use. Both assume no economical damage to nature as a consequence of water. German methodology adds hereby the assumption the forestry is not in use for wood production. For Flanders, this assumption does not pose, because of its low logging productivity.

Line elements

If one speaks of land use, one usually thinks of area classification types. However, line elements such as roads and railroads are also part of land use.

German methodology focuses on traffic line elements such as (rail)roads, cycle tracks and footpaths. Average construction costs are used for valuation. Moreover, cleaning and reparation is taken into account per $m^2$. An important remark is necessary here. Langeoog case is very specific concerning roads and railroads. The island (part of the East Frisian Islands) is carless (except for emergency services) and contains only one railroad track. Therefore, German researchers found it appropriate to enhance detail by taking the real area of roads and foot paths, rather than only length.

Danish researchers define road and railroad networks, using Ribe County (roads) and TOP10DK (railroads) as data layers. Valuation (DKK per km) is done for different types of roads such as path, secundary road 3-6 m, secundary road > 6 m and express road. Extra attention is given when breaching is the case (high flow velocities). Then, damage is calculated based on distance to breach: 100 m corresponds to a damage of 80%, 300 m to a damage of 10%.

Flanders fits to Danish method in that way vector data is used for defining roads and railroads, produced by the National Geographical Institute (NGI) of Belgium. Thereby, information was preserved concerning type (road for cars, bicycles or pedestrians) presence of banks, lane track number (number of traffic lanes), bridge category, median category (presence of central reserve), use of road and width. For railroads, additional information contains lane track number (number of rail tracks), railroad power source (electrified or not) and use. Valuation varies according to type and use of (rail)road and is expressed in euro/m.

Point elements

Besides line elements, point elements can be added if necessary. Thereby, the level of detail is determined by the importance of certain categories in total damage, and the availability and detail of existing land use maps.

In Flemish methodology, a comprehensive number of point elements is added, such as landscape and historical elements, emergency centers, churches and chapels, castles, windmills, musea, hospitals, fire and police stations, city halls, telecommunication antennas, schools, rest homes, prisons, train and bus stations, drinking water stations, electricity production etc. For every point element, a valuation is made based on a variety of sources.

In Denmark, the number of handled point elements is not that extensive. The main reason for this lies in the greater detail of land use data for buildings. In this way, most of the buildings mentioned above are taken as separate classes in building data layer, which belongs to surface data (not point data). However, one point element must be mentioned: electrical installation, which contains windmills and pomps.

Langeoog has only little facilities, so it is logical German methodology is also sparing with point elements. There are, however, point elements defined for drinking water stations and wind turbines (although the latter does not exist on Langeoog).

## 5.2 Influence of flow velocity on risk calculations

### Introduction

Damage and risk calculations as presented before are limited to inundations which are caused by overflow. The modifying damage factor was always water depth. However, overflow is not the only failure mechanism. In case of geotechnical failures, such as dike breaching, damage to buildings and/or constructions can be much larger in comparison to overflow. In the vicinity of the breach, high flow velocities can even cause total collapse of buildings. In general, one can assume that flow velocity will cause an additional damage on top of the present damage calculations.

Besides material damage, the number of casualties will also be higher in case of high flow velocities. This specific impact is subject of the following section.

An important boundary condition difference can be made between when using detailed 2-dimensional modelling and 1-dimensional hydraulic modelling :

- 2D-models provide hydrodynamic data in every cell of their structure (water depth, flow velocity...). These data allow defining areas where additional damage will occur as a consequence of high flow velocities;
- 1D-models don't posses this raster structure. The limited detail implies a conceptual approach for defining risky areas

In this section, a methodology is proposed for the calculation of additional damage because of high velocities. First a conceptual approach is given which is build upon a system of concentric circles. Secondly an approach for 2D-models is discussed. After that a specific case in damage calculation is discussed namely by extreme wave overtopping along sea dikes.

### Conceptual approach with concentric circles

Approach

Vrisou Van Eck (et al., 1999) defines the general relation between real damage and water depth:

$$S_w = \sum (\alpha * n_i * S_{\max})$$

With:

$S_w$ = real damage in an area

α = coefficient expressing the relation between damage and water depth (value between 0 and 1)

$n_i$ = number of entities (linear or surface)

$S_{max}$ = maximal or potential damage of a certain land use type

High flow velocities can lead to additional damage which has to be added to the real damage $S_w$. To avoid double counting, the maximal additional damage is calculated as follow:

$$S_{\max,b} = S_{\max} - S_w$$

With:

$S_{max,b}$ = maximal damage in case of breaching

The real additional damage in case of breaching $S_{w,b}$ is defined as a function of high flow velocities, which is determined by:

- distance to the breach: the closer to the breach, the higher the flow velocity will be. The velocity decreases rapidly with greater distances.
- resistance impact of certain land use types
- linear structures: these can realize a water-retaining function if higher than ground level (e.g. banks of roads en railroads)

To calculate the total damage in case of flooding, a simple sum is sufficient:

$$S_T = S_w + S_{w,b}$$

With:

$S_T$ = total real damage in case of flooding

As mentioned above, additional damage depends on the distance to the breach, discharge values and a resistance factor, which is subject to a certain land use type. These parameters (the impact of linear structures is added later on) are combined into one model, which consists of two concentric circles around the dike breach. These circles represent a certain damage caused by high flow velocities. The middle zone A comprises an area where damage is set to 100%. The flow rates are expected to be high enough to make buildings collapse. Therefore, the damage coefficient δ for zone A is set to 1. In the second - exterior - zone B, flow velocities are expected to be much lower, by which additional damage will be significantly less. The decline of the flow velocity is not only caused by the distance the water has travelled, but also by the resistance effects of land use types in zone A. Therefore, the damage coefficient δ contains a resistance coefficient $K_l$, which is multiplied by a constant value 0,5. This coefficient refers to the distance impact on flow velocity. A third zone C can be defined as the remaining area, outside circles A and B. In this zone, no additional damage is expected by flow velocities (Table ).

Now the zones are defined, the question raises which diameter to choose for circles A and B. Based on empirical data of several streams during multiple observations, following formula is derived:

For zone A: $r_A(m) = MIN\ (100\ ;\ MAX\ (\ 1\ ;\ 25\ *\ log\ Qmax)\ )$

For zone B: $r_B(m) = MIN\ (300\ ;\ MAX\ (\ 5\ ;\ 75\ *\ log\ Qmax)\ )$

Where Qmax the maximum measured discharge

Table 5 Radius and damage coefficient of zones A, B and C

| Zone | Radius (m) | Damage coefficient δ | Meaning |
|---|---|---|---|
| zone A | $r_A$ | 1 | high flow velocities cause maximal damage |
| zone B | $r_B$ | 0,5 * K | lower flow velocities cause less additional damage |
| zone C | --- | 0 | no additional damage |

Resistance coefficient $K_i$

The resistance coefficient $K_i$ has a value between 0 (full resistance) and 1 (no resistance) and is assigned to all land use types for the whole of Flanders. The categories of land use are taken from Vanneuville et al. (2006), which are based on a combination of CORINE Land Cover (CLC 2000) and Small Scale Land Use Map of Flanders and Brussels. The values were assigned on the basis of *expert judgment* in relation to similar resistance coefficients used in the hydraulic models.

It is of great importance to emphasize the fact that resistance coefficients are assigned only to land use categories of zone A. However, they have only impact on the damage coefficient of zone B. After all, the water flows through zone A to zone B. A weighted average of the different resistance coefficients leads to a total resistance coefficient $K_T$. Therefore, the surface of the different land use types is used:

$$\kappa_T = \frac{\sum_{i=1}^{n} A_i * \kappa_i}{\sum_{i=1}^{n} A_i}$$

With:

$K_T$ = total resistance coefficient

$A_i$ = surface of a land use type (in zone A)

$K_i$ = resistance coefficient for a certain land use type

The damage coefficient $\delta_B$ for zone B is thus defined as follow:

$$\delta_B = 0{,}5 * \frac{\sum_{i=1}^{n} A_i * \kappa_i}{\sum_{i=1}^{n} A_i}$$

Finally, the damage coefficient (either for zone A, which is equal to 1, or zone B) can be used to calculate the real additional damage in case of breaching.

$$S_{w,b} = \sum (\delta * n_i * S_{\max,b})$$

With

$S_{w,\,b}$ = real additional damage in case of breaching

$\delta$ = damage coefficient

$n_i$ = number of entities (linear or surface)

$S_{max,\,b}$ = maximal additional damage

Impact of banks

A special case is true when heightened linear structures intersect with zone A and/or zone B. These banks can be road banks, railroad banks, walls, embankments etc. The area behind these banks will be protected if they're not interrupted by passages. As a consequence, there will be no additional damage in the hinterland. The damage coefficient $\delta$ is thus set to zero. In case the banks are only partly in zone A or B, a "line of sight" is used to determine the protected zone.

Four distinct situations can be determined for a bank which intersects zone A or B completely or partially (Figure 18). Two situations need more explanation. Situation B shows a partially intersection through zone A. Let us assume the linear structure does not fail in zone A. A "line of sight" is drawn from the location of the breach to the end of the bank. In this case, the area behind the bank but within zone A is supposed to be insufficient "protected", so a damage factor of 1 is given. This is not the case for protected areas in zone B. There, a sufficient protection of the bank is supposed, which explains the damage factor of zero (Situation B and C in Figure 18).

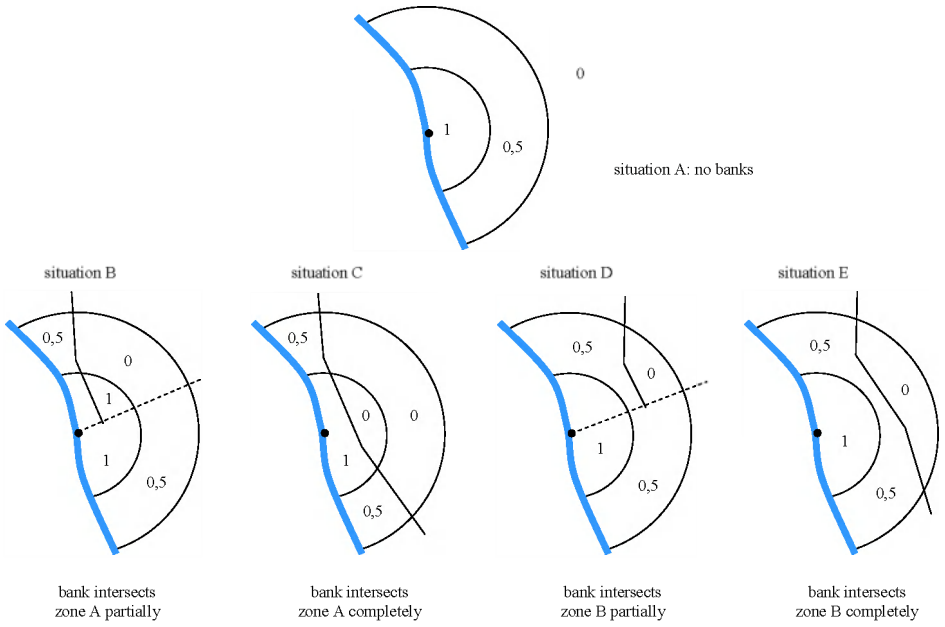


Figure 18 Partially or completely intersection of a bank in zone A or B, with indication of damage coefficient (abstraction is made of the resistance coefficient)

Banks can contain under-passes, culverts etc. If this is the case, one can speak of "artificial" breaches. The impact of these gaps is taken into account by assuming a damage function of 0,5 for the areas behind the banks (Situation C', D' and E' in Figure 19), unless the bank intersects zone A just partially. In that case, the damage function remains 1 (Situation B' in Figure 19).

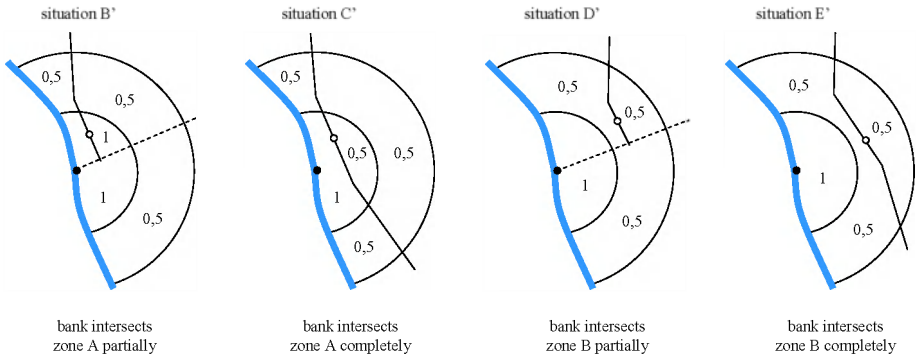


Figure 19 Impact of under-passes or culverts in heightened linear structures (location indicated by white bullets)

The vector database TOP50v-GIS, developed by the National Geographical Institute (NGI) of Belgium, contains geographical information which can be applied to map possible water-retaining structures in the inundated area. Table 6 gives an overview of these data layers.

Table 5 Overview of vector data layers developed by NGI, Belgium

| | | |
|---|---|---|
| **HYDRONET (hydrography)** | BNK (bank) | indicates the presence of parallel banks or levees at the left and/or right side of the road axis |
| | LEV (level) | level of the objects with respect to the ground level |
| **HYDROPNT** | HY26 | location of culverts |
| **RAILNET (railroad network)** | BNK (bank) | (analogous to BNK-Hydronet) |
| | LEV (level) | (analogous to LEV-Hydronet) |
| | BRC (Bridge Category) | indicates the type and location of a bridge |
| **ROADNET (road network)** | BNK (bank) | (analogous to BNK- Hydronet) |
| | LEV (level) | (analogous to LEV-Hydronet) |
| | BRC (Bridge Category) | (analogous to BRC-Hydronet) |
| **SCAPENET (linear structures of the landscape)** | LA1 | geographical relief (bank, embankment, steep, dune slope...) |
| | LA | artificial objects (wall, foundation...) |

The data layer "BNK" is described by a two character code, which indicates the heigthening of railroads, roads and waterways (levees). The structures are only interesting for the model if the heightening appears at both sides of the linear structure (Figure 20).

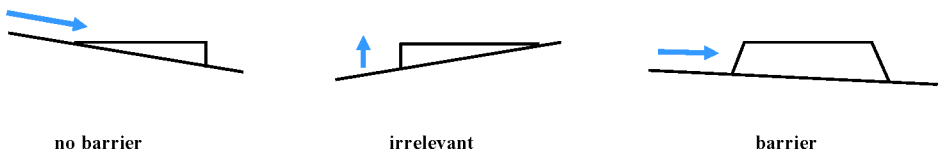


Figure 20 Heightening of linear elements: three possible situations (cross-section)

Besides "BNK" an interesting data layer is "LEV", which gives the height in cm with respect to the ground level. This layer can be used as an indication for the importance of the heightening.

Summary

Figure 21 gives a summary of the presented methodology.

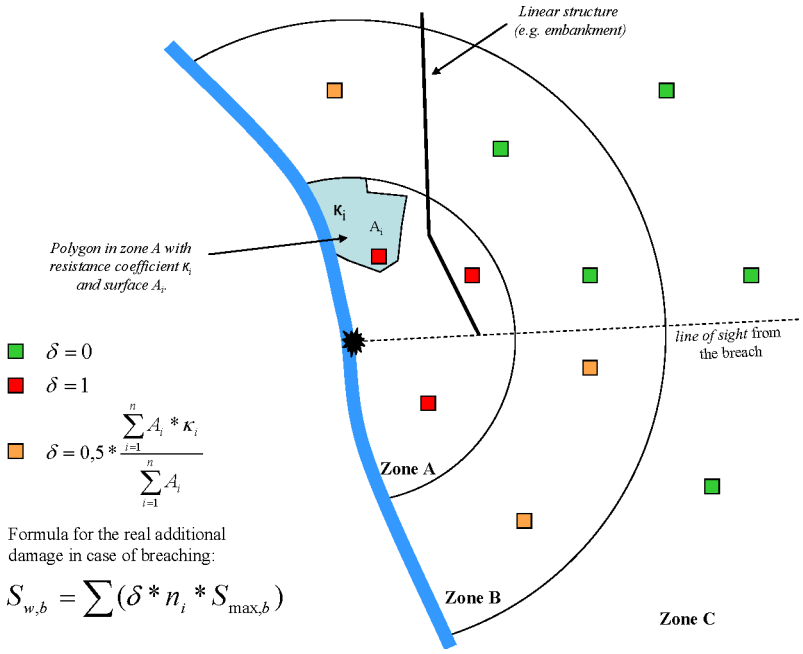


Figure 21 Summarizing figure: calculation of additional damage in case of breaching (1D modelling)

## Methodology for 2D modelling

### Approach

2D models are created with a very high level of detail and lots of hydrodynamic data, including water depth, vertical rise velocity and last but not least: flow velocity. In this section a damage function is proposed for the calculation of monetary damage which takes both water depth and high flow velocities into account (Figure 22).

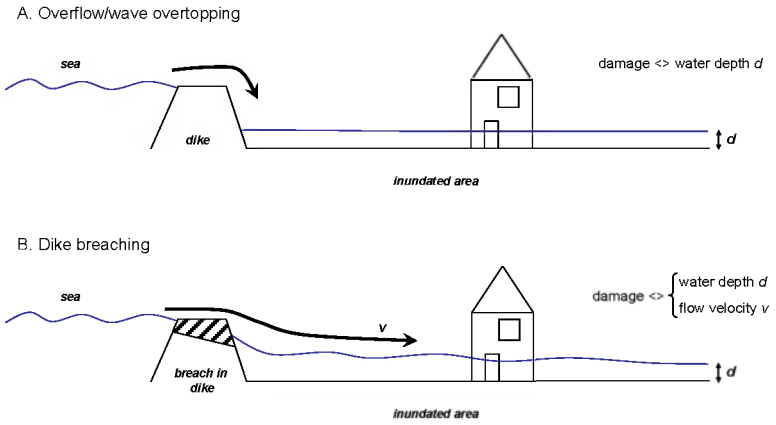


Figure 22 Schematic representation of damage factors in case of overflow/wave overtopping (A) and dike breaching (b)

Some publications give an indication of critical flow velocities. One of them is Vrisou van Eck et al. (1999) who proposes critical values of 7 m/s for concrete walls, and only 1 or 2 m/s for brickwork walls. Vrisou van Eck assumes a flow velocity of 3 m/s to be sufficient for maximal damage to structures (buildings). However, these flow velocities can only cause harm if they are accompanied by sufficient flow rates or water depths. Vrisou van Eck proposes a critical water depth of 0,5 m. It is important not to confuse this denotation of water depth (thus, in combination with flow velocity) and the denotation used by Vanneuville et al. (2002 and 2006), where water depth is the only damage factor (see Chapter 2).

In case of dike breaching, the maximal damage coefficient ß, caused by flow velocities can be defined as follow:

$$ß = 1 \quad \text{if} \quad v > 3 \text{ m/s} \quad \underline{\text{and}} \quad d \geq 0{,}5 \text{ m}$$

With:

ß = damage factor

d = water depth (m)

v = flow velocity (m/s)

This formula is a criterion, which means the condition is either true or false. To make this criterion more realistic, a continue function can be made based on the critical values given by Vrisou van Eck. Therefore, two new damage factors are defined: $ß_v$ for flow velocity, $ß_d$ for water depth. The total damage coefficient ß will be equal to the product of these two damage factors.

Analogous to the calculation method from Chapter 5.2 (section 1), the damage coefficient ß is used with a residual damage, i.e. maximal additional damage after the

damage calculation according to water depth (Chapter 2). This is done to eliminate a double counting of damage.

Damage functions

As mentioned above, damage factors $\beta_v$ and $\beta_d$ are defined as continuous functions. The shape of the function is chosen to be exponential:

- little damage will occur if water depth and flow velocity are low;
- damage will increase dramatically if one or both components increase, until the damage is maximal (damage coefficient = 1)

Figure 23 and Figure 24 represent an exponential course for both components. The formulae are constructed in that way they reach a maximal damage value with $\beta_d$ = 0,5 m and $\beta_v$ = 3,0 m/s:

$$\beta_d = \frac{\exp(3{,}6.d) - 1}{5} \qquad \text{with} \qquad \beta_d = 1 \quad \text{if} \quad d \geq 0{,}5$$

$$\beta_v = \frac{\exp(0{,}6.v) - 1}{5} \qquad \text{with} \qquad \beta_v = 1 \quad \text{if} \quad v \geq 3{,}0$$

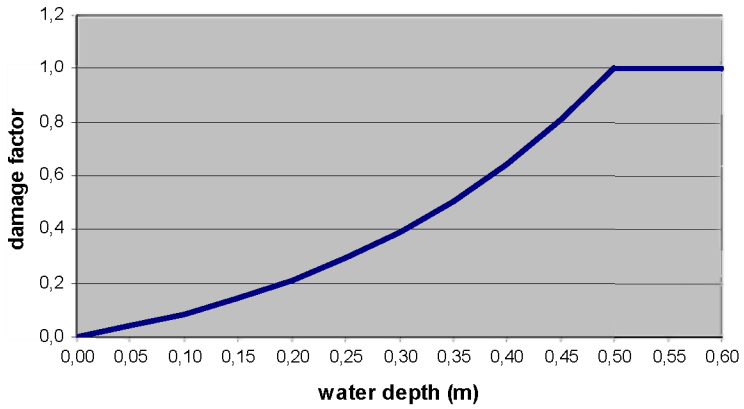


Figure 23 Damage function for water depth (m)

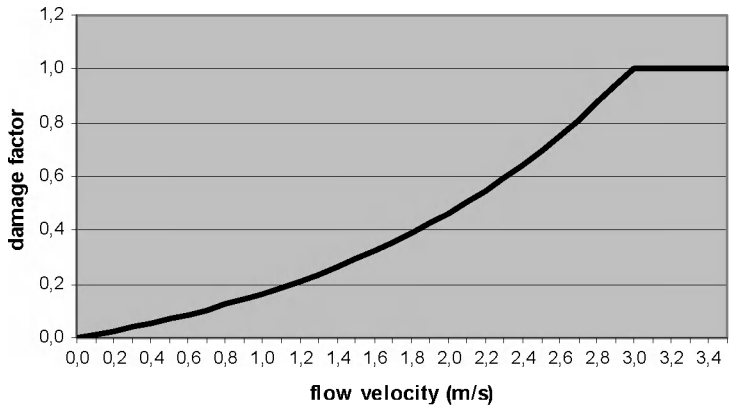


Figure 24 Damage function for flow velocity (m/s)

The multiplication of both components gives damage factor ß:

$$\beta = \beta_v . \beta_d$$

A relation between water depth, flow velocity and a percentage of additional damage (damage factor ß) is given in Figure 25.

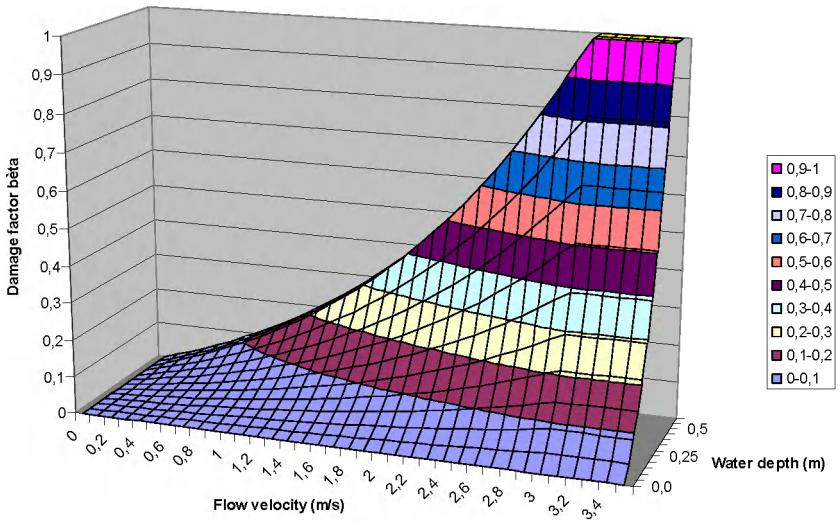


Figure 25 Relation water depth, flow velocity and percentage of additional damage (damage factor ß)

**Wave overtopping**

Approach

In this section a method is proposed for the calculation of damage along the embankments of the sea coast, where the effects of wave overtopping are very important. In this case, abstraction is made of breach growth.

The methodology has an analogous course to the damage calculations in case of breaching, as mentioned in the previous section. However, the critical values of Vrisou van Eck aren't completely usable in this situation. Her method was designed for breaching of dikes, where water depth and flow velocity are important parameters for damage calculation. In case of wave overtopping, it is possible that (very) high flow velocities cause damage, even with a rather low water depth. This explains why the latter isn't taken into account in the calculations for wave overtopping. The critical values for flow velocity are preserved, so the damage factor α is defined as follow:

α = 1 if v > 3 m/s

With:

α = damage factor

v = flow velocity (m/s)

Or, translated into a continuous function (see previous section):

$$\alpha = \frac{\exp(0{,}6.v) - 1}{5} \qquad \text{with} \quad \alpha = 1 \quad \text{if} \quad v \geq 3{,}0$$

The input for this function is given by the formula of Schüttrumpf, which calculates the maximal wave overtopping velocity across the dike. It is assumed that these values remain constant until they reach the first line of buildings. The damage factor $\alpha$ defines the procentual damage to these buildings (and other land use). Therefore, a buffer distance is used in a GIS, which defines a risk zone of 40 m inland[2], starting from the first housing blocks along the coast (Figure 26).

[2] Distance of 40 m is based on expert judgement

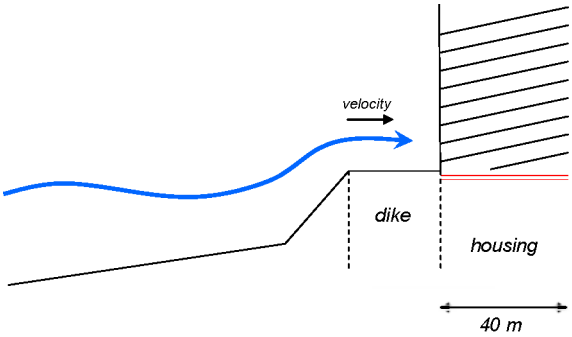


Figure 26 Schematic representation of the 40 m risk zone inland (red)

In case of breaching, maximal damage is assumed also in a buffer zone of 40 m inland.

## 5.3 Casualty calculations

### Introduction

In the previous section, all attention was given to material damage caused by floods. Unfortunately, floods can cause also numerous victims. As such, a methodology is necessary to estimate the number of casualties and to determine areas of risk for persons. In this section, a method is presented which takes into account water depth, rise velocity, flow velocity, and (conceptually) evacuation.

Casualties are defined as mortal victims (no injured persons). It has to be emphasized no monetary value is given to people. Casualty risk is defined as the number of mortal victims per square meter. As a result, a risk map of casualties can't be combined mathematically with a risk map of material damage. Because of this, the effects of land use adaptations (e.g. installation of water retaining infrastructure) to damage and casualties can be studied separately.

### General approach

The calculation method for casualty risks is largely analogous to the one for material damage. The maximum number of victims (expressed per square meter) is defined as the total number of inhabitants in the inundated area.

According to Vrisou van Eck (1999, p. 5-1, 5-3), the number of casualties N for a given flood is influenced by:

- number of inhabitants per square meter ($m^2$), represented by $A$
- drowning factor as a function of water depth (m), represented by $f_d$
- drowning factor as a function of rise velocity (m/hour), represented by $f_w$

Or, mathematically:

$$N = f_d * f_w * A$$

Notice the absence of water velocity in this formula. In case of dike breaching, one can assume the number of casualties being higher as a consequence of high flow velocity. In section 5.2, attention is given to this parameter as well as water depth and rise velocity.

Evacuation can, if well organised and executed, reduce the number of casualties significantly. As such, the number of people that are affected by flooding are only a percentage of the total number of inhabitants. This percentage is represented by an evacuation factor, which is discussed in section 5.2 at the end of this chapter.

$$A = f_e * I$$

With:

$A$ = number of remaining people per square meter (after evacuation)

$f_e$ = evacuation factor

$I$ = number of inhabitants per square meter

**Drowning factors**

Drowning factor water depth

Vrisou van Eck (1999, p. 5-1) defines a drowning factor water $f_d$ depth as follows:

$$f_d = e^{(1{,}16d - 7{,}3)} \quad \text{and} \quad f_d \leq 1$$

With:

$d$ = water depth (m)

The exponential course of the function is represented in Figure 27.

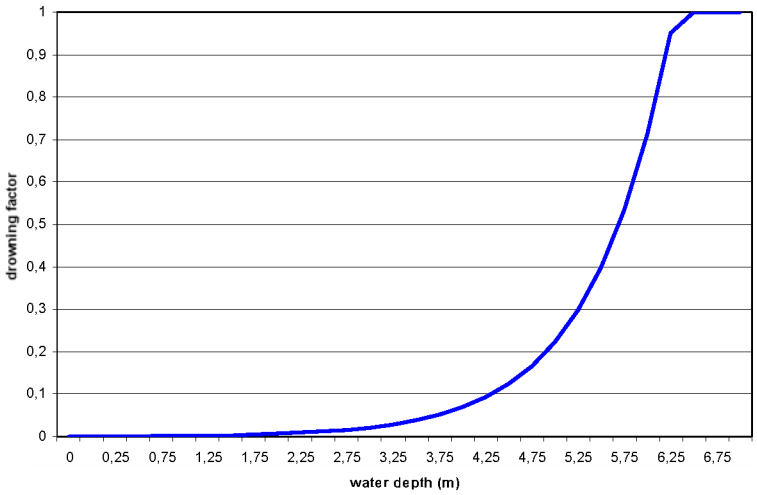


Figure 27 Drowning factor water depth

Drowning factor rise velocity

Vrisou van Eck (1999, p. 5-3) determines a linear course for drowning factor rise velocity (Figure 28). For a rise velocity of less than 0,3 m/hour, none casualties are expected. In case the rise velocity exceeds 3 m/hour, the drowning factor $f_w$ is set to 1. Thus:

| | | |
|---|---|---|
| $f_w = 0$ | voor | $w \leq 0{,}3$ |
| $f_w = 0{,}37 * w - 0{,}11$ | voor | $0{,}3 < w < 3{,}0$ |
| $f_w = 1$ | voor | $w \geq 3{,}0$ |

With:

w = rise velocity in m/hour

The availability of rise velocity values differ for 1D- and 2D-modelling. In case of 1D-modelling, a technique has been worked out using *flood branches*. These branches are built up with several points, which contain information on water depth for a specific time interval. As such, the maximal rise velocity per hour can be derived.

For 2D-models, rise velocity is provided together with other data (water depth, flow velocity). These grids can be immediately used in the risk calculation.

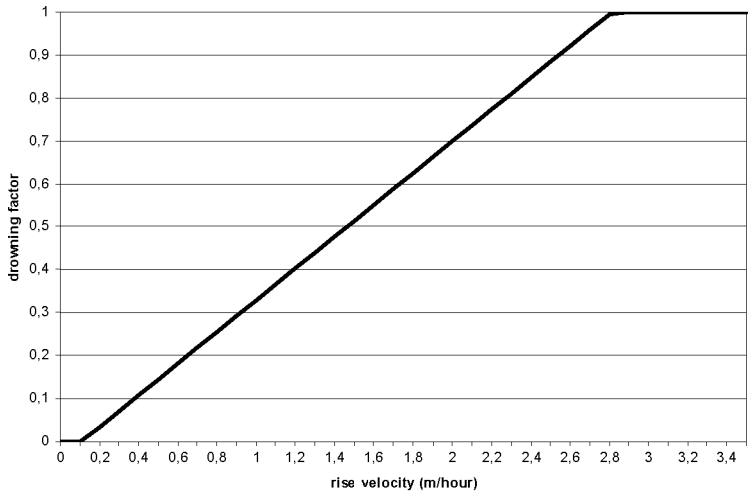


Figure 28 Drowning factor rise velocity

Drowning factor flow velocity

Besides water depth and rise velocity, a third factor can influence the number of fatalities, certainly when breaching is the case. This factor is flow velocity. In 1989, Abt (et al., in Jonkman, 2007) did as one of the first experimental study on human (in)stability in flowing water. Based on empirical data, he estimated the value of the critical product (between water depth and flow velocity) as a function of the subject's height (L -[m]) and mass (m - [kg]):

$$d.v = 0{,}0929(e^{0.001906Lm+1.09})^2$$

For heights between 1,5 m and 2 m and masses between 50 kg and 100 kg, the product has a range between 1 and 2 $m^2/s$. However, the formula may only be applied to healthy adults. For children and elderly people, the limit value for instability will be much lower. As information on height and mass of humans is not available in detail, one limit value has to be introduced for everyone. Besides, instability doesn't necessarily leads to death. If conditions are well (not too cold water temperature, little debris...), (healthy) people can float or swim for a while. Therefore, the actual drowning factor should be taken higher.

Let us assume an average person with a height of 1,8 m and a mass of 75 kg. Using the formula given, the product *d.v* is 1,37 $m^2/s$. This value is just slightly lower than the criterion product for building collapse, proposed by Vrisou Van Eck (1999), which was discussed in Chapter 5.2:

if d > 0,5 m and v > 3 m/s (= 1,5 $m^2/s$) then: damage factor = 100 %

Thus, the value of 1,5 $m^2/s$ has a double meaning. First, it is slightly higher than an average instability limit, taking into account the difference between instability and drowning. Second, 1,5 $m^2/s$ is set as the minimum value for buildings to collapse. If this is fulfilled, one may assume that all inhabitants, if not evacuated, die. So, the limit values of Vrisou Van Eck can be translated as follow:

if d > 0,5 m and v > 3 m/s (= 1,5 $m^2$/s) then: number of casualties = 100 %

One should notice that this criterion is unrelated to other functions for water depth and rise velocity. Therefore, this criterion is called “disjunct”, which means it can never be applied together with the other factors (it is either true or not) (Jonkman, 2004).

A special case can be distinguished along the coast, where people are exposed to wave overtopping on promenade dikes. Here, no breaching is assumed. In literature, critical values are proposed for overtopping discharges (Van der Meer in Verhaeghe, 2002).

Allsop (2005) defines following limiting values for pedestrians (in l/m/s):

| | |
|---|---|
| Q < 0,003 | pedestrian experiences no trouble |
| 0,003 < Q < 0,03 | bothersome, but no danger |
| 0,03 < Q | dangerous |

Despite the fact that this criterion is based on quantitative data, the expression of risk is still qualitative. After all, what is dangerous? Is dangerous synonymous for fatal? Notwithstanding this fundamental problem, one can translate the given values to damage factors using a logarithmic function (Swillens, 2002) (Table 7) and put into a graph (Figure 29). An average value (black line in Figure 29) is calculated for practical use in the risk model.

Table 7 Critical overtopping discharges for pedestrians
(based on Verhaeghe, 2002; Allsop, 2005)

| | Damage factor | Lower limit discharge (l/m/s) | Upper limit discharge (l/m/s) |
|---|---|---|---|
| no danger | 0 | / | 0,003 |
| little danger | 0,5 | 0,003 | 0,03 |
| danger | 1 | 0,03 | / |

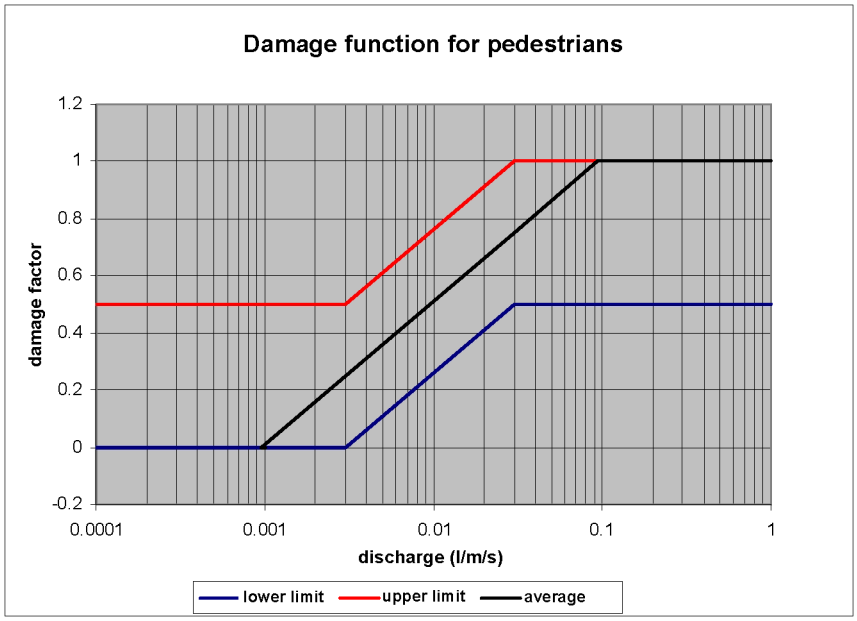


Figure 29 Damage factor for pedestrians caused by overtopping discharges (with uncertainty band)

Mathematically, these criterions can be defined as follow (l/m/s):

$f(q) = 0$ if $q \leq 9{,}47.10^{-4}$

$f(q) = 0{,}2171.\ln(q) + 1{,}5114$ if $9{,}47.10^{-4} \leq q \leq 0{,}095$

$f(q) = 1$ if $0{,}095 \leq q$

The use of this function however is very doubtful as explained before. One can assume that most people will seek shelter in their houses, or evacuate to more safe areas.

**Evacuation**

Until now, impacts of evacuation were not taken into account in the risk methodology. Only for cars a fixed evacuation coefficient of 70 % was assumed. Obviously, there is need for an area dependent variable.

If people are warned hours before the storm surge peaks (moment of inundation), it is likely that most of them will leave the area of risk. One could say people have a certain time period in which they can participate to evacuation procedures. This is called *available time*. However, the available time must be equal or larger than the required time, which is the time period necessary for a safe evacuation. The latter is dependent to the size of the inundation, the population density of the area, the facilities of the traffic network and the coordination and organization of the evacuation.

In this study, evacuation is defined as the procedures initiated by the government to bring people in safety, *before* the inundation takes place. People, who are saved during the inundation (rescue operations) or bring themselves in safety (escaping), are not taken into account.

Much research has been done on evacuation models and -factors, but the presented factors are rarely quantified. On the one hand, there is a shortcoming of available data for calibrating the models. On the other hand, evacuation is subject to a great numbers of complex factors which influence each other in multiple ways. Four factors are seen as important for a basic implementation of evacuation in the risk methodology: available and required time for evacuation, the traffic network and the population density.

Available time / required time

As mentioned above, the available time gives an indication of the available time period for evacuation, starting from the first warning sign and ending at the moment of the actual inundation. If this time period is less than the required time, a certain amount of people will still be present in the risk area at the moment of inundation.

Assume a sigmoidal course for evacuation, starting at the moment of warning (Figure 30). Initially, only few will evacuate. People need time to realize and recognize what's going on , and they need also time for preparing the evacuation. Obviously, the duration of these actions will differ from person to person.

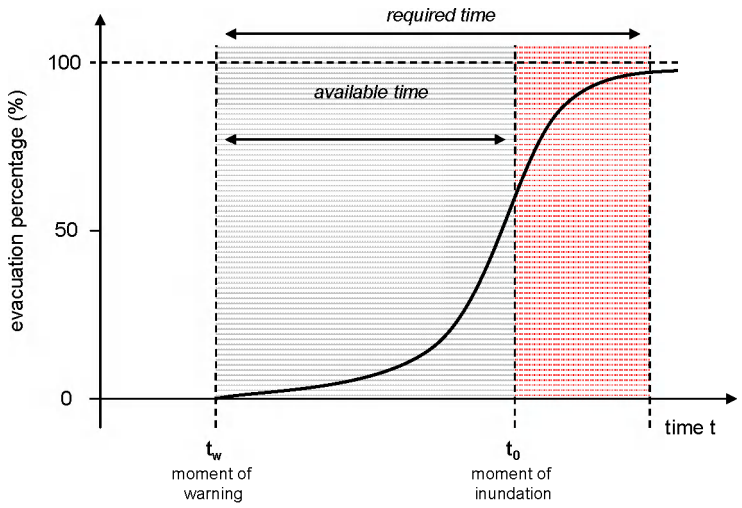


Figure 30 Available time / required time: evacuation curve

For example, the realization and recognizing of a possible inundation will happen quicker for people who experienced such hazards earlier. Likewise, the preparation for evacuation will take less time for persons who are familiar with evacuation procedures. Besides personal factors, the required time is influenced by multiple external factors (Sanders et al., 2004):

- number of cars available: too less causes problems, too many also (traffic jams);

- the amount of goods people want to take with them;
- people at work, children at school… the more people outside of the house, the more difficult it will be to gather everyone.

After a while, more people will evacuate in a short time, which is reflected in the evacuation curve by a steep slope (Figure 30). From then on, the curve turns off to just less than 100 %. The gap is clear: not everyone will evacuate. It is reasonable to think that some people refuse to evacuate because of economic considerations and/or denial of threat refuse. It's also possible they haven't received a warning at all (Jonkman en Cappendijk, 2006).

Figure 30 indicates the inundation by a red zone in time. The evacuation process stops at this moment. In this case, this means only 60 % of the people has left the area of risk. 40 % stays behind. During the inundation, more people can escape or being rescued, but initially, they are exposed to water.

It's not obvious to estimate the available time for a given type of inundation. This is even harder for estimating the required time. However, Kolen and Geerts (2006) give an overview of the available time, estimated for several failure mechanisms along the North Sea. A 5 %, 50 % and 95 % change of appearance is given (Table 8).

Table 8 Indicative values for available time (in hours) for flooding from the North Sea (source: Kolen en Geerts, 2006)

| Failure mechanism | 5% | 50% | 95% |
|---|---|---|---|
| overtopping/overflow | 10 | 15 | 58 |
| piping | 16 | 21 | 33 |
| sliding | 20 | 33 | 59 |
| erosion dike body | 32 | 46 | 60 |
| piping (big infrastructure) | 10 | 21 | 36 |
| piping (small infrastructure) | 9 | 15 | 26 |
| malfunction of infrastructure | 12 | 21 | 58 |
| dune erosion | 19 | 25 | 31 |

As mentioned earlier, the required time is suspect to multiple factors which influence each other in a complex and repeating way. In the next section, two important factors are discussed: traffic network and population density.

Traffic network / population density

One may assume a well accessible area be better suited for evacuation compared to an area with very little transport possibilities. To determine the quality of the road

network in a certain area, a "scoring" is proposed. The many different types of roads are classified into a limited number of classes. Therefore, two road classifications can be used: either the road code given by the National Geographical Institute of Belgium (NGI) or the Functional Road Classification (FRC) used in MultiNet[3] by Tele Atlas Belgium. Both classification methods are more or less the same and can be linked to each other. The scoring system gives the highest scores to the roads with the highest capacity. Small roads and country paths are given the lowest scores.

These scores possess no absolute meaning, and may therefore only be used for comparison between different areas. The size of these areas can be chosen: either the level of the municipality, or the level of statistical sector. The latter is preferred for its greater level of detail.

A second factor is population density, which, in combination with traffic network, can be used as an indicator for traffic intensity. Therefore the different scores for roads of a certain statistical sector can be added and then divided with the population density (per $m^2$). This gives again a relative value which now takes into account the accessibility of a sector in combination with the number of inhabitants. In this way evacuation has become an area dependent variable.

[3] vector, version 2006.07 (AGIV-product), owner: Tele Atlas Data Gent

# 6. Case study

## 6.1 Study area and models

### Introduction

The case study 'Vlaanderen/Zeeuws-Vlaanderen' was an important outcome of COMRisk (IMDC, 2005-b). This COMRisk case study is further elaborated on in this study, namely considering the hydraulic modelling part together with damage and casualties calculations was further elaborated. Besides a sensitivity analysis, also an uncertainty analysis is performed, both using the methodological improvements as described in previous chapters.

### Study area

The COMRisk study area contained the Flemish and Dutch coastal flood plain between Zeebrugge and Breskens. Here, for practical reasons (limiting computation time, storage capacity, data availability for damage calculations, …) the study area was limited to the Flemish part only. Given the fact that failure of the Flemish coastal defence can result in flooding in the Netherlands, an area east of the Dutch-Flemish border was retained to the study area. Figure 31 shows the adjusted study area.


Figure 31: Study area (source: mappy.com)

### Software

Hydraulic calculations were executed using the most recent commercially available version of MIKE FLOOD (DHI, 2007). MIKE FLOOD is a dynamically linked one-dimensional and two-dimensional flood modelling package. This software allows to model some areas in 2D detail (flooding of the coastal plain), while other areas can be modeled in 1D (breach growth and the flow through the breach).

### 1D breach model

Breach locations and time of occurrence of the breaches were adopted from the COMRisk case study. Breaches in the Dutch part were not accounted for. In total, the maximum number of breaches reduces thereby from 18 to 8.

Figure 32 shows the location and Tabel 9 mentions the time of breaching. Breach growth is described by time series for crest level and breach width. The initial breach depth is set to zero for all breaches. The lowest crest level equals 6, 5 and 4 m AD, respectively for breaches at Knokke (233-236), at Het Zoute (241-243) and at the Zwindijk. Growth in depth takes place in less then 15 minutes for those breaches at Knokke, while it takes slightly more then 1 hour at Het Zoute and Zwindijk. Initial width is set at 90, 60 and 20 m, respectively at Knokke, Het Zoute and Zwindijk. Breaches at Knokke do not show any growth in depth, while for those at Het Zoute and Zwindijk a growth rate of 120 m/h is chosen. Maximum width at Het Zoute equals 150 m. The maximum width of the breach at Zwindijk is 300 m.

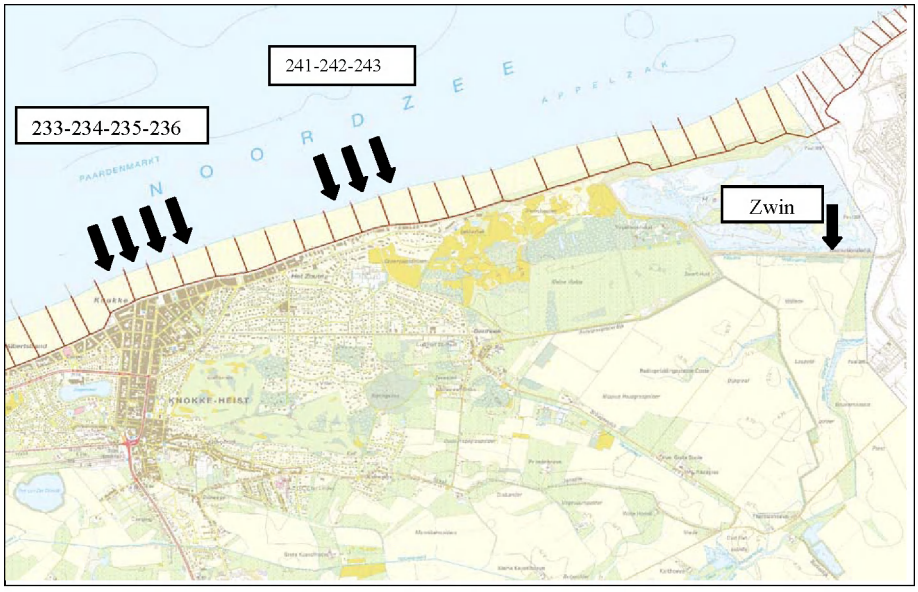


Figure 32: Breach locations

Table 9: Time of breaching

| Breach | T = 4000 years | T = 10000 years | T = 40000 years |
|---|---|---|---|
| 233 | high tide 2 + 1 hour | high tide 2 + 1 hour | high tide 1 + 1 hour |
| 234 | - | high tide 2 | high tide 2 |
| 235 | - | high tide 2 + 1 hour | high tide 2 + 1 hour |
| 236 | - | high tide 2 + 1 hour | high tide 2 + 1 hour |
| 241 | - | high tide 2 | high tide 2 |
| 242 | high tide 2 | high tide 2 | high tide 1 |
| 243 | high tide 2 | high tide 2 | high tide 1 |
| Zwin | - | - | high tide 2 |

**2D flood model**

The 2D flood model is based on the elevation model used in the COMRisk case study (file "dtm_ZV_VL_TOT_DIJKEN_200min_COR-40000j-zee15m-95.dfs2"). Figure 33 shows the adjusted elevation model, where the 700 most eastern situated columns were deleted and the southern border was set inactive.

The exact source and procedure of the elevation data showed in Figure 33 is not known. More over, the resulting elevation model contains some rather unrealistic pits (e.g. at the centre of Knokke) and flat plains (e.g. at Het Zoute). It is clear that (secondary) dike structures were appended based on terrestrial measurements. Figure 33 also shows a number of dikes (Leopold canal, canal Damme-Sluis, Zwin, …), but others (e.g. old Zwin dikes more south) are not taken into account.

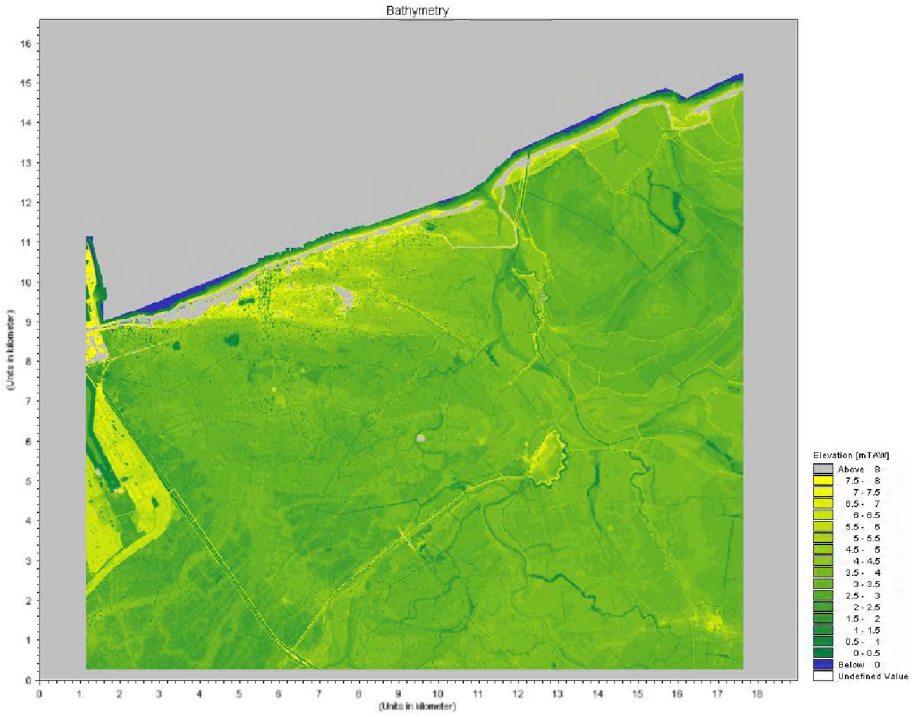


Figure 33: Elevation model

The coastal plan contains a range of land use types. Within COMRisk land use was not explicitly taken into account. Here, in the Flemish part, Corine Land Cover 2000 was used to derive the land use. Table 10 sums up the applied land use classes. For the Dutch part no detailed information regarding the land use was available. Based on airborne data agriculture was assumed to be the dominant land use. Figure 34 shows the spatial distribution of the different land use classes.

Table 10: Land use classes

| Land use | Class |
|---|---|
| Urban | 1 |
| Industry/infrastructure | 2 |
| Recreation | 3 |
| Agriculture | 4 |
| Forest | 5 |
| Nature | 6 |
| Beach/dune | 7 |
| Aquatic nature | 8 |
| Water | 9 |

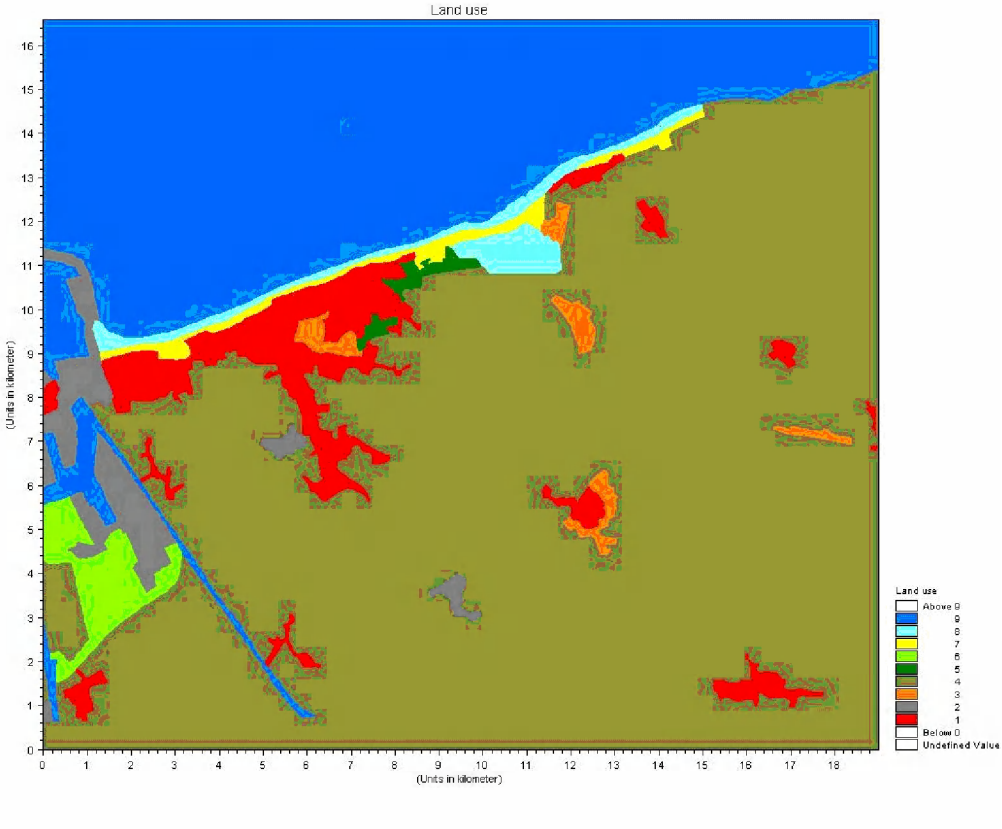


Figure 34: Land use

### Coupling 1D and 2D models

The 1D breach model and the 2D flood model are combined near the breach locations. This connection is realized at the landward side of the see defence. Each breach in MIKE 11 is linked to 1 or more grid cells of MIKE 21. The number and locations of associated grid cells is to be specified by the user.

In theory, when a breach is growing in width, the number of associated grid cells should increase. However, during simulation the number of grid cells cannot be changed within MIKE FLOOD. Based on some exploring simulations, it was concluded that a decrease in the number of associated cells could lead to a decrease of the flow through the breach. So the most conservative approach would be to choose the number of grid cells based on the maximum width of the breach (cfr. COMRisk).

On the other hand, when a breach is growing in depth, the associated grid cells should be situated lower as well, which in practice means more landward. Again, it is not possible within MIKE FLOOD to change the location of the associated grid cells during simulation. In addition, associated grid cells of which the elevation exceeds the crest level of the breach tend to cause numerical instabilities and lead to physical unrealistic behaviour. As a consequence, it was chosen to link 1D and 2D elements at locations where the elevations corresponds to the minimal crest level of the breach. This was not always the case within COMRisk.

Furthermore to overcome some remaining numerical issues, some of the (COMRisk) links were relocated over a short distance. The number of associated grid cells was kept. Finally, some numerical parameters were adjusted (eg. exponential smoothing).

### Boundary conditions

The hydraulic boundary conditions were adopted from COMRisk. Figure 35 shows the applied storm events. A symmetrical tidal event with duration of 45 hours together with a 1000-year storm surge of again 45 hours was used. For higher return periods, it is assumed that the central part of longer lasting storm surges was superimposed on the 45 hour lasting tidal event.

Since there were no breaches for the 1000-year event, only the following storm events were studies, eg. the 4000-, 10000- and 40000-year events.

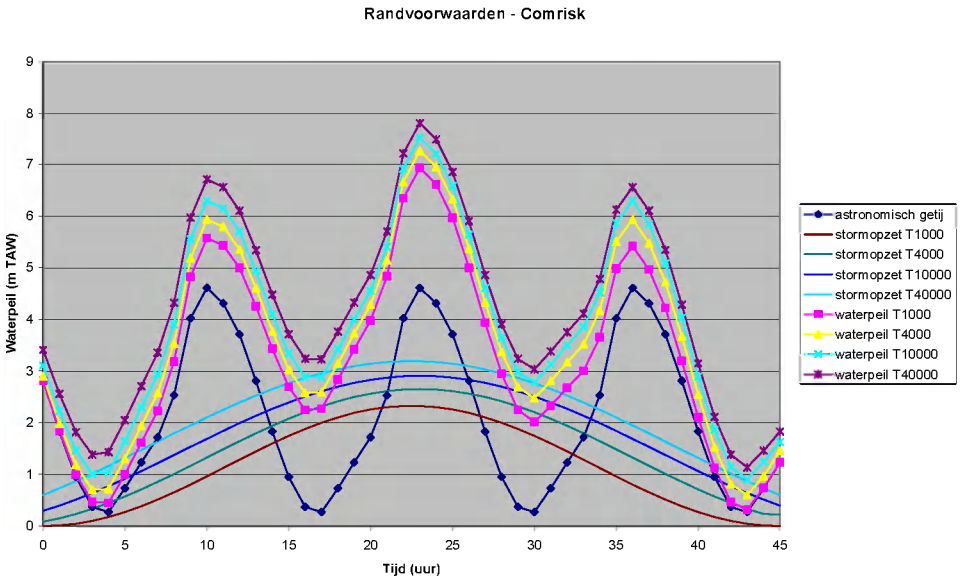


Figure 35: Water level and storm surge (Source: COMRisk)

## 6.2 Sensitivity analysis hydraulic model

**Procedure**

The model as described in the previous chapter is considered as a reference model. The impact of several factors (model parameters, model options, boundary conditions, …) was examined by altering one factor at a time, and comparing the results of the altered model to those of the reference model.

The examined factors can be divided in 4 groups:

- Parameters and options of the 1D breach model (Mike11)
- Parameters and options of the 2D flood model (Mike21)
- Parameters and options of the coupled models (MikeFlood)
- Boundary conditions

**1D breach model**

*Time of breaching*

The time of breaching is obtained from a number of preliminary calculations which are subject to considerable uncertainties (cfr. 6.4). The impact of time of breaching was estimated by means of two additional simulations: one in which time of breaching was set 30 minutes earlier and one in which it was set 30 minutes later.

*Horizontal growth rate*

In the COMRisk study the horizontal breach growth rate was described by means of time series. According to the reports the horizontal growth rate was estimated at 30 meter per hour. However, in the models a very high growth rate of 120 meter per hour was implemented. In order to evaluate the impact of hereof, a simulation with a

growth rate of 30 meter per hour was run. The maximum breach dimensions were not modified, but the time required to attain these dimensions has increased.

*Vertical growth rate*

In the COMRisk study the vertical breach growth rate was also described by means of time series. The duration of the vertical growth ranges from a few minutes to slightly over one hour, depending on the depth of the breach. Values reported in literature (e.g. Zwin experiment '94) suggest that vertical growth could be even faster. In order to evaluate the importance of the vertical growth a simulation was run in which the vertical growth rate was doubled. The lowest breach bottom level was not modified.

*Growth by erosion*

In Mike11 breach growth can also be obtained from erosion calculations. The user has to specify initial and final breach dimensions, but the model itself will calculate the growth rate from the Engelund-Hansen sediment transport equation.

Growth by erosion potentially offers two advantages: (1) growth rate can depend on dike properties and (2) growth rate varies as a function of flow through the breach. The first advantage can only be used when the dike material properties (grain size, porosity, critical shear stress for erosion) are known. In reality, this is rarely the case. The second advantage is more important. When breach growth is slow, the possibility exists that flow through the breach may be temporarily interrupted in between two tidal cycles, while breach dimensions have not reached their maximum yet. When constructing time series, this phenomenon is difficult to incorporate in advance and often growth is allowed to continue linearly, even though the flow through the breach temporarily ceases. When using growth by erosion, growth rates will be automatically adjusted to the changing boundary condition and this problem does not present itself.

The parameters of the erosion based breach growth model were calibrated by comparison to the Verheij-vanderKnaap equation. For details reference is made to section 4.1.

Two simulations were run. In both simulations initial depth was set at 0,2 m and initial width and maximum depth were copied from the COMRisk study. The maximum width is computed by the model itself. In the first simulation, the (COMRisk) assumption was made that the buildings located on the dike at Knokke do not collapse making horizontal growth impossible for the breaches at Knokke. In the second simulation, horizontal growth was allowed for the breaches at Knokke too.

*Breach flow equations*

In Mike11, flow through a breach is computed by means of general equations for flow through a structure. As an alternative, breach flow can also be computed by means of the equations used in the National Weather Service's DAMBRK model.

In the COMRisk study, the standard equations were used. For comparison purposes, a simulation was run using the NWS DAMBRK equations. The time series specifying the breach dimensions were not modified.

**2D flood model**

*Roughness*

Surface roughness is a typical calibration factor. In the absence of data for calibration, literature values need to be used. Mike11 offers the possibility to use a constant or spatially distributed surface roughness.

In the COMRisk study, a uniform roughness was assigned to the entire model area. The average value (1/Manning = Strickler = 32) corresponds to Mike21's default value. In addition, the impact of a higher (Strickler coefficient = 20) and a lower (Strickler coefficient = 40) roughness were examined. The hydraulic impact of these changes was described by means of limnigraphs at a limited number of locations. In order to allow for a comparison to other factors, these two variants were repeated.

Mike21's default value is a typical value for a sea bottom. The average roughness of a land surface is probably higher than the average roughness of a sea bottom. In addition, the surface roughness varies as a function of land use. An additional simulation was run, in which different roughness values were assigned to a number of land use classes. These values are listed in Table 11.

Table 11: Roughness coefficients

| Land use | Roughness coefficient (Strickler) |
|---|---|
| Urban | 10 |
| Industry/infrastructure | 15 |
| Recreation | 20 |
| Agriculture | 25 |
| Forest | 10 |
| Nature | 30 |
| Beach/dune | 30 |
| Aquatic nature | 30 |
| Water | 35 |

*Eddy viscosity*

Eddy viscosity is a second important calibration parameter. In the absence of data for calibration, literature values need to be used once again.

Mike21 offers the possibility to use a variable eddy viscosity. The variable form is based on the Smagorinsky formulation. The use of this formulation can cause numerical problems when sections of a model repeatedly flood and dry. A test using the Smagorinsky formulation did indeed suffer from numerical problems. Therefore, the use of a constant eddy viscosity is necessary.

In the COMRisk study, a turbulent viscosity was set to 1,1 $m^2/s$. This value was justified as "the value for water at a temperature of 15 °C".

In literature, a number of rules of thumb for estimating eddy viscosity can be found. Application of these rules of thumb to the study area results in values ranging from 0,2 to 4 $m^2/s$. Please note that these rules of thumb are probably derived from marine experience and may not apply to overland flow. In order to evaluate the impact of eddy viscosity, simulations with a low (0,1 $m^2/s$) and a high (10 $m^2/s$) were run.

In Mike21 the turbulent viscosity term in the momentum equation can be formulated in two ways: one based on velocities and one based on fluxes. The former is more accurate, but the latter offers better numerical stability. The reference simulation was based on the velocity formulation (Mike21 default), but the flux formulation was tested too.

*Coriolis force*

Mike21 is originally a model for marine applications. Therefore, its default settings automatically activate Coriolis forces. The user has the possibility to deactivate this force.

In the COMRisk study, Coriolis forces were applied. For overland flow, the influence of this force is probably very limited. In order to test this hypothesis, a simulation without Coriolis forces was run.

*Flooding and drying parameters*

Mike21 uses two parameters to determine if a section of the elevation model is dry or wet: the flooding depth determines when a dry cell will flood and the drying depth determines when a wet cell will dry out. For marine and estuarine applications, values of 0,2 and 0,1 m are recommended.

In the COMRisk study, a flooding depth of 0,01 m and a drying depth of 0,005 m were used. The impact of these values was examined by increasing them to 0,02 and 0,01 m.

*Elevation model*

The impact of the elevation model was evaluated by means of a series of new elevation models, described in section 4.2. Four different versions were considered:

- Fine (20x20 m)
- Coarse (40x40 m)
- Fine with linear structures
- Coarse with linear structures

Each breach is linked to a limited number of elevation model grid cells. For the fine elevation model, the number of cells was estimated by dividing the maximum breach width (roughly projected in the east-west direction) by the fine elevation model grid size (20 m). When converting to a coarser elevation model, the number of cells to which the breaches are linked needs to be reduced. Initially, the number of cells was once again estimated by dividing the maximum breach width by the coarse model grid size (40 m). This reduces the number of cells per link by a factor 2. As the area of a coarse grid cell is four times higher than the area of a fine grid cell, the total area per link is still twice as high. A number of tests indicated that the increase in surface area cause an increase of the discharge through the breach. In order to reduce this influence, the number of cells in the links to the coarse elevation model was further reduced by trial and error until the total volume passing through the breaches when using the coarse elevation model (with linear structures) was almost equal to the total volume passing the breaches when using the fine elevation model (with linear structures).

**Coupled models**

*Simulation period*

In the COMRisk study, simulations were terminated at the end of the design storm. Even if one assumes that no inflow of sea water occurs after the end of the storm, the water already present in the flood plain can still continue to redistribute. To check the influence of redistribution, the simulation duration was increased by 12 hours. The assumption was made that no additional inflow through the breaches is possible during the period following the storm.

If the breach bottom level is below the astronomical high tide level, additional inflow can occur during the tidal cycles following the storm. For the breaches specified in the COMRisk study, this is only true for the breach in the Zwin dike, which forms during a storm with a return period of 40000 years. Therefore, this phenomenon was not investigated any further. When the simulation period is increased, other phenomena such as infiltration and evaporation will gain importance too. These were not investigated either.

*Time step*

In MikeFlood the couplings between Mike11 and Mike21 are of an explicit nature. The criterion for numerical stability of such links (Courant number < 1) imposes the use of a very small time step (a few seconds).

In the COMRisk study, a time step of 2 seconds was used. A rough estimate indicates that in this case the Courant number is probably less tan 1 for small return periods and about 1 for the largest return period. Theoretically speaking, there might be possibilities for a further increase of the time step. Test simulations have indicated that increasing the time step to 4 seconds causes strong oscillations in the breach flow for small return periods and causes the simulation to crash for the largest return period. As a result, increasing the time step seems impossible without additional measures.

The use of the numerical options described in the next paragraph influences the stability of the coupled model in a positive way. After optimizing the numerical options, the time step could be doubled to 4 seconds. Higher values were not tested.

*Numerical options*

The standard coupling between Mike11 and Mike21 allows the exchange of volume and momentum. In case of numerical problems, stability can be increased by disabling momentum transfer. This option was already applied in the COMRisk study. To evaluate the potential impact, a verification simulation including momentum transfer was run.

The latest release of MikeFlood contains an option named “exponential smoothing”. By means of an “exponential smoothing factor” a time delay is introduced in the transfer of water levels from Mike21 to Mike11. This reduces the possibility of oscillations in the breach hydrographs, but could also influence the shape of the hydrographs. For testing purposes, a very low smoothing factor (0,1) was imposed. When applying this factor, it takes several minutes for the water levels in Mike11 to approach those in Mike21 to 0,1% or less. This factor does not seem to influence normal hydrographs, but proved very effective in dampening oscillations in irregular hydrographs. Therefore, it was always used. As some couplings become unstable without the use of this factor, a full verification of its influence was impossible.

*Output interval*

The simulation results are saved with a specific time interval. The size of this interval could influence the derived variables (maximum inundation depth, maximum velocity, maximum rise) used in damage and casualty calculations. In order to evaluate the impact of the output interval, it was reduced from half an hour to 10 minutes.

**Boundary conditions**

*Symmetrical storm surge*

A first scenario consisted of limiting storm surge duration to 45 hours for all return periods. This leads to the symmetrical boundary conditions shown in Figure 36.

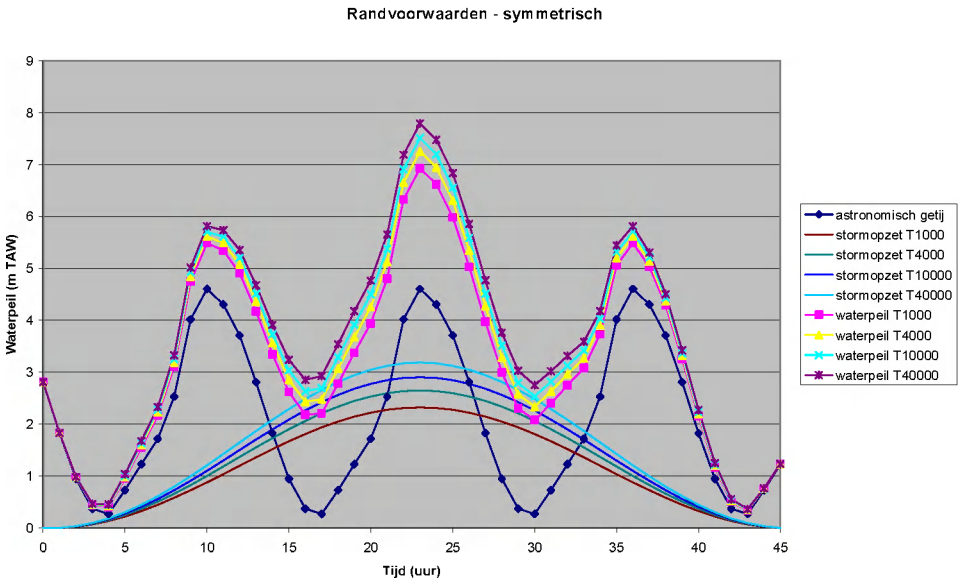


Figure 36: Symmetric water level and storm surge

Because of the considerable decrease of the maximum water level during the first tidal cycle, a number of dikes which fail at the first high tide (T= 40000 years) in the reference situation will fail at a later time. For these dikes, the time of breaching was moved to a point on the rising limb of the second tidal cycle where the water level equals the maximum water level of the first tidal cycle in the reference situation. The time of breaching was delayed, but the water level at which breaching occurs remains unchanged.

*Asymmetrical storm surge*

A second scenario is based on an asymmetrical storm surge. It is based on a storm duration of 35 hours before the central high tide and 55 hours afterwards. The resulting boundary conditions are shown in Figure 37.

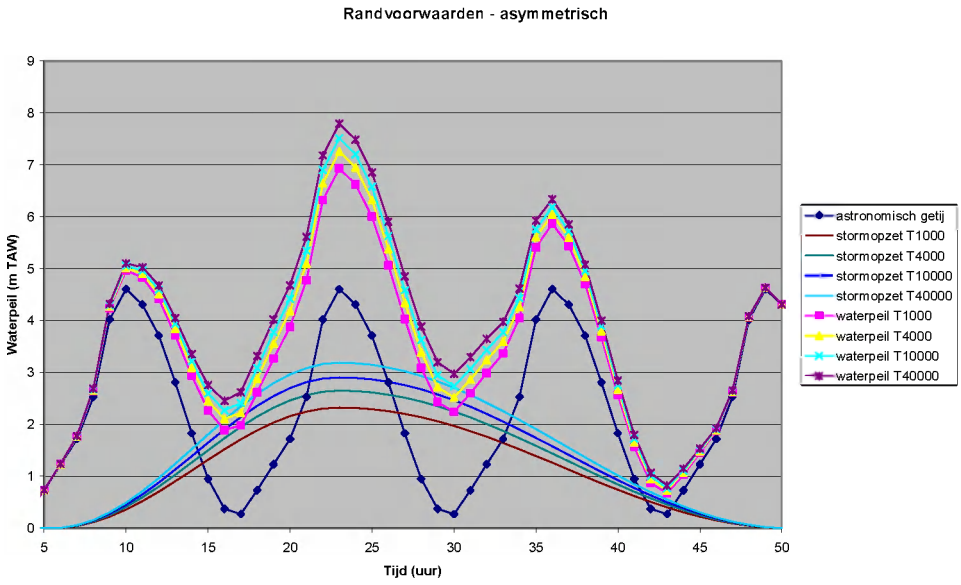


Figure 37: Asymmetrical water level and storm surge

In case of an asymmetrical storm, the maximum water level during the first tidal cycle is even lower than for the symmetrical storm. For those dikes which fail during the first tidal cycle in the reference situation, the time of breaching was delayed again, following the method described for the symmetrical storm.

*Wind*

Mike21 offers the possibility to take the influence of wind friction on the water surface into account. In the default setting, this option is not active. It needs to be activated by the user.

The influence of wind on the sea level is already incorporated in the boundary conditions (storm surge). The potential influence of wind on the distribution of flood water in the coastal plain needs to be estimated separately. In the COMRisk study, this influence was neglected. In order to evaluate the influence of wind action, a simulation including wind action was run.

The calculation of wind friction requires knowledge of wind speed (10 m above the water surface), wind direction and a wind friction coefficient. The wind direction was set to NNW. This direction is perpendicular to the coast line and is likely to have the largest influence on the distribution of flood water in the coastal plain. The maximum wind speed was estimated form the statistical analysis presented in the “Hydraulic Boundary Conditions for the Flemish Coast” (Hydraulisch Randvoorwaardenboek Vlaamse Kust, IMDC 2005-a) for the direction NNW and an aggregation period of 2 hours. The published values are valid for an altitude of 25 m above the water surface. They were reduce by a factor 0,9 in order to estimate the wind speed at an altitude of 10 m above the water surface and subsequently by a factor of 0,8 to account for lower wind speeds above land. The final values are 23,7, 25,2 and 26,6 m/s for return periods of 4000, 10000 and 40000 years. The temporal variation of wind speed was described by the relationship used for storm surge ($\cos^2$). The result is shown in Figure 38. The default wind friction coefficient (0,0026) is intended for strong winds above sea. In case of overland flow, part of the water surface will be shielded by landscape elements which are not flooded and the use of the default value would result in an

overestimation of the true impact of wind friction. Based on literature values, the wind friction coefficient was lowered to 0,0008.

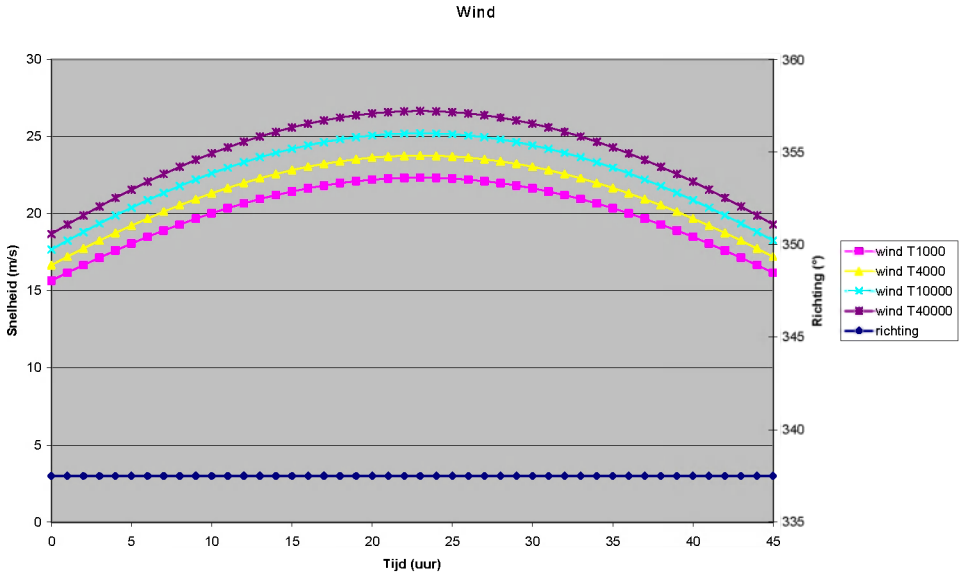


Figure 38: Wind

*Wave overtopping*

A major number of breaches along the Flemish coast are caused by wave overtopping. In addition, there are a number of locations were overtopping occurs without breaching.

In the COMRisk study, overtopping discharges were not taken into account. In order to evaluate the potential impact of these discharges, they were added to the model in a strongly simplified way. The overtopping discharge per unit width was estimated from the COMRisk report. This information is summarized in Table 12. For dikes which do not fail during the second, but during first or third tidal cycle, it was not clear to which tidal cycle these values apply. Overtopping discharges for a return period of 10000 years were obtained by interpolation between 4000 and 40000 years.

The maximum overtopping discharges were obtained by multiplying the unit discharges by an estimated overtopping width. This overtopping width includes the width of streets and squares in a section, augmented by half the width of the sea dike in the vicinity of these streets (to account for lateral inflow). Overtopping occurring in front of buildings or dunes is probably reflected and was not taken into account. For the Zwin, the average overtopping along the entire dike was multiplied by the total length of the dike. Overtopping discharges were injected on the landward side of the dike, for a period of 2 hours surrounding the highest water level. This was done by means of a triangular hydrograph with a base width of two hours and a height corresponding to the maximum overtopping discharge. For dikes failing during the first or last tidal cycle, this is probably not correct.

Table 12: Wave overtopping

| Section | Width (m) | T=1000 Q (l/s/m) | T=4000 Q (l/s/m) | T=10000 Q (l/s/m) | T=40000 Q (l/s/m) |
|---|---|---|---|---|---|
| 220 | 30 | 0,8 | 22,7 | 51,5 | 195,5 |
| 233 | 75 | 0,2 | 185,8 | 268,6 | 682,4 |
| 234 | 112,5 | 0,0 | 60,9 | 109,3 | 351,6 |
| 235 | 150 | 0,0 | 0,7 | 51,4 | 305,1 |
| 236 | 137,5 | 0,0 | 0,5 | 73,4 | 437,8 |
| 240 | 47,5 | 0,0 | 0,0 | 9,7 | 58,0 |
| 241 | 0 | 0,0 | 0,0 | 64,1 | 384,7 |
| 242 | 20 | 0,0 | 138,8 | 234,5 | 712,7 |
| 243 | 0 | 0,2 | 184,0 | 271,1 | 706,6 |
| 246 | 0 | 0,0 | 0,0 | 3,9 | 23,3 |
| Zwin | 2000 | 0,0 | 0,2 | 0,8 | 3,7 |

**Results**

*Reference model*

Figure 39 through Figure 45 show the results for the reference simulation. Figure 39, Figure 41 and Figure 43 show the breach hydrographs for return periods of 4000, 10000 and 40000 years. Figure 40, Figure 42 and Figure 44 show the maximum flooded depth for the same return periods.

The hydrographs indicate that for most breaches, the largest volume of flood water enters the coastal plain during the second tidal cycle. For the breach in the Zwin dike, the third tidal cycle is very important too. The hydrographs also indicate that some breaches contribute a lot more to the floods than others. In particular, the volume originating from the breach in the Zwin dike is very large. Most hydrographs also show a short period of negative flows at the end of a tidal cycle. This indicates that the flood water is transported inland very slowly and partially returns to sea at low tide.

The flood maps indicate that floods mainly occur on Flemish soil and propagate into Netherlands to a very limited extent. The extent of floods resulting from a storm with a return period of 40000 years is obviously limited by the dikes of canals in the coastal plain (Leopold canal and canal from Damme to Sluis).

Figure  shows the propagation of a flood with a return period of 40000 years. The flood wave moves from the coast (Knokke, Het Zoute, Zwin) in south-easterly direction (Zwin polders, Retranchement), subsequently turns towards the south (Sint-Anna, Westkapelle) and finally moves towards the southwest over a wide front (Oostkerke, Ramskapelle).

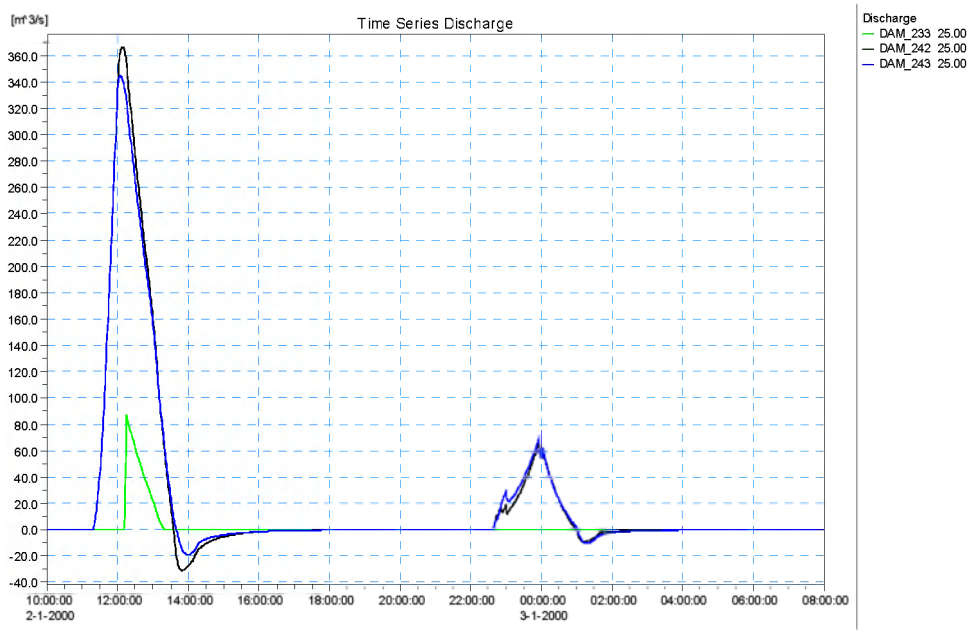


Figure 39: Breach hydrographs (T = 4000 years)

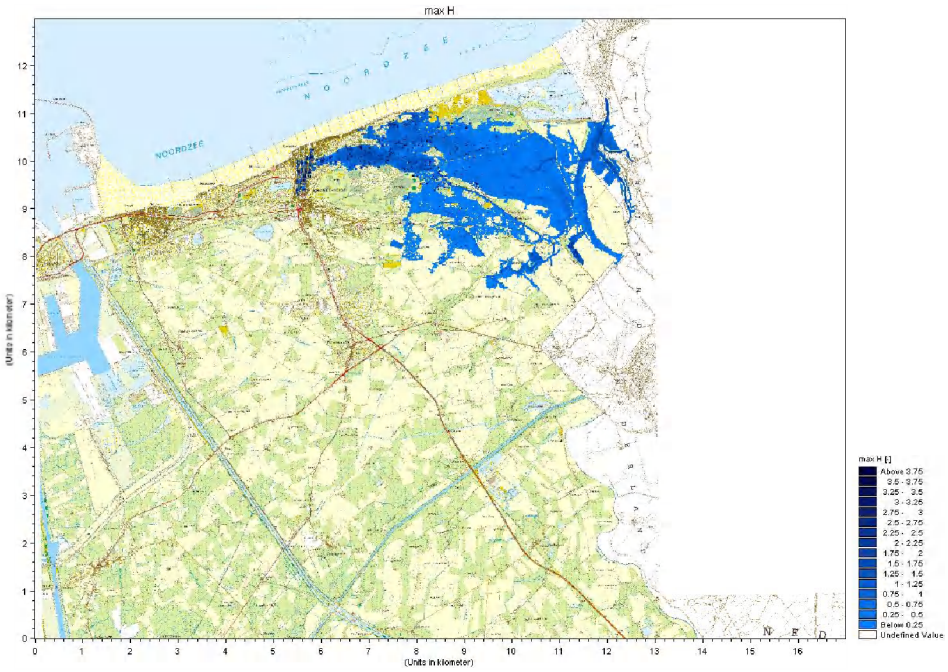


Figure 40: Inundations (T = 4000 years)

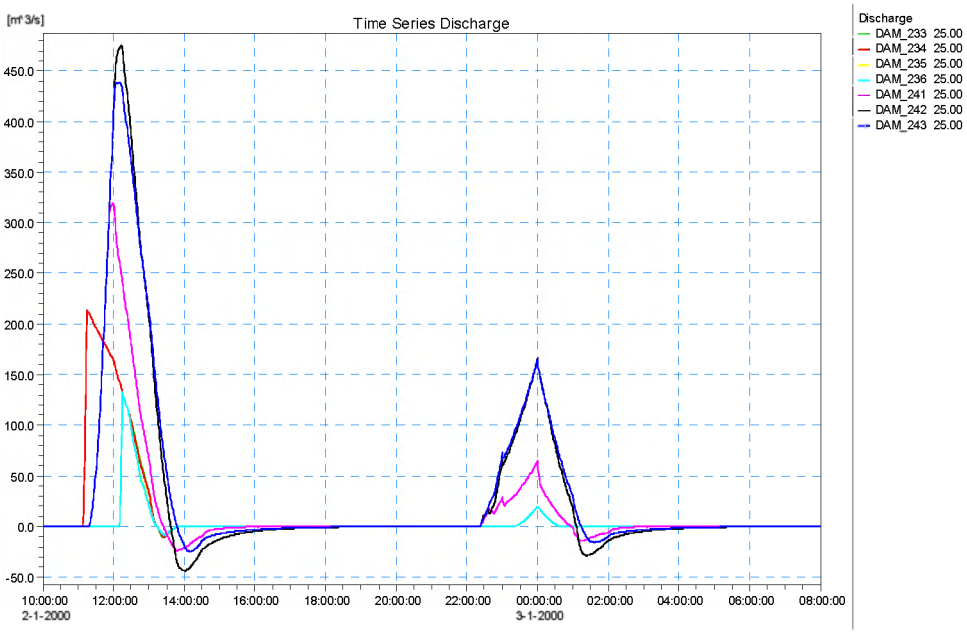


Figure 41: Breach hydrographs (T = 10000 years)

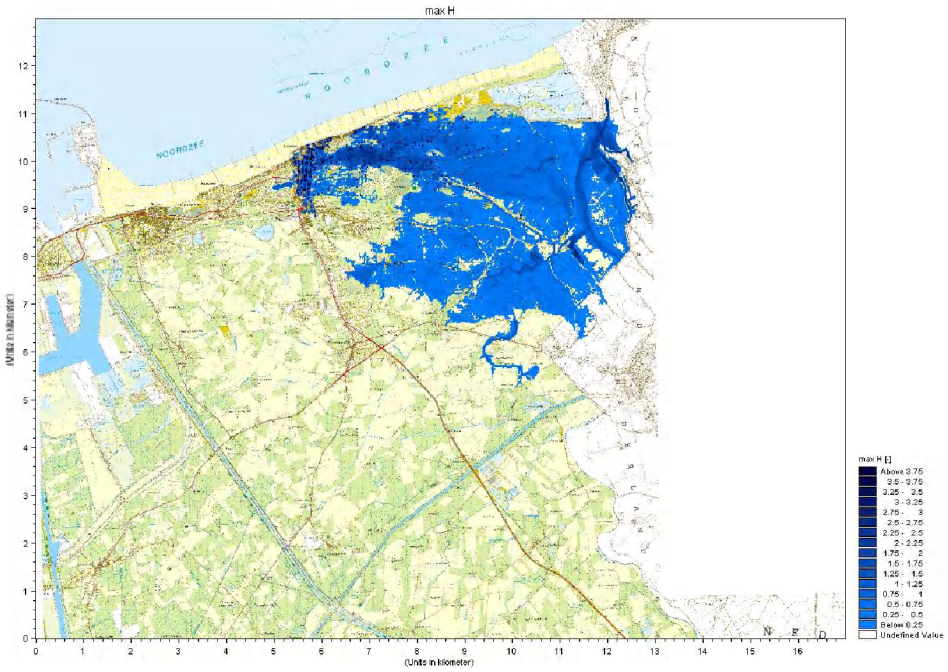


Figure 42: Inundations (T = 10000 years)

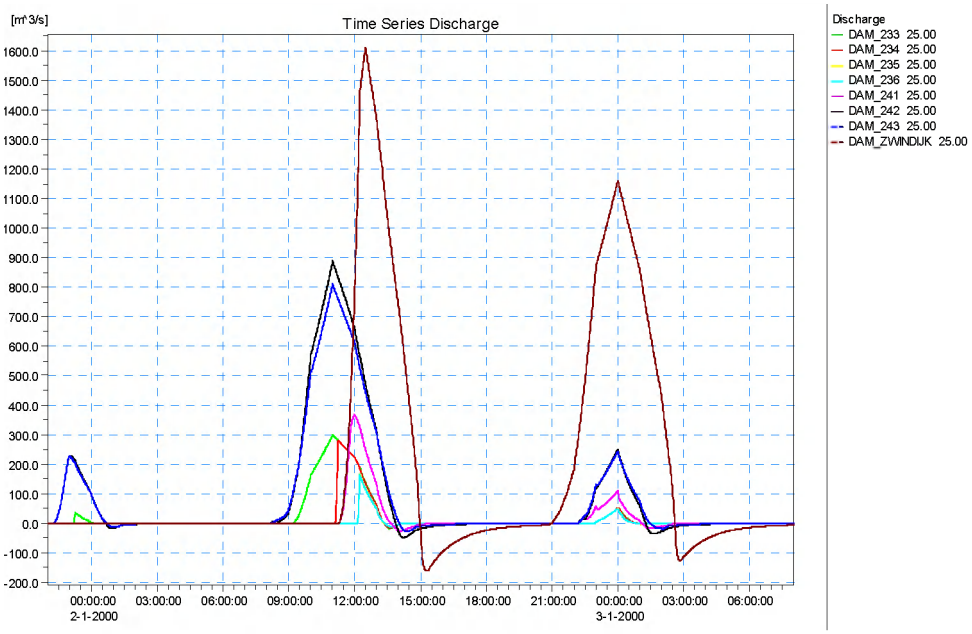


Figure 43: Breach hydrographs (T = 40000 years)

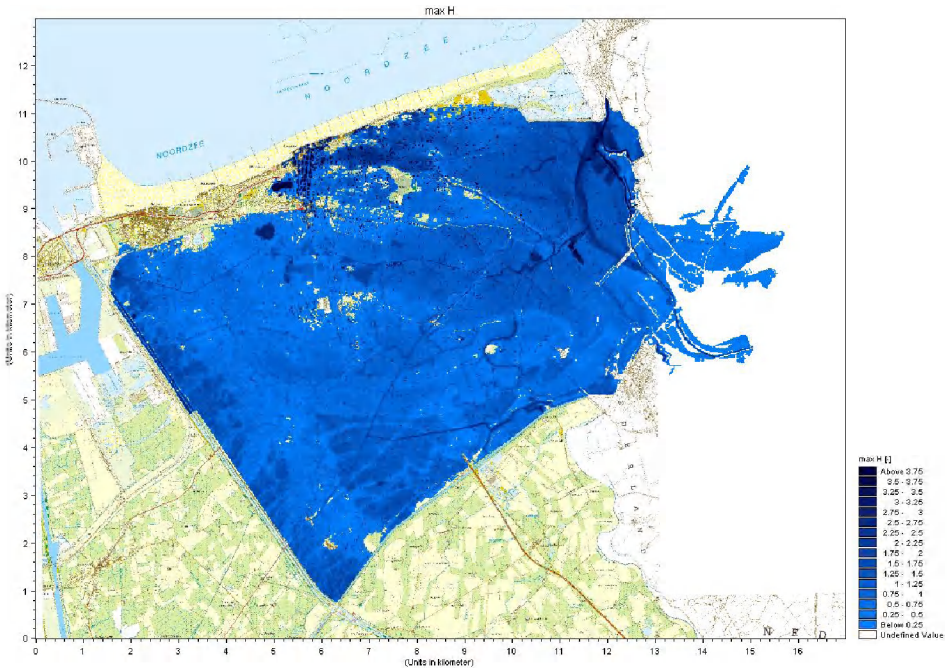


Figure 44: Inundations (T = 40000 years)

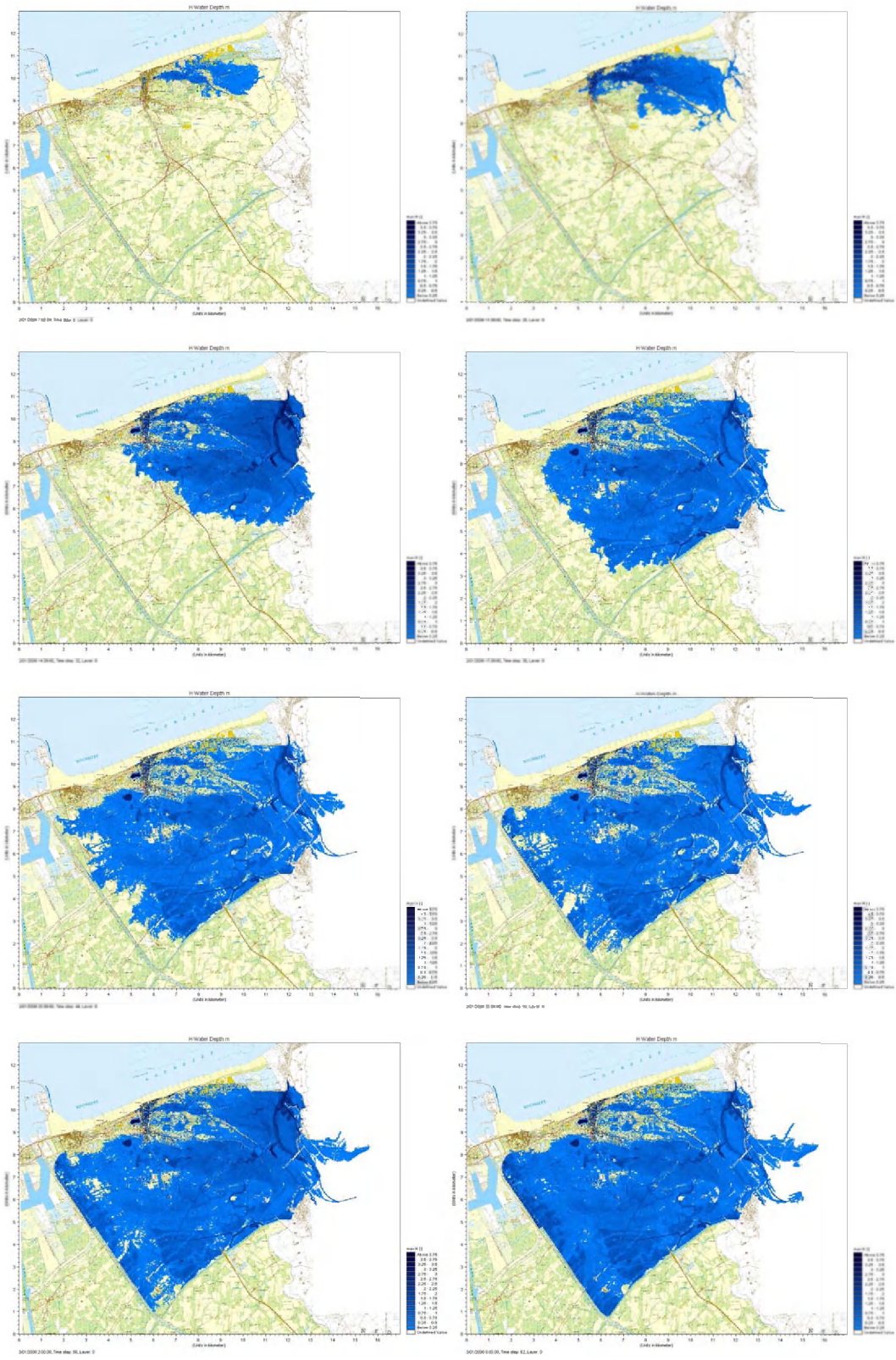

Figure 45: Inundation after 3, 12, 15, 18, 21, 24, 27 en 30 hours (T = 40000 years)

*Breaching*

Table 13 presents an overview of maximum breach width, computed by the erosion based breach growth models. Two cases can be distinguished: one in which no horizontal growth is allowed for breaches at Knokke (233-236) ("erosion 1") and a second one where horizontal growth does take place ("erosion 2").

Table 13: Breach width

| Breach | T=4000 time series | T=4000 erosion 1 | T=4000 erosion 2 | T=10000 time series | T=10000 erosion 1 | T=10000 erosion 2 | T=40000 time series | T=40000 erosion 1 | T=40000 erosion 2 |
|---|---|---|---|---|---|---|---|---|---|
| 233 | 90 | 90 | 99 | 90 | 90 | 97 | 90 | 90 | 200 |
| 234 | - | - | - | 90 | 90 | 114 | 90 | 90 | 109 |
| 235 | - | - | - | 90 | 90 | 96 | 90 | 90 | 95 |
| 236 | | | | 90 | 90 | 96 | 90 | 90 | 95 |
| 241 | | | | 150 | 72 | 72 | 150 | 73 | 72 |
| 242 | 150 | 83 | 83 | 150 | 89 | 89 | 150 | 131 | 131 |
| 243 | 150 | 80 | 80 | 150 | 86 | 86 | 150 | 116 | 115 |
| Zwin | - | - | - | - | - | - | 300 | 166 | 166 |

For the breaches at Het Zoute (241-243) the breach width increases as the return period increases. For the breaches at Knokke (233-236) this is not the case because breaches do not grow or interact with each other. During a storm with a return period of 40000 years, breach 233 grows very quickly, thereby hampering the growth of neighbouring breaches. The growth of the breaches at Knokke hardly influences the growth of the breaches at Het Zoute and the Zwin.

Table  presents an overview of the total volumes passing through the breaches when using different elevation models (relative to a reference = fine with linear structures). The use of a coarse elevation model leads to an increase of volumes for all return periods, whereas the addition of linear structures leads to a decrease of volumes, in particular for the largest return periods. Both effects can probably be explained by a change of backwater effects in the flood plain. The use of a coarser elevation model flattens the landscape. This leads to a decrease of backwater effects and an increase of breach flows. The addition of linear structures creates new barriers in the landscape. These cause increased water levels downstream of the breaches and a decrease of breach flows. The results from the simulations involving a fine elevation model with linear structures and a coarse elevation model with linear structures agree very well (Table 14).

Table 14: Relative volume passing through breaches

| Elevation model | T=4000 Volume (%) | T=10000 Volume (%) | T=40000 Volume (%) |
|---|---|---|---|
| Fine | - | - | - |
| Coarse | 9 | 7 | 5 |
| Fine with linear structures | -1 | -9 | -18 |
| Coarse with linear structures | 2 | -12 | -20 |

*Flooding*

The outcomes of the different simulations were compared in terms of 5 hydraulic indicators: flood volume, flooded area, maximum flow depth, maximum flow velocity and maximum rise velocity.

The flood volume is the total volume of water in the flood plain at the end of the simulation (total inflow - return flow).

The flooded area is the total area of all cells in the 2D flood model which were (temporarily) flooded in the course of a storm.

The maximum depth, maximum velocity and maximum rise were computed twice: as a spatial average of all flooded cells and as a spatial average of all cells. As all cells do not flood simultaneously and the maxima do not all occur at the same time, these indicators do not represent one specific situation which occurred in the course of a storm, but an envelope of all conditions which occurred during a storm. The spatially distributed values of these variables will be used for the calculation of damage and casualties.

In order to quickly evaluate the impact of the studied parameters on damage and casualty calculations, an additional hydraulic index was defined, which combines a number of relevant quantities:

$$I = \sqrt[4]{A\ d\ v\ r}$$

where:

I = hydraulic index

A = flooded area ($m^2$)

d = maximum flow depth (m)

v = maximum flow velocity (m/s)

r = maximum rise velocity (m/h)

The results are summarized in Table 15, Table 16 and Table 17. For each scenario and each return period, these tables list the relative deviation (in percent) of all indicators from the reference situation. For the results related to the elevation models, the fine grid with linear structures was used as a reference.

The impact of a factor can vary depending on the return period under consideration. For return periods of 4000 and 10000 years, only part of the study area is flooded, whereas for a return period of 40000 years, the entire area between the coast and the dikes of the canals in the coastal plain is flooded. As a result, the impact of some factors is more clearly visible for return periods of 4000 and 10000 years than for a return period of 40000 years. The impact of some other factors (e.g. breach growth by erosion and boundary conditions) is stronger for a return of 40000 years.

Table 15: Procentual deviations of hydraulic indicators: volume, area, index

| Simulation | T=4000 volume (%) | T=4000 area (%) | T=4000 index (%) | T=10000 volume (%) | T=10000 area (%) | T=10000 index (%) | T=40000 volume (%) | T=40000 area (%) | T=40000 index (%) |
|---|---|---|---|---|---|---|---|---|---|
| Earlier breaching | 51 | 42 | 16 | 42 | 28 | 16 | 12 | 3 | 8 |
| Later breaching | -41 | -29 | -24 | -34 | -30 | -18 | -11 | -3 | -7 |
| Slower horizontal growth | -15 | -10 | -9 | -11 | -9 | -5 | -13 | -4 | -9 |
| Faster vertical growth | 33 | 24 | 13 | 25 | 17 | 10 | 6 | 1 | 4 |
| Breach growth by erosion | 5 | 3 | 0 | 0 | 0 | -1 | -26 | -11 | -15 |
| Breach growth by erosion (growth Knokke) | 5 | 3 | 1 | 2 | 1 | 0 | -23 | -8 | -12 |
| Alternative breach flow equations | 5 | 3 | 2 | 5 | 4 | 3 | 10 | 2 | 5 |
| Lower surface roughness | 7 | 5 | 5 | 8 | 6 | 5 | 5 | 1 | 4 |
| Higher surface roughness | -18 | -11 | -12 | -19 | -18 | -9 | -14 | -6 | -9 |
| Variable surface roughness | -49 | -40 | -28 | -47 | -40 | -23 | -28 | -15 | -16 |
| Alternative formulation viscosity | 1 | 1 | 1 | 1 | 1 | 1 | 1 | 0 | 1 |
| Lower eddy viscosity | 1 | 2 | 1 | 2 | 2 | 1 | 1 | 0 | 1 |
| Higher eddy viscosity | -17 | -11 | -10 | -18 | -18 | -7 | -11 | -3 | -7 |
| No Coriolis force | 0 | 0 | 0 | 0 | 0 | 0 | 0 | 0 | 0 |
| Modified flood/dry parameters | -1 | -1 | 1 | 0 | -1 | 1 | 0 | 0 | 0 |
| Longer simulation duration | 2 | 5 | -1 | 1 | 8 | -1 | 0 | 2 | 0 |
| Larger time step | 1 | 1 | 0 | 1 | 0 | 0 | 0 | 0 | 0 |
| Momentum transfer | 0 | 0 | 0 | 0 | 0 | 0 | 0 | 0 | 0 |
| Output interval | 0 | 0 | 5 | 0 | 0 | 5 | 0 | 0 | 3 |
| Symmetrical storm surge | -12 | -3 | -1 | -21 | -11 | 1 | -35 | -14 | -6 |
| Asymmetrical storm surge | 8 | 6 | 0 | -6 | 0 | 0 | -22 | -5 | -5 |
| Wind friction | 4 | 9 | 2 | 5 | 7 | 2 | 4 | 0 | 3 |
| Wave overtopping | 2 | 1 | 1 | 2 | 2 | 1 | 2 | 0 | 1 |
| Fine elevation model | - | - | - | - | - | - | - | - | - |
| Coarse elevation model | 10 | 29 | 4 | 7 | 14 | 1 | 5 | 4 | 0 |
| Fine elevation model with linear structures | -1 | -39 | 7 | -10 | -26 | -3 | -18 | -7 | -9 |
| Coarse elevation model with linear structures | 3 | -40 | 13 | -12 | -22 | -3 | -20 | -7 | -11 |

Table 16: Procentual deviations of hydraulic indicators: depth, velocity, rise (flooded area)

| Simulation | T=4000 depth (%) | T=4000 velocity (%) | T=4000 rise (%) | T=10000 depth (%) | T=10000 velocity (%) | T=10000 rise (%) | T=40000 depth (%) | T=40000 velocity (%) | T=40000 rise (%) |
|---|---|---|---|---|---|---|---|---|---|
| Earlier breaching | 9 | 5 | 8 | 11 | 11 | 13 | 8 | 10 | 12 |
| Later breaching | -23 | -19 | -23 | -11 | -18 | -14 | -7 | -7 | -8 |
| Slower horizontal growth | -9 | -8 | -9 | -3 | -5 | -4 | -10 | -10 | -11 |
| Faster vertical growth | 9 | 11 | 9 | 7 | 7 | 9 | 4 | 4 | 5 |
| Breach growth by erosion | 0 | 0 | -1 | -1 | -2 | -1 | -17 | -15 | -17 |
| Breach growth by erosion (growth Knokke) | 0 | 0 | -1 | 0 | -1 | 0 | -14 | -11 | -14 |
| Alternative breach flow equations | 2 | 3 | 2 | 2 | 3 | 3 | 6 | 5 | 6 |
| Lower surface roughness | 1 | 14 | 0 | -1 | 14 | -1 | 1 | 14 | 1 |
| Higher surface roughness | -6 | -26 | -3 | 3 | -23 | 3 | -5 | -25 | -2 |
| Variable surface roughness | -16 | -45 | -11 | -9 | -39 | -3 | -13 | -28 | -9 |
| Alternative formulation viscosity | 0 | 2 | 0 | 0 | 2 | 0 | 0 | 2 | 0 |
| Lower eddy viscosity | 0 | 2 | 0 | 0 | 1 | 0 | 1 | 2 | 1 |
| Higher eddy viscosity | -8 | -15 | -6 | -1 | -10 | 0 | -7 | -11 | -4 |
| No Coriolis force | 0 | 0 | 0 | 0 | 0 | 0 | 0 | 0 | 0 |
| Modified flood/dry parameters | 1 | 1 | 1 | 1 | 1 | 1 | 0 | 0 | 0 |
| Longer simulation duration | 0 | -4 | -3 | -1 | -5 | -5 | 0 | -1 | -1 |
| Larger time step | -1 | -1 | -1 | 0 | 0 | 0 | 0 | 0 | 0 |
| Momentum transfer | 0 | 0 | 0 | 0 | 0 | 0 | 0 | 0 | 0 |
| Output interval | 1 | 18 | 3 | 1 | 15 | 3 | 0 | 9 | 5 |
| Symmetrical storm surge | -2 | 2 | 1 | 0 | 6 | 6 | -15 | -3 | 6 |
| Asymmetrical storm surge | 1 | -4 | -4 | -1 | -1 | 0 | -10 | -5 | 2 |
| Wind friction | -4 | 2 | -1 | -3 | 3 | -2 | 2 | 8 | 3 |
| Wave overtopping | 1 | 0 | 1 | 1 | 0 | 0 | 1 | 1 | 1 |
| Fine elevation model | - | - | - | - | - | - | - | - | - |
| Coarse elevation model | -6 | 6 | -9 | -7 | 3 | -6 | -1 | 4 | -5 |
| Fine elevation model with linear structures | 33 | 24 | 30 | 10 | 0 | 7 | -6 | -14 | -8 |
| Coarse elevation model with linear structures | 44 | 37 | 39 | 4 | 6 | 5 | -8 | -15 | -12 |

Table 17: Procentual deviations of hydraulic indicators: depth, velocity, rise (total area)

| Simulation | T=4000 depth (%) | T=4000 velocity (%) | T=4000 rise (%) | T=10000 depth (%) | T=10000 velocity (%) | T=10000 rise (%) | T=40000 depth (%) | T=40000 velocity (%) | T=40000 rise (%) |
|---|---|---|---|---|---|---|---|---|---|
| Earlier breaching | 54 | 49 | 53 | 42 | 42 | 44 | 11 | 13 | 15 |
| Later breaching | -46 | -43 | -46 | -38 | -43 | -40 | -10 | -11 | -11 |
| Slower horizontal growth | -18 | -18 | -18 | -11 | -13 | -13 | -13 | -13 | -15 |
| Faster vertical growth | 36 | 38 | 35 | 25 | 24 | 27 | 5 | 6 | 6 |
| Breach growth by erosion | 3 | 2 | 2 | -1 | -2 | -1 | -26 | -24 | -26 |
| Breach growth by erosion (growth at Knokke) | 3 | 2 | 2 | 1 | 0 | 1 | -22 | -19 | -21 |
| Alternative breach flow equations | 5 | 6 | 4 | 5 | 7 | 6 | 8 | 8 | 8 |
| Lower surface roughness | 5 | 19 | 4 | 6 | 21 | 6 | 2 | 15 | 2 |
| Higher surface roughness | -16 | -34 | -14 | -16 | -37 | -15 | -11 | -29 | -7 |
| Variable surface roughness | -50 | -67 | -47 | -45 | -63 | -42 | -26 | -39 | -23 |
| Alternative formulation viscosity | 1 | 3 | 1 | 1 | 3 | 1 | 1 | 2 | 1 |
| Lower eddy viscosity | 2 | 4 | 2 | 2 | 4 | 2 | 1 | 2 | 1 |
| Higher eddy viscosity | -18 | -24 | -17 | -19 | -27 | -19 | -10 | -15 | -7 |
| No Coriolis force | 0 | 0 | 0 | 0 | 0 | 0 | 0 | 0 | 0 |
| Modified flood/dry parameters | 0 | 0 | 0 | 0 | 0 | 0 | 0 | 0 | 0 |
| Longer simulation duration | 5 | 1 | 1 | 6 | 2 | 3 | 2 | 0 | 0 |
| Larger time step | 0 | 0 | 0 | 0 | 0 | 0 | 0 | 0 | 0 |
| Momentum transfer | 0 | 0 | 0 | 0 | 0 | 0 | 0 | 0 | 0 |
| Output interval | 1 | 18 | 3 | 1 | 15 | 3 | 0 | 9 | 5 |
| Symmetrical storm surge | -5 | -2 | -2 | -11 | -5 | -5 | -27 | -16 | -9 |
| Asymmetrical storm surge | 7 | 2 | 2 | -1 | -1 | 0 | -15 | -10 | -3 |
| Wind friction | 5 | 12 | 8 | 4 | 11 | 5 | 2 | 8 | 4 |
| Wave overtopping | 2 | 1 | 1 | 2 | 2 | 2 | 1 | 2 | 2 |
| Fine elevation model | - | - | - | - | - | - | - | - | - |
| Coarse elevation model | 22 | 37 | 18 | 7 | 18 | 8 | 3 | 8 | -2 |
| Fine elevation model with linear structures | -18 | -24 | -20 | -19 | -26 | -20 | -12 | -20 | -15 |
| Coarse elevation model with linear structures | -13 | -17 | -16 | -20 | -18 | -19 | -14 | -21 | -18 |

The time of breaching very strongly influences the hydraulic results. Vertical growth rate, horizontal growth rate and growth model (time series or erosion) can all exert an important influence. The large impact of the breach growth model for a return period of 40000 years is caused by the large change of the dimensions of the major breach in the Zwin dike (cfr. Table 13). The choice of breach flow equations turns out to be of minor importance.

Changes in surface roughness and eddy viscosity have a comparable impact. The spread on surface roughness values (20 - 40) is much lower than the spread on eddy viscosity values (0,1 - 10). Therefore the relative impact of surface roughness is higher than the relative impact of eddy viscosity. The use of a variable surface roughness causes a significant decrease of flooding. The dominant land use (agriculture) has a higher roughness than the default value (25 instead of 32) and a number of areas near the coast (urban and infrastructure) has a significantly higher roughness (10 instead of 32).

The impact of the Coriolis force turns out to be negligible, as expected. The flood and dry parameters do not have a strong impact either.

The simulation duration has a limited influence on hydraulic results. It should be noted that this conclusion is influenced by the assumption that breach bottom levels are not eroded to a level below astronomical high tide. Therefore, an increase of the simulation duration will only result in redistribution of flood water, but not to additional inflow. If the breach bottom levels were eroded to a level below astronomical high tide, an increase of the simulation duration could lead to additional inflow.

A larger time step has a very limited influence. The same holds for momentum transfer. This means that time step and numerical options can be optimized to obtain faster and more robust simulations.

The use of an asymmetrical storm surge has graver consequences than the use of a symmetrical storm surge. This is mainly caused by an increase of the level of the third high tide. The impact of wave overtopping and wind turns out to be limited.

The use of a coarse elevation model leads to worse flooding (larger volume) a larger spatial distribution (larger area). The incorporation of linear structures has an opposite effect (smaller volume and smaller area).

A number of parameters also influence the propagation speed of the flood wave. Figure 46 shows the evolution of water depth in a number of locations for simulations with a constant and a variable roughness. Near the coast, the use of a higher variable roughness leads to higher peak water levels. At the other locations, peak water levels drop. The use of a higher variable roughness also causes a delay of the flood wave. Near the coast this delay amounts to no more than half an hour, but further inland, it can increase to more than 8 hours.

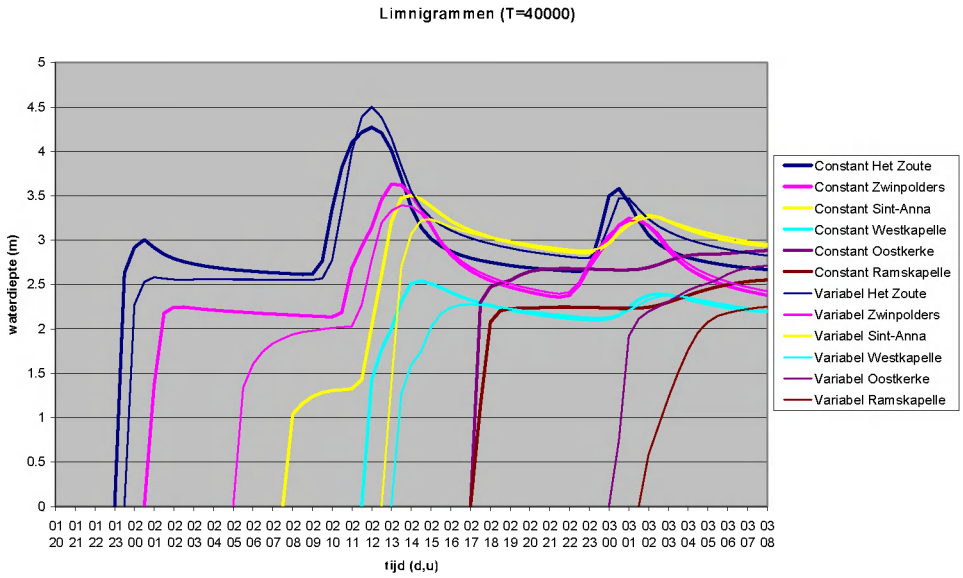


Figure 46: Limnigraphs (T = 40000 jaar)

The impact of the elevation models on the spatial distribution of floods is shown in Figure 47, Figure 48 and Figure 49. These figures clearly show that the use of a coarser elevation model can lead to the inundation of additional areas (Zwin polders in Figure 48) and overtopping of flattened canal embankments (Leopold canal in Figure 49). The addition of linear structures solves both problems.

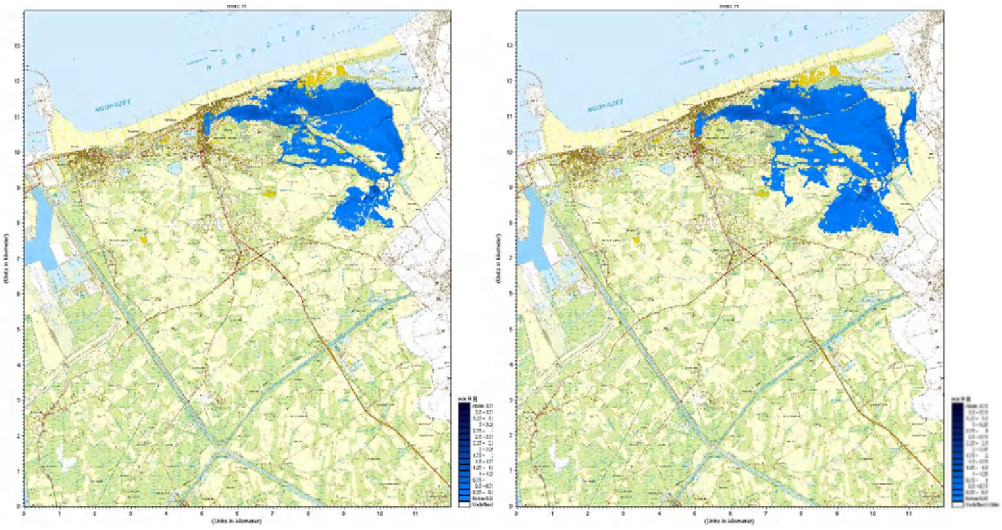

fine (20x20 m) coarse (40 x 40 m)

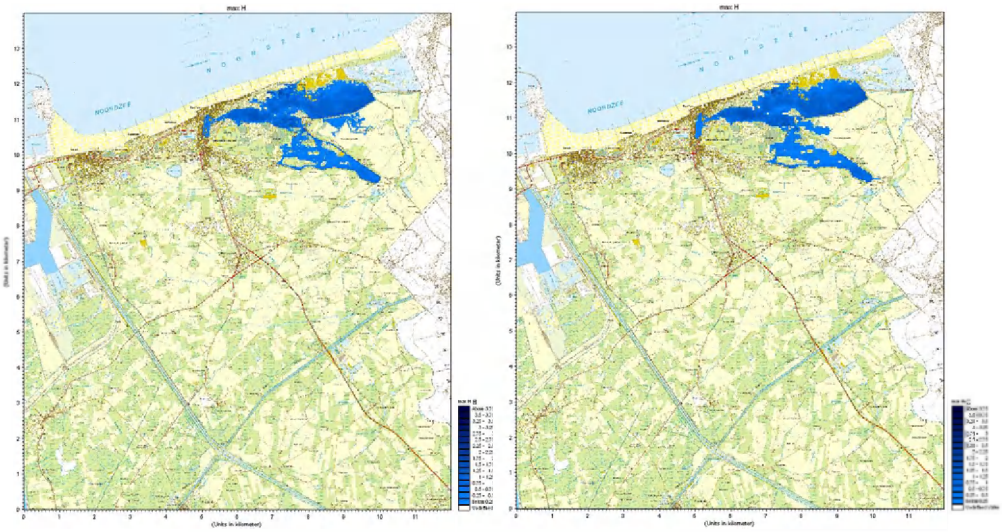

fine with linear structures coarse with linear structures

Figure 47: Flooding (T = 4000 year)

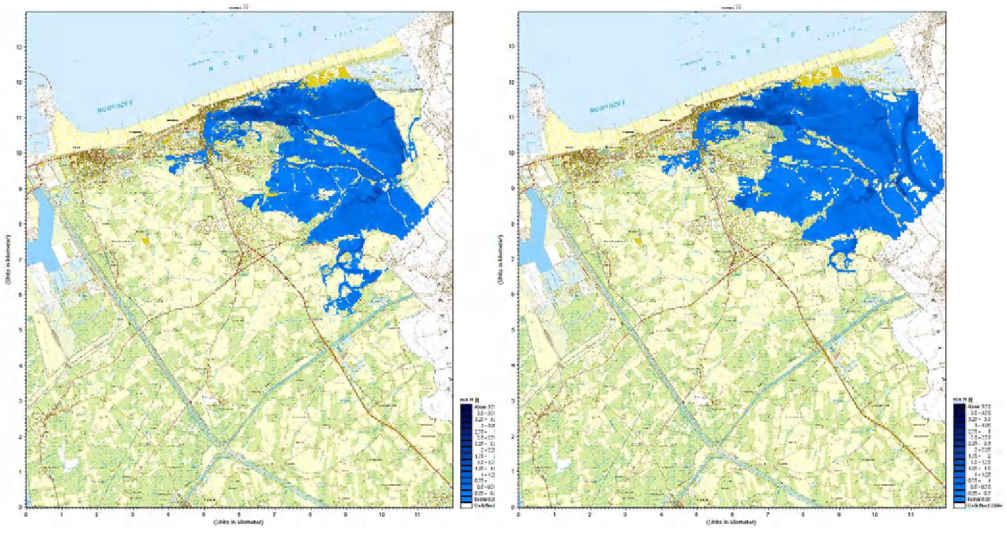

fine (20x20 m) coarse (40x40 m)

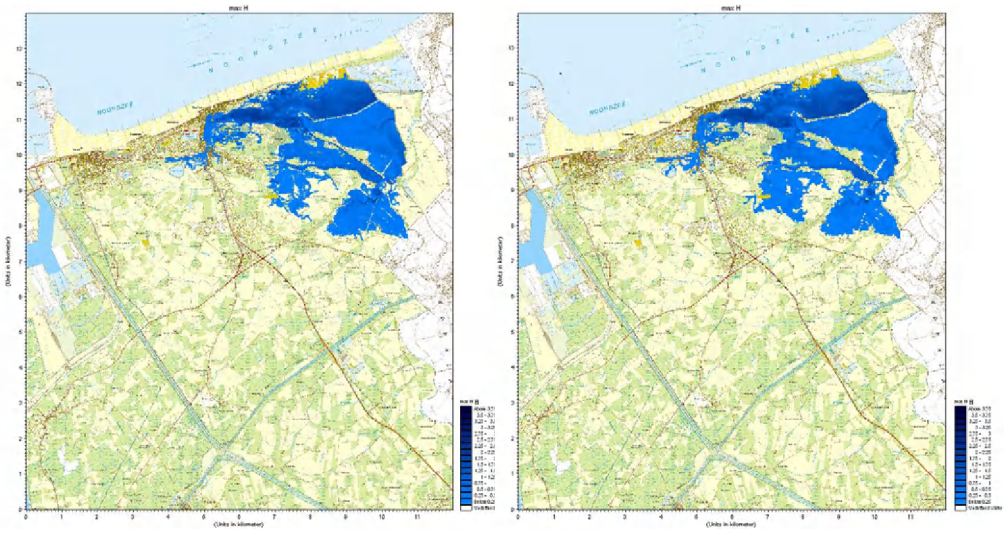

fine with linear structures coarse with linear structures

Figure 48: Flooding (T = 10000 year)

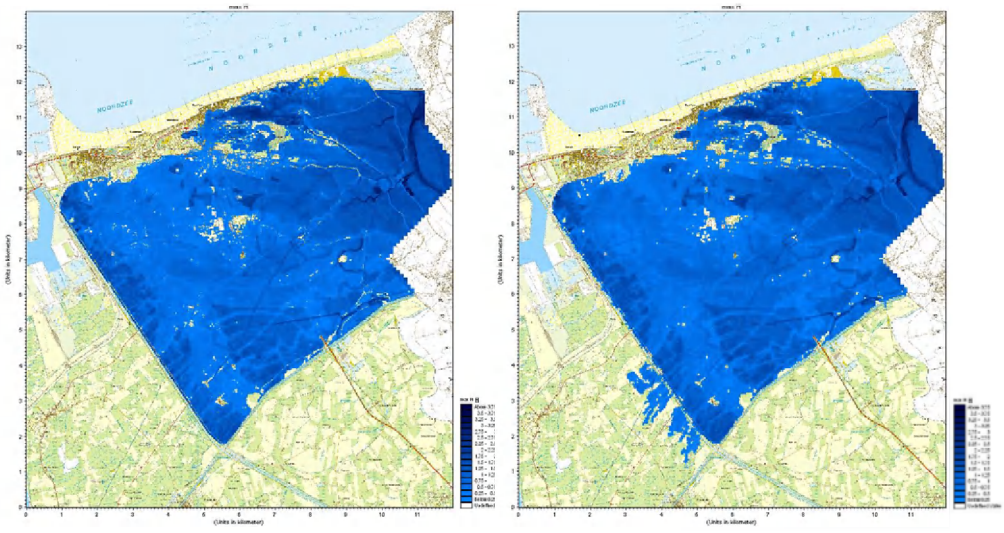

fine (20x20 m) coarse (40x40 m)

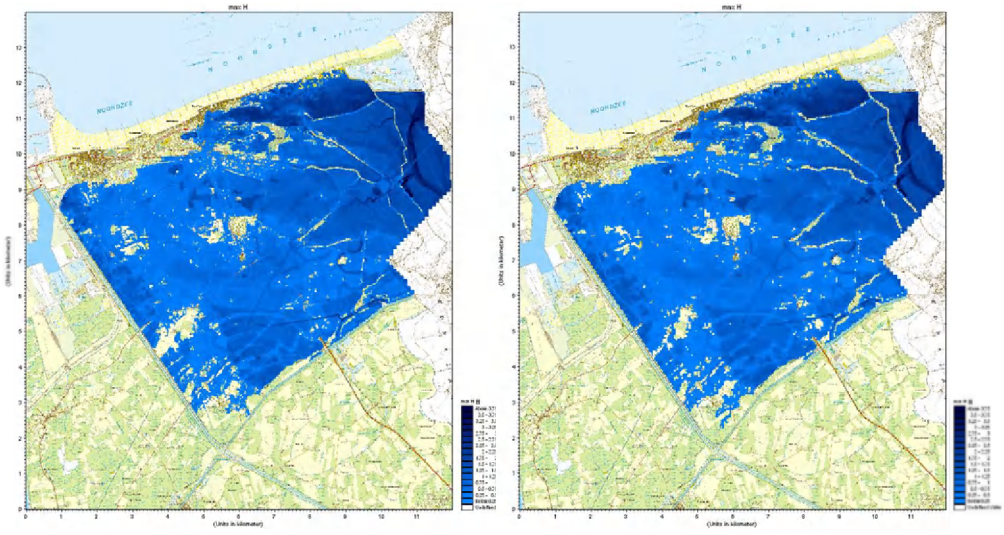

fine with linear structures coarse with linear structures

Figure 49: Flooding (T = 40000 year)

*Damage and casualties*

For a number of scenarios with a large impact on flooding, the damage and casualties in the coastal plain were calculated. A distinction was made between damage and additional damage. The damage to the coastal defence itself was not taken into account.

Damage is based on the maximum depth of flooding and occurs in all areas where a minimum depth of flooding occurs. The additional damage is based on the maximum flow velocity and mainly occurs in the vicinity of breaches. The number of casualties depends on both maximum flow depth and maximum rise velocity.

For a full description of the method used for calculating damage and casualties, the reader is referred to chapter 5.

The calculation of damage and casualties was limited to Flanders. Possible damage and casualties in the Netherlands were neglected due to lack of data. The results are shown in Table 18. For each scenario and each return period, this table lists the relative deviation (in percent) of damage and casualties from the reference situation.

The calculation of casualties led to unexpectedly high numbers. Further analysis revealed that these high numbers are caused by anomalies in the COMRisk elevation model. In a number of locations isolated grid cells with an inexplicably low surface level can be found. During a flood, these little “pits” rapidly fill with water, resulting in a high depth of flooding, a high rise velocity and a high number of casualties. Therefore, the results from the casualty calculations should be interpreted cautiously.

The results for damage and casualties often show other trends than the hydraulic results, even when compared to the most related hydraulic indicator. These differences are caused by the spatial variation of land use (damage) and population density (casualties). When spatially averaging hydraulic results, all grid cells are given an equal weight, regardless of land use and population density. During the calculation of damage and casualties, land use and population density do get taken into account.

Table 18: Damage and casualties

| Simulation | T=4000 damage (%) | T=4000 additional damage | T=4000 casualties (%) | T=4000 damage (%) | T=4000 additional damage | T=4000 casualties (%) | T=4000 damage (%) | T=4000 additional damage | T=4000 casualties (%) |
|---|---|---|---|---|---|---|---|---|---|
| Earlier breaching | 55 | 45 | 139 | 26 | 23 | 34 | 11 | 30 | 15 |
| Later breaching | -63 | -62 | -80 | -29 | -32 | -45 | -12 | -17 | -16 |
| Slower horizontal growth | -15 | -23 | -18 | -2 | -5 | -2 | -4 | -10 | -2 |
| Faster vertical growth | 29 | 28 | 56 | 15 | 1 | 20 | 5 | 8 | 5 |
| Breach growth by erosion (growth at Knokke) | 8 | -4 | 14 | 4 | 4 | 9 | 0 | 9 | 21 |
| Variable surface roughness | -26 | -64 | -20 | 0 | -47 | 9 | -4 | -54 | 13 |
| Output interval | 0 | 0 | 1 | 1 | 0 | 23 | 1 | 0 | 8 |
| Symmetrical storm surge | -4 | -3 | -6 | -2 | -3 | -2 | -18 | -19 | -15 |
| Asymmetrical storm surge | 5 | 2 | 7 | 0 | -1 | 0 | -12 | -13 | -13 |
| Wind friction | 2 | 1 | 1 | 0 | 2 | -1 | -2 | 0 | -3 |
| Wave overtopping | 15 | 2 | 28 | 6 | 1 | 6 | 7 | 9 | 21 |
| Fine elevation model | - | - | - | - | - | - | - | - | - |
| Coarse elevation model | 37 | 83 | -38 | -2 | 16 | -7 | -2 | 13 | -29 |
| Fine elevation model with linear structures | -18 | -29 | 38 | -27 | -42 | 30 | -3 | -12 | 36 |
| Coarse elevation model with linear structures | -20 | -26 | 38 | -27 | -30 | 40 | -4 | -12 | 33 |

*Risk*

The different factors were ranked based upon their impact on annual risk. A distinction was made between damage risk and casualty risk. The results are shown in Table 19. As mentioned before, the casualty risk may be distorted by anomalies in the elevation model.

Table 19: Risk

| Simulation | Damage risk (%) | Casualty risk (%) |
|---|---|---|
| Earlier breaching | 47 | 92 |
| Later breaching | -55 | -59 |
| Slower horizontal growth | -14 | -11 |
| Faster vertical growth | 25 | 38 |
| Breach growth by erosion | 6 | 15 |
| Variable surface roughness | -25 | -7 |
| Output interval | 1 | 7 |
| Symmetrical storm surge | -5 | -7 |
| Asymmetrical storm surge | 3 | 1 |
| Wind friction | 1 | 0 |
| Wave overtopping | 12 | 22 |
| Fine elevation model | - | - |
| Coarse elevation model | 32 | -32 |
| Fine with linear structures | -19 | 37 |
| Coarse with linear structures | -19 | 37 |

**Conclusion**

Time of breaching and breach growth strongly influence damage risk and casualty risk. Apart from this, the most influential parameter in the flood model is the surface roughness.

The resolution of the elevation model and the absence of linear structures can strongly influence the result of a risk evaluation. The relative importance of both factors depends on the type of risk (damage or casualties). When flood resisting structures are taken into account, the influence of elevation model resolution can be reduced. This requires an optimization of the couplings between the 1D breach model and the 2D flood plain model.

The following recommendations are made based on the previous analyses:

- 2D flood model:
    - Use of variable roughness
    - Neglecting Coriolis Forces

    - Detailed representation of line-shaped structures in the elevation model
- 1D breach model:
    - Use of erosion-based breach growth
    - Use of default flow formulae
- 1D/2D coupled models:
    - Careful link selection
    - numerical robustness
    - retaining 30 min output frequency
- Boundary conditions:
    - Use of asymmetric storm surge
    - taking into account wind effects
    - taking into account overtopping discharges

## 6.3 Uncertainty analysis hydraulic model

**Procedure**

The uncertainty associated with the hydraulic model was roughly estimated by means of a strongly simplified procedure, analogous to the one presented in the European IMPACT project (HR Wallingford, 2005).

1. Determine the most probable values for the parameters in the 1D breach model and the 2D flood model
2. Select a combination of parameter values for the 1D breach model resulting in minimal and maximal breach development
3. Select a combination of parameter values for the 2D flood model resulting in minimal and maximal flood propagation
4. Run a number of simulations with the coupled 1D and 2D models:
    - an initial simulation using the most probable parameter values for the breach and flood models
    - at least two additional simulations using the corresponding minimal and maximal breach and flood models
    - possibly the remaining six combinations of minimal, most probable and maximal breach and flood models

The application of this procedure results in 3 or 9 simulations for each return period.

The procedure was evaluated by means of a fine (high resolution) elevation model. In practice, this may not be feasible because of high computational requirements. A possible, intermediate solution would be to run the initial simulation by means of the fine elevation model in order to determine the most probable conditions and subsequently 3 to 9 additional simulations by means of a coarser elevation model in order to establish uncertainty margins surrounding these conditions. The initial simulation should be repeated using the coarse elevation model in order to identify unacceptably large resolution effects.

### 1D breach model

The number of breaches, the location of the breaches, the (initial) geometry of the breaches and the time of breaching all greatly influence the hydraulic model results. The variability of these factors is shown in the analysis of the uncertainty associated with coastal defence failure behaviour (chapter 7). That the breach characteristics are most dominant in the risk analysis will be made obvious in paragraph 6.4. In this paragraph an uncertainty analysis will be presented of the horizontal breach growth, one of the breach characteristics.

So, given the number, the location and the initial geometry of the breached, an important source of uncertainty in the breach model is horizontal breach growth. When buildings have been constructed on a sea dike, breaches caused by wave overtopping will develop in the empty spaces (roads, squares,…) between blocks of buildings. It is not clear if the flow through the breaches will be strong enough to cause the adjoining buildings to collapse and to carry out the debris.

When breaching is caused by wave overtopping, the assumption is made that the dike section which is being overtopped will fail simultaneously over its entire length. In this case, the initial breach width equals the width of the open space between the buildings. When breach growth is being modelled by mean of an erosion based breach growth model (described in 4.1), horizontal breach growth can be varied by means of the “Side Erosion Index” (SEI). Three different scenarios were identified:

- slow horizontal growth (SEI = 0)
- average horizontal growth (SEI = 2 = calibrated value)
- fast horizontal growth (SEI = 15)

The calibrated value for the SEI results in a horizontal growth of approximately a few meters per hour. The maximum value for the SEI results in a horizontal growth of a few tens of meters per hour. This corresponds to the highest values reported in literature.

### 2D flood model

The uncertainty analysis was carried out by means of the new elevation model, constructed following the procedure described in paragraph 4.2.

The primary source of uncertainty in the flood model is surface roughness. When surface roughness is varied as a function of land use, uncertainty increases as roughness increases. Literature values for the roughest surfaces exhibit the largest spread. This increase in uncertainty was taken into account by applying a fixed margin of uncertainty to the Strickler roughness coefficient “k”. A fixed absolute margin of uncertainty will automatically produce a larger relative margin of uncertainty for rougher surfaces, characterized by a lower k-value.

Three scenarios were identified:

- low roughness (large k, small n)
- average roughness (average k and n)
- high roughness (small k, large n)

The values for Strickler’s “k” are shown in Figure 50 and those for Manning’s “n” in Figure 51.

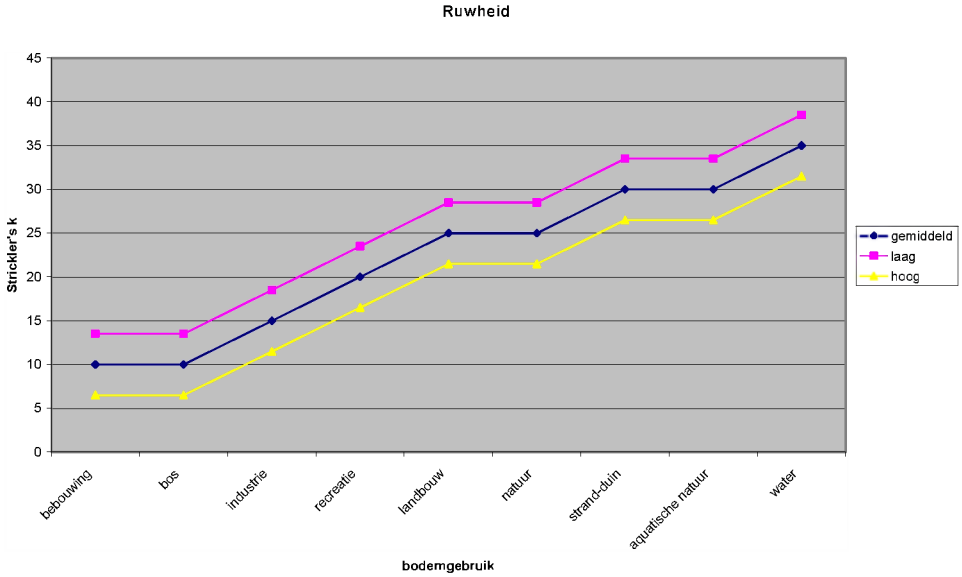


Figure 50: Variation of surface roughness (Strickler)

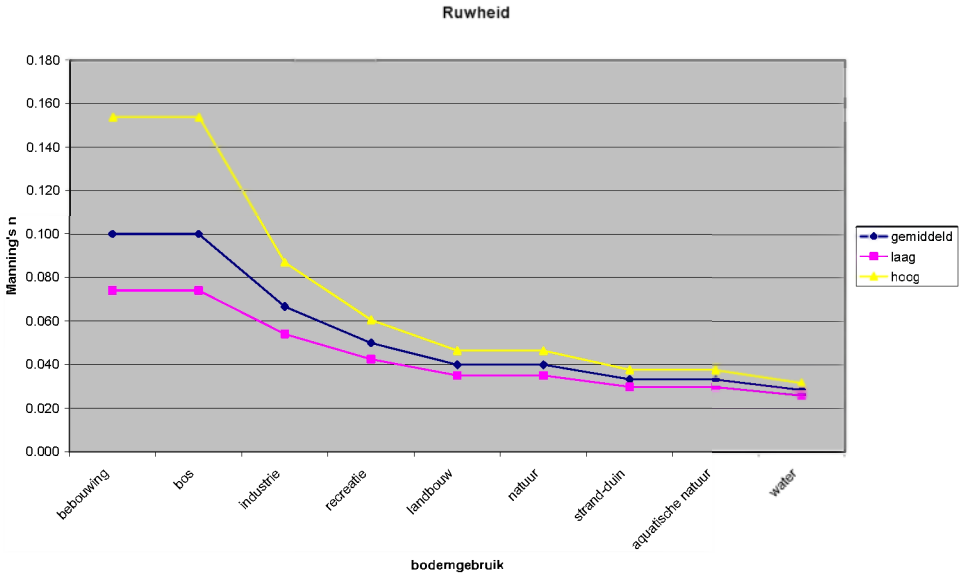


Figure 51: Variation of surface roughness (Manning)

### Coupled models

The three scenarios for horizontal breach growth and the three scenarios for surface roughness combine into nine scenarios for the coupled models:

- average breach growth rate and average surface roughness
- slow breach growth rate and high surface roughness

- fast breach growth rate and low surface roughness
- average breach growth rate and low surface roughness
- average breach growth rate and high surface roughness
- slow breach growth rate and average surface roughness
- fast breach growth rate and average surface roughness
- slow breach growth rate and low surface roughness
- fast breach growth rate and high surface roughness

The first scenario represents the "most probable" reference condition. The second and third scenarios establish the most extreme combinations. These three scenarios are necessary to obtain an idea of the overall uncertainty margins.

Computational facilities permitting, the fourth through seventh scenario can also be simulated. These offer an insight in the individual contributions from the breach growth model and the flood model to the overall uncertainty. For completeness, the last two combinations can be simulated too.

**Results**

*Horizontal breach growth*

Table 20 shows the maximum breach width for the reference scenario and both extreme scenarios: slow breach growth rate and high surface roughness (= minimal flooding) and high breach growth rate and low surface roughness (= maximal flooding).

Table 20: Breach growth : maximum breach width (m)

| Breach | T=4000 min. | T=4000 ref. | T=4000 max. | T=10000 min. | T=10000 ref. | T=10000 max. | T=40000 min. | T=40000 ref. | T=40000 max. |
|---|---|---|---|---|---|---|---|---|---|
| 233 | 60 | 62 | 73 | 60 | 61 | 68 | 60 | 64 | 89 |
| 234 | - | - | - | 60 | 68 | 110 | 60 | 69 | 115 |
| 235 | - | - | - | 60 | 62 | 77 | 60 | 62 | 74 |
| 236 | | | | 60 | 66 | 100 | 60 | 63 | 80 |
| 241 | | | | 60 | 66 | 99 | 60 | 66 | 102 |
| 242 | 60 | 67 | 106 | 60 | 68 | 115 | 60 | 74 | 133 |
| 243 | 60 | 68 | 114 | 60 | 71 | 136 | 60 | 87 | 188 |
| Zwin | - | - | - | - | - | - | 96 | 161 | 398 |

In the reference situation breach growth is very limited, except for the breach in the Zwin dike. This is caused by the short duration of breach flow and backwater effects.

The short duration of breach flow is caused by the high elevation of the coastal plain in the vicinity of the breaches; For a storm with a return period of 40000 years, the available time for breach flow after the peak water level (second high tide) is limited to about 5 hours for a breach with a bottom level of 6 m AD (Knokke), about 8 hours for a breach with a bottom level of 5 m AD (Het Zoute) and about 11 hours for a breach with a bottom level of 4 m AD (Zwin).

The backwater effects are caused by the fact that most breaches occur in urbanized areas. The built-up areas (Knokke, Het Zoute) have a high surface roughness (Manning's n = 0,1) which delays the flow of water towards the coastal plain. The low flow velocity and high downstream water levels reduce the breach growth rate to a level below that for free outflow conditions. The only exception is the breach in the Zwin dike, which occurs in a rural area with a much lower roughness (Manning's n = 0,04).

*Flooding*

The results for the different scenarios were compared by means of the hydraulic indicators used for the sensitivity analyses (cfr. section 6.2).

The results are summarized in Table 21, Table 22, Table 23, Figure 52 and Figure 53. For each scenario and each return period, the tables list the relative deviation (in percent) of all indicators from the reference situation.

Figure 52 shows the maximum depth of flooding for the reference scenario and the two extreme scenarios: slow breach growth rate and high surface roughness (= minimal flooding) and high breach growth rate and low surface roughness (= maximal flooding).

Figure 53 shows the maximum depth of flooding as a function of breach growth rate and surface roughness for a return period of 10000 years.

The uncertainty associated with horizontal breach growth and surface roughness turns out to be considerable. For return periods of 4000 and 10000 years the uncertainty associated with surface roughness is dominant. For a return period of 40000 years, the influence of horizontal breach growth is the largest. This shift can be explained by the strong impact of the breach in the Zwin dike, which only occurs with a return period of 40000 years.

Table 21: Procentual deviations of hydraulic indicators: volume, area, index

| Scenario | T=4000 volume (%) | T=4000 area (%) | T=4000 index (%) | T=10000 volume (%) | T=10000 area (%) | T=10000 index (%) | T=40000 volume (%) | T=40000 area (%) | T=40000 index (%) |
|---|---|---|---|---|---|---|---|---|---|
| Average breach growth rate and average surface roughness | - | - | - | - | - | - | - | - | - |
| Slow breach growth rate and high surface roughness | -28 | -22 | -11 | -25 | -26 | -11 | -29 | -24 | -16 |
| Fast breach growth rate and low surface roughness | 34 | 19 | 15 | 29 | 39 | 8 | 81 | 88 | 26 |
| Average breach growth rate and high surface roughness | -26 | -20 | -10 | -24 | -25 | -11 | -14 | -13 | -6 |
| Average breach growth rate and low surface roughness | 22 | 13 | 10 | 18 | 27 | 4 | 12 | 19 | 2 |
| Slow breach growth rate and average surface roughness | -2 | -1 | -1 | -2 | -3 | -1 | -17 | -15 | -9 |
| Fast breach growth rate and average surface roughness | 9 | 7 | 3 | 8 | 11 | 2 | 60 | 66 | 20 |
| Slow breach growth rate and low surface roughness | 18 | 11 | 8 | 15 | 23 | 2 | -8 | -5 | -5 |
| Fast breach growth rate and high surface roughness | -20 | -17 | -8 | -19 | -22 | -8 | 36 | 36 | 15 |

Table 22: Procentual deviations of hydraulic indicators: depth, velocity, rise (flooded area)

| Scenario | T=4000 depth (%) | T=4000 velocity (%) | T=4000 rise (%) | T=10000 depth (%) | T=10000 velocity (%) | T=10000 rise (%) | T=40000 depth (%) | T=40000 velocity (%) | T=40000 rise (%) |
|---|---|---|---|---|---|---|---|---|---|
| Average breach growth rate and average surface roughness | - | - | - | - | - | - | - | - | - |
| Slow breach growth rate and high surface roughness | -1 | -18 | 1 | 2 | -21 | 3 | -10 | -22 | -9 |
| Fast breach growth rate and low surface roughness | 12 | 24 | 6 | -7 | 7 | -3 | -6 | 21 | 18 |
| Average breach growth rate and high surface roughness | 0 | -18 | 1 | 3 | -20 | 3 | 0 | -11 | 2 |
| Average breach growth rate and low surface roughness | 6 | 20 | 2 | -8 | 4 | -6 | -7 | 3 | -5 |
| Slow breach growth rate and average surface roughness | -1 | -1 | -1 | 1 | 0 | 0 | -6 | -9 | -7 |
| Fast breach growth rate and average surface roughness | 3 | 2 | 2 | -2 | -2 | 0 | -6 | 12 | 19 |
| Slow breach growth rate and low surface roughness | 4 | 16 | 0 | -8 | 4 | -6 | -7 | 0 | -9 |
| Fast breach growth rate and high surface roughness | 2 | -17 | 2 | 5 | -18 | 5 | -3 | 7 | 25 |

Table 23: Procentual deviations of hydraulic indicators: depth, velocity, rise (total area)

| Scenario | T=4000 depth (%) | T=4000 velocity (%) | T=4000 rise (%) | T=10000 depth (%) | T=10000 velocity (%) | T=10000 rise (%) | T=40000 depth (%) | T=40000 velocity (%) | T=40000 rise (%) |
|---|---|---|---|---|---|---|---|---|---|
| Average breach growth rate and average surface roughness | - | - | - | - | - | - | - | - | - |
| Slow breach growth rate and high surface roughness | -22 | -36 | -21 | -24 | -41 | -24 | -31 | -41 | -30 |
| Fast breach growth rate and low surface roughness | 33 | 47 | 26 | 30 | 50 | 35 | 77 | 127 | 122 |
| Average breach growth rate and high surface roughness | -21 | -35 | -20 | -23 | -40 | -23 | -13 | -23 | -11 |
| Average breach growth rate and low surface roughness | 20 | 35 | 14 | 17 | 33 | 20 | 10 | 22 | 12 |
| Slow breach growth rate and average surface roughness | -2 | -2 | -2 | -2 | -4 | -3 | -20 | -23 | -21 |
| Fast breach growth rate and average surface roughness | 10 | 9 | 9 | 9 | 9 | 11 | 56 | 86 | 98 |
| Slow breach growth rate and low surface roughness | 15 | 29 | 11 | 13 | 28 | 15 | -12 | -5 | -13 |
| Fast breach growth rate and high surface roughness | -15 | -31 | -15 | -18 | -36 | -18 | 32 | 45 | 70 |

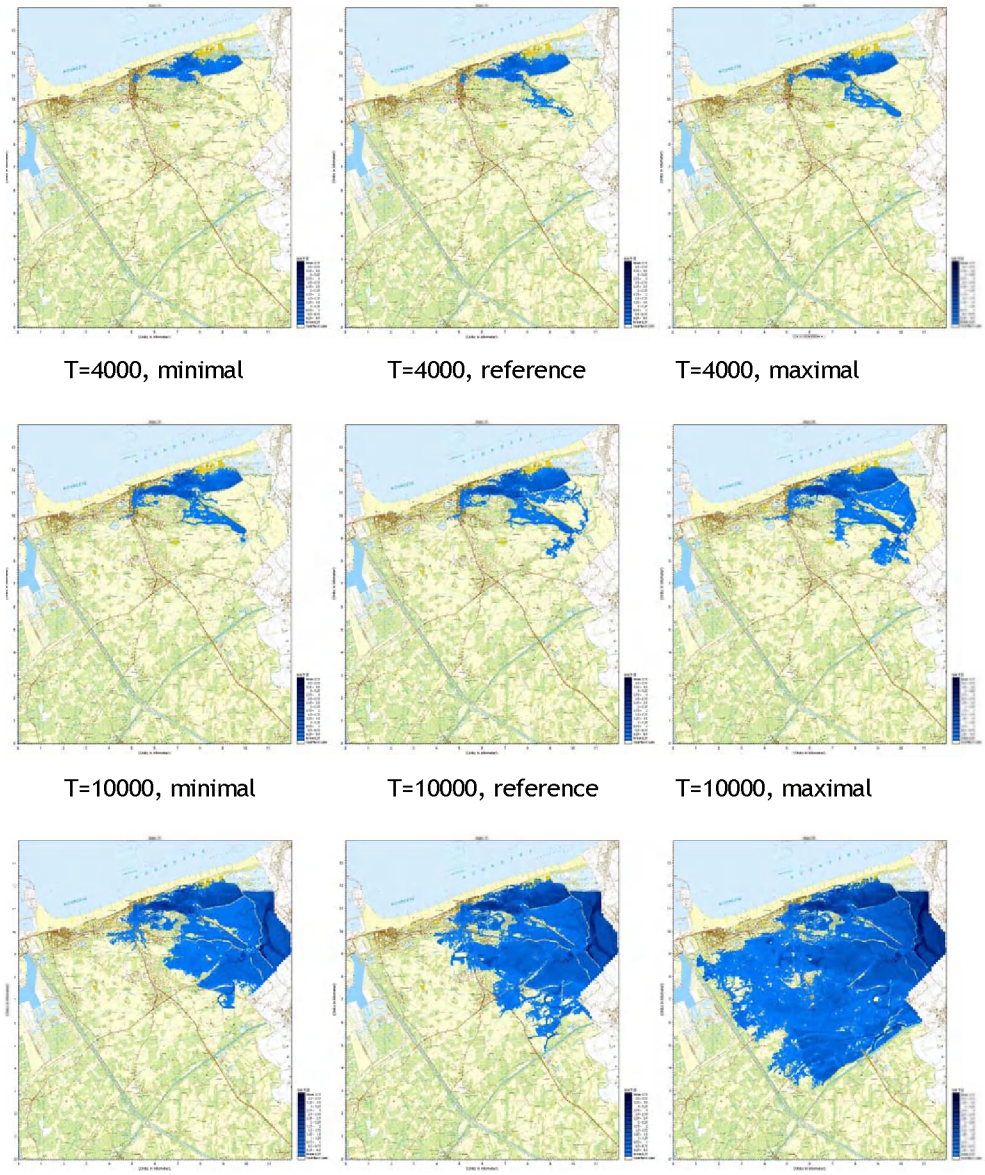


Figure 52: Flooding as a function of scenario and return period.

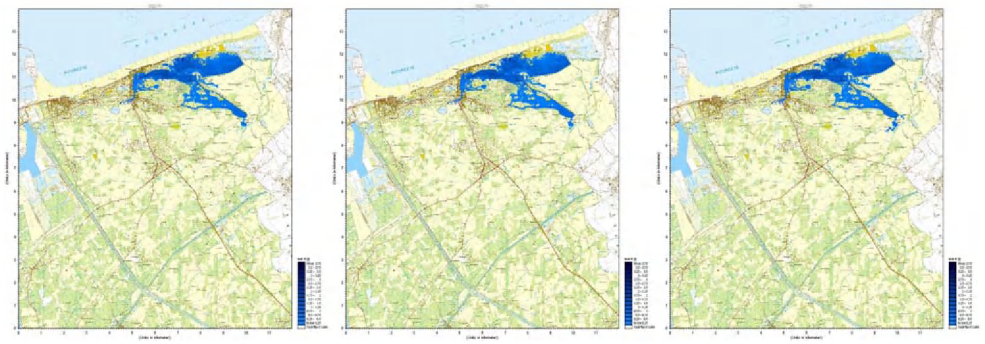

slow growth
high roughness

average growth
high roughness

fast growth
high roughness

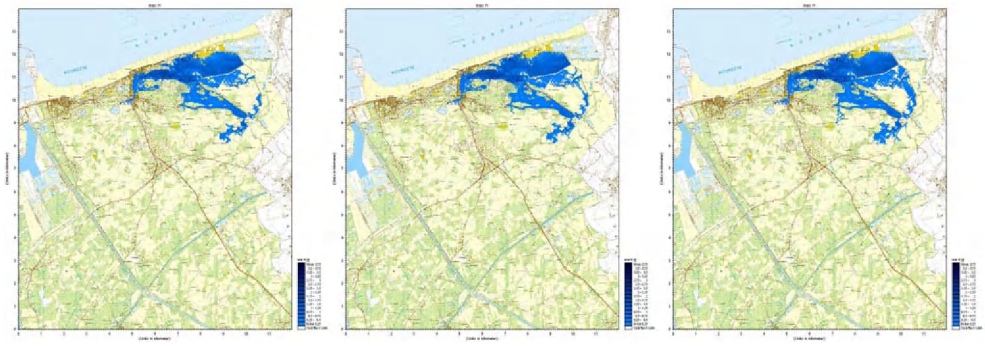

slow growth
average roughness

average growth
average roughness

fast growth
average roughness

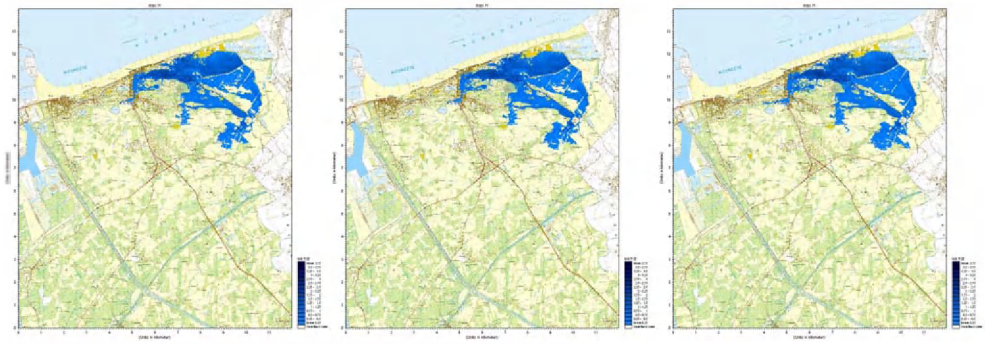

slow growth
low roughness

average growth
low roughness

fast growth
low roughness

Figure 53: Flooding as a function of breach growth and surface roughness (T=10000)

*Damage and casualties*

For each scenario, damage and casualties in the coastal plain were calculated. A distinction was made between damage and additional damage. The damage to the coastal defence itself was not taken into account.

For a description of the methods used for calculating damage and casualties, the reader is once again referred to chapter 5.

The calculation of damage and casualties was limited to Flanders. Possible damage and casualties in the Netherlands were neglected. The results are shown in Table 24. For each scenario and each return period, this table lists the relative deviation (in percent) of damage and casualties from the reference situation.

The uncertainty surrounding damage and casualties shows the same trends as the uncertainty surrounding hydraulic results: for return periods of 4000 and 10000 years the uncertainty associated with surface roughness is dominant and for a return period of 40000 years the influence of horizontal breach growth is the largest.

Table 24: Damage and casualties

| Simulation | T=4000 damage (%) | T=4000 additional damage | T=4000 casualties (%) | T=4000 damage (%) | T=4000 additional damage | T=4000 casualties (%) | T=4000 damage (%) | T=4000 additional damage | T=4000 casualties (%) |
|---|---|---|---|---|---|---|---|---|---|
| Average breach growth rate and average surface roughness | - | - | - | - | - | - | - | - | - |
| Slow breach growth rate and high surface roughness | -32 | -32 | -54 | -29 | -39 | -50 | -37 | -45 | -54 |
| Fast breach growth rate and low surface roughness | 46 | 38 | 82 | 34 | 79 | 71 | 62 | 75 | 313 |
| Average breach growth rate and high surface roughness | -30 | -31 | -52 | -28 | -39 | -49 | -19 | -31 | -26 |
| Average breach growth rate and low surface roughness | 30 | 34 | 58 | 21 | 48 | 38 | 9 | 29 | 21 |
| Slow breach growth rate and average surface roughness | -2 | -1 | -4 | -2 | -4 | -4 | -15 | -14 | -32 |
| Fast breach growth rate and average surface roughness | 11 | 6 | 17 | 7 | 10 | 12 | 38 | 46 | 232 |
| Slow breach growth rate and low surface roughness | 25 | 29 | 49 | 17 | 40 | 29 | -3 | 18 | -15 |
| Fast breach growth rate and high surface roughness | -25 | -26 | -46 | -23 | -38 | -42 | 22 | 2 | 174 |

*Risk*

The different factors were ranked based upon their impact on annual risk. A distinction was made between damage risk and casualty risk. The results are shown in Table 25.

Table 25: Risk

| Scenario | Damage risk (%) | Casualty risk (%) |
|---|---|---|
| Average breach growth rate and average surface roughness | - | - |
| Slow breach growth rate and high surface roughness | -33 | -54 |
| Fast breach growth rate and low surface roughness | 48 | 144 |
| Average breach growth rate and high surface roughness | -28 | -45 |
| Average breach growth rate and low surface roughness | 26 | 45 |
| Slow breach growth rate and average surface roughness | -4 | -12 |
| Fast breach growth rate and average surface roughness | 16 | 76 |
| Slow breach growth rate and low surface roughness | 20 | 30 |
| Fast breach growth rate and high surface roughness | -16 | 15 |

**Conclusion**

The uncertainty associated with hydraulic flood modelling can be significant (up to 10% and more). By means of two additional simulations, this uncertainty can be roughly estimated. The relative importance of the major sources of uncertainty (horizontal breach growth and roughness) are function of the considered return period as well as the examined risk (damage or casualties).

## 6.4 Uncertainty analysis failure behaviour

The sensitivity analysis and uncertainty analysis presented in the previous sections were based on the breaches (number, location, (initial) geometry and time of breaching) identified in the course of the failure behaviour of the coastal defences, carried out as part of the COMRisk case study "Vlaanderen/Zeeuws-Vlaanderen" (IMDC, 2005-b). The calculations clearly identify the time of breaching and the breach geometry as a major source of uncertainty. The uncertainty associated with the coastal defence failure analysis could cause the number and location of the breaches to change too.

A recent analysis of the failure behaviour of the coastal defences along the eastern part of the Flemish coast was carried out was based on new data and a methodology different from the one used in the COMRisk case study (no report available yet). This new analysis indicates that most probably no breaches will occur along the eastern part of the coast, not even during a storm with a return period of 40000 years. Comparing this result to the results of the COMRisk case study leeds to the conclusion that the uncertainty associated with failure behaviour outweighs the uncertainty associated with hydraulic modelling. Uncertainty analysis should therefore be focused on failure behaviour. The next chapter outlines a method for performing such an analysis.

# 7. Uncertainty on coastal flood risk calculations

## 7.1 Introduction

A coastal flood risk calculation estimates the damage by coastal flooding for a certain time horizon. Five different sources of uncertainty can be distinguished: unpredictability of the weather; uncertainty on the extreme value probability distribution of storm surges; unknown future values of economic growth rate, population growth rate, sea level rise rate and discount rate; limited knowledge of the behaviour of the coastal system; limited amount of measurements about the state of the coastal system. From a general analysis for the Belgian coastal zone it will be shown that the combined effect of these different sources of uncertainty results in a very large uncertainty on the calculated risk, namely a sigma of a factor more than 10. Some important sources of uncertainty are impossible to decrease substantially by doing research or measurements. Therefore the only option for coastal management is to deal with these large uncertainties. It is suggested to use calculation results relatively, namely to compare scenarios of coastal management in order to determine which scenario can best use an available budget for investment. Also it is concluded that risk calculation results would best be compared as ratios between scenarios (in %), not as differences (in euro/year).

**The Belgian coastal zone**

The Belgian coastal zone is part of the North West European low-lying coastal areas along the Southern North Sea, with a length of 65 km. In Belgium this area has an average width of 20 km and is located an average of 2 m below the surge level of an annual storm. The natural sea defences are sandy beaches and dunes. However, hard defence structures have replaced the dunes almost everywhere in the coastal towns and ports, and hence representing approximately two thirds of the Belgian coastal defence line. The Belgian standard of coastal protection is to be safe against a surge level with a return period of 1000 years (not fixed by law however). At present it is investigated if and how this standard could be modified using risk calculations.

## 7.2 Sources of uncertainty on coastal flood risk calculations

A coastal flood risk calculation aims at estimating the damage by coastal flooding for a certain time horizon. It is important to distinguish the different sources of uncertainty which influence a prediction of damage for a certain time horizon, for a given coastal zone. Five different sources of uncertainty are being distinguished here:

1) the unpredictability of the weather

2) the uncertainty on the extreme value probability distribution of extreme storm surge events

3) unknown future values of economic growth rate, population growth rate, sea level rise rate and discount rate, for the time horizon under consideration

4) the limited knowledge of the behaviour of the coastal system during a coastal flooding event

5) the limited amount of measurements about the actual state of the coastal system.

In the following sections a method will be presented to estimate the impact of these five sources of uncertainty on the damage, with a preliminary application for coastal flood risk assessment of the Belgian coastal zone.

## 7.3 Uncertainty caused by the unpredictability of the weather

The predictability of the weather is very limited (~a few days), compared to the time horizon T considered when doing coastal flooding risk calculations (~100 years). The chance of occurrence of a coastal flooding is very small (for the Belgian coast ~1/10000 years) compared to the time horizon considered in actual coastal zone management (~100 years). So for the Belgian coast in 99 out of 100 possible futures there is no coastal flooding damage during the time horizon under consideration. Coastal flooding damage in a specified time horizon T is the result of a Poisson process. Weather systems change each few days. For every independent weather system there is a chance of occurrence of an extreme storm surge that results in coastal flooding. Because the considered time horizon T (~100 years) is much smaller than the return period R of coastal flooding (~10000 years) the expected damage E(D) can be calculated as E(D)=T/R×S in which S is the damage in case of a coastal flooding. For clarity of the arguments the damage due to coastal flooding is simplified to a constant value S. In other words, the relation between damage S and return period R is simplified as a step-function. This binary approach is to be generalised for a more realistic case in which the damage S is an increasing function of the return period R, but this is out of the scope of this paper. So the expected damage (euro) and risk (euro/year) are defined by the following equations.

$$E(D) = \frac{T}{R} \cdot S$$

$$risk = \frac{E(D)}{T} = \frac{S}{R}$$

The variation around the expected value for damage during the time horizon considered can be expressed by the coefficient of variation valid for a Poisson process $\mu = \sqrt{R}/\sqrt{T}$.

For the Belgian coast typical values are R ~10000 years and T ~100 years, so $\mu \sim 10$. This means a very large uncertainty on the damage, namely a factor ~10.

## 7.4 Uncertainty on the extreme value probability distribution of extreme storm surges

The extreme value probability distribution is essentially the result of an extrapolation of storm surge events recorded during the past decades/century. For the Belgian coast almost 100 years of reliable storm surge measurements are available. However, such a dataset remains very limited when one has to determine storm surge levels of extreme events with return periods of ~10000 years. Because of the importance of extreme storm surge levels in coastal management, in Belgium several detailed statistical studies were carried out in previous years. Extreme value probability distributions were determined, and also the uncertainties on the distributions. The results of Probabilitas (1999) are shown in Figure 54.

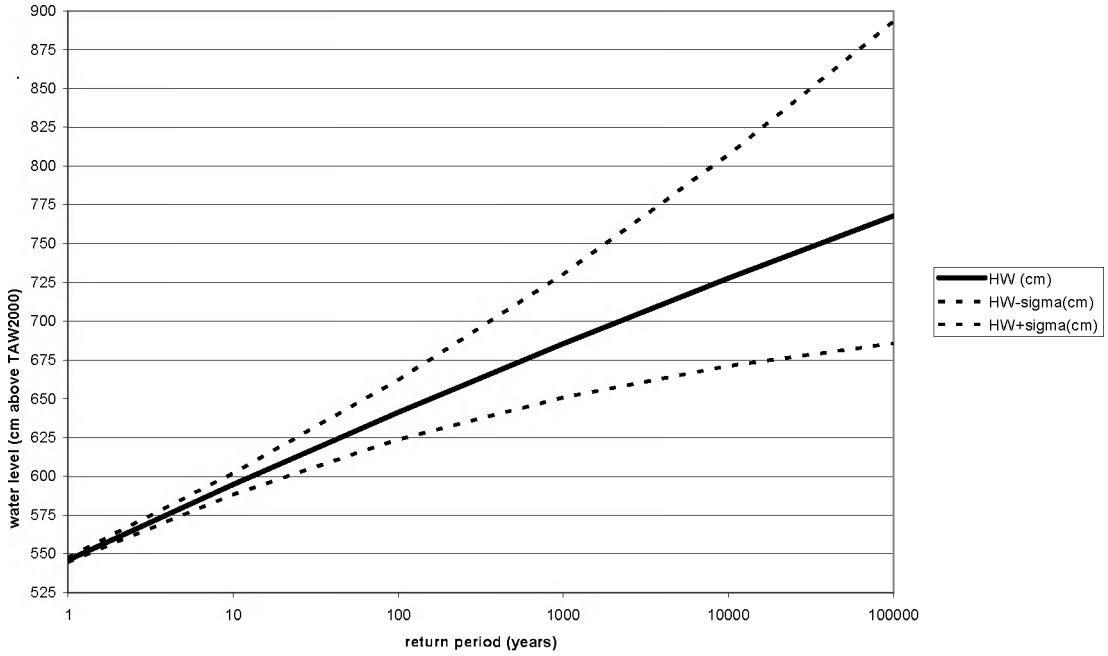


Figure 54 Probability of exceedance of storm surge level in Oostende including uncertainty estimate (Probabilitas 1999).

It is obvious that the uncertainty is larger for higher storm surge levels. For a typical level causing coastal flooding (return period of 10000 years) the uncertainty on the return period is approximately a factor 10. This results in a very large uncertainty on the expected damage during a considered time horizon, namely a sigma of a factor of ~10.

## 7.5 Uncertainty on the future values of economic growth rate, population growth rate, sea level rise rate and discount rate

When considering a time horizon for a coastal flooding risk calculation, e.g. T = 100 years, it is essential also to consider some continuously evolving system characteristics. Namely, four elements are continuously changing: the economic value and the size of the population in the coastal zone prone to flooding, the sea level -which is rising with or without an effect of climate change-, and the discount rate. For sake of clarity a constant rate for these parameters is assumed.

A first systematic changing element is the amount of values at risk of coastal flooding. More specifically is meant the rate of growth of the economical values and also the rate of population growth in the coastal zones prone to flooding. For the Belgian coastal zone the actual (at present) rates are measured to be 2 % per year for economical growth and 0,2 % per year for population growth (especially elderly enjoying retirement at the coast). Predictions of these socio-economic rates for the coming ~100 years are very uncertain. Estimates of the expected variation can be determined from the rates in the previous century, or by using results of global scenario studies which are regularly performed by planning bureaus.

A second systematic changing element is the sea level rising. For the Belgian coast the actual rise of the high water level (relative to the height of the coastal defences) is 1,8 mm per year (see Verwaest & Verstraeten, 2005). A rising of the average sea level results in a rising of the probabilities of extreme storm surge levels, and thus also a rising of the coastal flooding risks. For the Belgian coast the risks have been rising with 0,7 %/year due to the sea level rise of 1,8 mm/year. Predictions of sea level rise in the 21st century are very uncertain. Depending on the size of the impact of the global warming different scenarios are foreseen, ranging from a very optimistic scenario of no acceleration of sea level rise, to a very pessimistic scenario of an acceleration to a 5 times higher rate of sea level rise (~90 cm/100 years = 5 x 1,8 mm/year). This very pessimistic scenario results in a yearly increase of the coastal flooding risks with 3,5 % (3,5 % = 5 x 0,7 %).

A third systematic changing element is the discount rate. In our capitalist economies money brings more money, thanks to the interest rate. This also means that future costs have to be valued less at present day. In Belgian the actual discount rate is about 4 % (corrected for inflation). Predictions of the discount rate for the coming century are very uncertain. An estimate of the expected variation can be determined from the discount rates in the previous century or from socio-economic projections.

Combining the different rates of change, considering them to be independent of each other and small (<<1), results in a net rate of change. Estimates for the different rates for the Belgian coastal zone are summarised in Table 26.

Table 26 Rates of change for the 21st century:

expected values and uncertainties for the Belgian coastal zone

| | Expected value ([+] means resulting in larger coastal flooding risks, [-] means the opposite) | Estimate of uncertainty on the rate of change (+- sigma) |
|---|---|---|
| Rate of change of economic assets at risk | 2 %/year [+] | $\sigma$ = +- 2 %/year |
| Rate of change of population at risk | 0,2 %/year [+] | $\sigma$ = +- 1 %/year |
| Rate of sea level rise | 2 %/year [+] | $\sigma$ = +- 1 %/year |
| Discount rate | 4 %/year [-] | $\sigma$ = +- 2 %/year |
| Net rate of change from an economical point of view (excluding population change) | 0 %/year | $\sigma$ = +- 3 %/year |

According to the estimates above, the expected value of the net rate of change from an economical point of view (excluding population change) for the Belgian coast is “no change”. However, positive or negative net change rates are possible, most probably less than +- 6% (~ +- 2 x sigma).

Considering a constant net rate of change r (positive means increasing flooding risks), the calculation of the expected damage in a certain time horizon T is with the following equation.

$$E(D) = \frac{T}{R} \cdot S \cdot \frac{(1+r)^T - 1}{rT}$$

This equation is a modification to take into account the effect of changing conditions during the time horizon T considered. It differs from the classical risk formula only by the multiplication with a so called rate factor. The rate factor is thuss defined by equation:

$$ratefactor = \frac{(1+r)^T - 1}{rT}$$

For typical values of the time horizon T, the rate factor is calculated for different values of r. The results are given in Table 27.

Table 27 The rate factor calculated for different values of T and r.

| | $T$ = 50 years | $T$ = 100 years | $T$ = 200 years |
|---|---|---|---|
| $r$ = -6 %/year | 0,32 | 0,17 | 0,08 |
| $r$ = -5 %/year | 0,37 | 0,20 | 0,10 |
| $r$ = -4 %/year | 0,44 | 0,25 | 0,12 |
| $r$ = -3 %/year | 0,52 | 0,32 | 0,17 |
| $r$ = -2 %/year | 0,64 | 0,43 | 0,25 |
| $r$ = -1 %/year | 0,79 | 0,63 | 0,43 |
| $r$ = 0 %/year | 1 | 1 | 1 |
| $r$ = +1 %/year | 1,29 | 1,70 | 3,16 |
| $r$ = +2 %/year | 1,69 | 3,12 | 12,87 |
| $r$ = +3 %/year | 2,26 | 6,07 | 61,39 |
| $r$ = +4 %/year | 3,05 | 12,38 | 318,72 |
| $r$ = +5 %/year | 4,19 | 26,10 | 1729,16 |
| $r$ = +6 %/year | 5,81 | 56,38 | 9593,74 |

One can observe from Table 27 that for larger values of the net rate of change r and/or larger values for the time horizon T the rate factor becomes largely different from 1.

For the case of the Belgian coastal zone (r= 0 % +- sigma 3%) the coefficient of variation of the rate factor is of the order of ~10 if one takes the time horizon 2100 (~ 100 years). This results in a very large uncertainty on the expected damage for coastal flooding, namely a sigma of a factor ~10. However, if one takes the time horizon 2050 (~ 50 years) the uncertainty is much less, namely a sigma of a factor ~2.

## 7.6 Uncertainty caused by the limited knowledge of the behaviour of the coastal system during an extreme storm surge event

Coastal flooding events are very rare. For the Belgian coastal zone ~1/10000 years. So, not much empirical evidence can be gathered easily to understand the behaviour of the coastal

system during extreme storm surge events. Scientific progress is made by combining empirical studies of worldwide occurring coastal flooding events, and model studies of the local coastal system under consideration (mathematical modelling as well as physical model experiments). Present scientific understanding of the behaviour of the coastal system during a coastal flooding event is limited. From experts (see for example Oumeraci 2005) it is clear that especially on the failure behaviour of sea defences and the process of breach growth a lot more scientific research is needed. Anyway calibration of models will remain difficult due to the lack of in situ measurements (wave impact, breaching and breach growth, flood propagation) of extreme events having a very low probability of occurrence.

Estimating the uncertainty on the coastal flooding risk caused by the present lack of scientific understanding about the failure behaviour of sea defences is only possible by questioning experts. For the Belgian coastal defences an uncertainty of 0,5 m on the storm surge level at which a certain coastal defence fails resulting into breach formation and coastal flooding, corresponds to an uncertainty of approximately a factor 10 on the flooding risks. From expert opinions one may preliminary estimate that this source of uncertainty is resulting in an uncertainty on the expected damage with a sigma of a factor ~3 (corresponding to a storm surge difference of ~0,25 m).

## 7.7 Uncertainty caused by the limited knowledge of the behaviour of the coastal system during an extreme storm surge event

Many measurements are needed to characterise the state of the coastal system with respect to its vulnerability for coastal flooding damage. Measurements are needed on the one hand for characterising the coastal defences, and on the other hand for characterising the zones prone to flooding. Main characteristics of the coastal defences are its height (relative to storm surge level), its erosion resistance and its structural stability. Main characteristics of the zones prone to flooding are its height (relative to storm surge level), its area, its land use and its population density.

For the Belgian coastal zone detailed measurement results are available for all main characteristics of both the coastal defences and the zones prone to flooding. The least information is existing regarding the erosion resistance and the structural stability parameters of the hard coastal defence structures. Therefore a measurement campaign is being carried out in which geotechnical parameters and structural parameters are determined for the hard coastal defence structures along the Belgian coastline (mainly sea walls).

In previous studies estimates were made of the uncertainty on coastal flooding risks in Belgium caused by a lack of data (e.g. Verwaest, 2000). From these studies it can be preliminary estimated that for the Belgian coastal zone a coefficient of variation of ~3 results for the expected damage, mainly caused by the aforementioned lack of detailed measurements on the composition of the hard coastal defence structures.

Other parameters which are less well known are the hydraulic roughness of the flooding zones (e.g. urban areas in which flooding concentrates in streets, or the effect of the flow via existing drainage systems in the polders) and the damage functions for different types of valuables (e.g. the relation between the flood water level and the proportion of the value of a house damaged by flooding, or the damage to point objects -not detectable from land use maps- with a very high localised value such as drinking water wells, historical buildings etcetera). Ongoing research aims at further reducing uncertainties on these parameters.

## 7.8 The combined effect of the different sources of uncertainty

From the analysis of the effect of the five different sources of uncertainty on the coastal flooding damage for a given time horizon, it is clear that the combined effect results in a very large uncertainty on the expected coastal flooding damage for the Belgian coastal zone, namely a sigma of a factor more than 10. In Table 3 the effect of all uncertainty sources is summarised.

Table 28 Summary of the effect of the different sources of uncertainty for a risk calculation. Estimates from preliminary analysis for the Belgian coastal zone.

| | Source of uncertainty | Resulting uncertainty on the expected damage in terms of a sigma factor. |
|---|---|---|
| 1 | Unpredictability of the weather | ~10 (coefficient of variation) |
| 2 | Extrapolated values for exceedance frequencies of extreme storm surge levels | ~10 |
| 3 | Future net rate of change (combined effect of economical growth, population growth, sea level rise and discount rate) | ~10 (2100)<br>~2 (2050) |
| 4 | Limited understanding of the behaviour of the coastal system during an extreme storm surge | ~3 |
| 5 | Limited understanding on the state of the coastal system | ~3 |
| | All uncertainty sources combined | more than 10 |

Given the nature of the stochastics the result of a flood risk calculation can be tentatively assumed to be lognormal. This is a simple distribution that can represent a sigma of a factor e.g. 10 or more. An important characteristic of a lognormal stochast is the large difference between the median value (50% probability to have a higher value, 50% probability to have a lower value) and the expected value (weighted average). It can be shown that the expected value is a factor m larger than the median value, with m given by the following equation in function of the sigma factor $\sigma$.

$$m = \sqrt{\sigma}^{\ln(\sigma)}$$

For larger values of $\sigma$ the factor m becomes increasingly larger, as can be seen from Table 29.

Table 29 Lognormal distribution with sigma factor $\sigma$, resulting in a factor $m$ difference between expected value and median value.

| sigma factor $\sigma$ | factor $m$ |
|---|---|
| 2 | 1,3 |
| 5 | 3,7 |
| 10 | 14,2 |
| 20 | 88,9 |
| 50 | 2104,8 |

For the Belgian coastal zone the factor m is at least 10, given the estimate of a sigma factor of more than 10.

## 7.9 How to use coastal flood risk assessment results in coastal management?

Some important sources of uncertainty are impossible to decrease substantially by doing research or measurements, e.g. the uncertainty on the extreme value probability distribution of storm surge levels. Therefore the only option for coastal management is to deal with these large uncertainties with a sigma of a factor more than 10. Because the uncertainty on a risk calculation is that large, it is concluded that coastal flood risk calculations would best be used relatively, namely to compare scenarios of coastal management in order to determine which scenario can best use an available budget for investment.

For a given coastal zone, there is a complete correlation between different scenarios for three of the five sources of uncertainty (namely the first three in the Table 28). Also there is partial correlation between scenarios for the other two sources of uncertainty (the last two in Table 28). Taking into consideration the estimates of the different sources of uncertainty (see Table 28), a justifiable assumption is to simplify the degree of correlation between different scenarios as full (100 %) correlation.

The difference in risk between two scenarios "1" and "2" then has :

- an expected value : $E = E_1 - E_2 = m \cdot (median_1 - median_2)$
- a standard deviation : $\sigma_E = E \cdot \sqrt{m^2 - 1} \cong m \cdot E$ (m >> 1)
- a coefficient of variation : $\mu_E = \frac{\sigma_E}{E} \cong m$

The ratio of risks of two scenarios "1" and "2" then has :

- an expected value : $\varepsilon = \frac{E_1}{E_2} = \frac{median_1}{median_2}$
- a standard deviation : $\sigma_\varepsilon = 0$
- a coefficient of variation : $\mu_\varepsilon = \frac{\sigma_\varepsilon}{\varepsilon} = 0$

Because we estimated the factor m to be at least 10 for the Belgian coastal zone it is concluded that risk calculation results would best be compared as ratios between scenarios (in %), not as differences (in euro/year).

For example, if for a certain scenario of coastal defence improvement works the risk is calculated to be 1 million euro/year, while in the reference situation the risk is calculated to be 2 million euro/year, then it can be stated quantitatively that the improvement scenario has reduced the risk with 50 %. Contrary to this, the avoided risk by the improvement scenario (in euro/year) cannot be given with accuracy.

# 8. Conclusions

## 8.1 Key message

It was concluded that the uncertainty on a risk estimation is very large namely at least a factor 10, mainly due to uncertainties on the hydraulic load extreme statistics and on the failure behaviour of coastal flood defences. The effect of the uncertainty on future developments (sea level rise, societal evolution…) is comparetively small if one takes a time horizon until 2050, but it becomes the dominating source of uncertainty if one takes a time horizon of (more than) 100 years (2100 and beyond).

Due to large uncertainties coastal flood risk assessments cannot be used as absolute numbers. To compare scenarios, coastal flood risk ratios (in %) are relatively accurate while coastal flood risk differences (in euro/year) cannot be given with accuracy.

So, although theoretically coastal flood risk calculations are suitable to

- compare risks between different locations;
- compare risks for a given location between different scenarios (e.g. alternative measures can be evaluated to determine the risk reduction achieved by each measure);

…in practice, due to very large uncertainties influencing the results of the risk calculations, risk calculations are primarely of use to compare scenarios for a given system where uncertainties are strongly correlated (e.g. the system of the Belgian coastal zone). Moreover, within such a system, the coastal risk comparisons are to made as percentages relative to each other in order to cancel out most uncertainty, due to the (quasi) lognormal distribution of the sources of uncertainty. Coastal risk comparisons as differences are surrounded by very large uncertainties, and therefore are unsufficient to pretend to be a base for a cost-benefit analysis aiming to find a optimal balance between investment costs of coastal defence measures and risk reduction achieved by the same investments.

Nevertheless, coastal risk calculations remain an important supporting tool for coastal flood risk management. The results -including their uncertainties- can best be used in a multi criteria analysis, where economic, social and ecological perspectives are combined.

## 8.2 Other messages

A method is developed to include a time horizon in a flood risk calculation. Flood risk calculations can be multiplied by a so called rate factor if one aims to have a time horizon of several decades (e.g. 2050). This rate-factor combines the impacts of climate change and of growth in the coastal zone as well as discount rate.

Regarding flood modelling:

- a model with a relatively coarse grid has the advantage that the calculation time is relatively short. These fast running hydraulic models are very useful for comparison between scenarios if the one-dimensional topographic elements such as secondary dikes or embankments parallel to roads, railways and waterways are implemented in a correct way, namely as continuous elements in the bathymetry of the model.

- for a given number of breaches, the main sources of uncertainty in hydraulic modelling are breach growth and hydraulic roughness (uncertainties regarding other parameters of hydraulic modelling have a negligible effect). However, the resulting uncertainty on the risk is relatively small compared with the uncertainty on the risk caused by the uncertainty on the number of breaches.

The methodologies for calculating risks are still evolving. It is work in progress. More research is going on at the moment and is needed in the future. Given the extent and the nature of the uncertainties involved, research to improve the knowledge on the failure behaviour of coastal flood defences is especially recommended.

# 9. References

## 9.1 Publications from the SAFECoast action3b project

Vanderkimpen, P., Peeters, P., Flood modeling for risk evaluation: a MIKE FLOOD sensitivity and uncertainty analysis, River flow 2008, 3-5 September 2008, Ceşme-Izmir, Turkey (abstract accepted)

Vanderkimpen, P., Melger, E., Peeters, P., Flood modeling for risk evaluation: a MIKE FLOOD vs. SOBEK 1D2D benchmark study, River flow 2008, 3-5 September 2008, Ceşme-Izmir, Turkey (abstract accepted)

Verwaest, T., Van Poucke, Ph., Reyns, J., Van der Biest, K., Vanderkimpen, P., Peeters, P., Kellens, W., Vanneuville, W., 2008, SAFECoast: Comparison between different flood risk methodologies: action 3B report, SAFECoast Interreg IIIb North Sea project, Flanders Hydraulics Research, Belgium

Verwaest, T., Vanneuville, W., Peeters, P., Mertens, T., De Wolf, P., Uncertainty on coastal flood risk calculations, and how to deal with it in coastal management. Case of the Belgian coastal zone. 2nd IMA international conference on flood risk assessment, 4-5 September 2007, university of Plymouth, UK

Verwaest, T., Viaene, P., Verstraeten, J., Mostaert, F., Kellens, W., Vanneuville, W., Monitoring, understanding and blocking sea level rise (De zeespiegel meten, begrijpen en afblokken), De Grote Rede, 15, december 2005, pp. 15-25

## 9.2 Literature

Allsop, N.W.H., 2005. D38: Report on Hazard analysis. Rapport in het kader van CLASH WP6, Coördinator HR Wallingford, 28 p.

CPB, NMP, CBS, 2004, “Welvaart en Omgeving” (Prosperity and Environment)

Federal Planning Bureau, 2007, Growth and productivity in Belgium, working paper 5-07, March 2007

Federal Planning Bureau, 2006, Het klimaatbeleid na 2012 - analyse van scenario's voor emissiereductie tegen 2020 en 2050, (The climate policy after 2012 - Analysis of scenarios for the reduction of emissions by 2020 and 2050), July 2006, commissioned by the Federal Minister of the Environment.

Gauderis J., De Nocker L., Bulckaen D., Sigmaplan - Maatschappelijke kosten-batenanalyse - syntheserapport (Sigma plan - analysis of social costs and liabilities - synthesis report 2005, commissioned by Waterways and Sea Canal NV, Ministry of Mobility and Public Works.

IMDC, 2005-a, book of hydraulic boundary conditions (Hydraulisch Randvoorwaardenboek), commissioned by Coastal Division, Ministry of Mobility and Public Works.

IMDC, 2005-b, COMRISK: Flood Risk in Flanders/Zeeuws-Vlaanderen, commissioned by Coastal Division, Ministry of Mobility and Public Works and supported by Interreg.

IPCC, Climate change 2007 : the physical science basis - summary for policymakers - contribution of working Group 1 to the 4th assessment report of the intergovernmental panel on climate change, February 2007

Jonkman, B., 2004. Methode voor de bepaling van het aantal slachtoffers ten gevolge van een grootschalige overstroming. Onderbouwing van de slachtofferfuncties voor de Standaardmethode Schade en Slachtoffers als gevolg van overstromingen, Ministerie van Verkeer en Waterstaat, Rijkswaterstaat, DWW, 82 p.

Jonkman, B., Cappendijk, P., 2006. Veiligheid Nederland in Kaart - Inschatting van het aantal slachtoffers ten gevolge van een overstroming, Ministerie van Verkeer en Waterstaat, Rijkswaterstaat DWW

Jonkman, B., 2007. Loss of life estimation in flood risk assessment, theory and applications, doctoraatsthesis, Technische Universiteit Delft, 354 p.

Kellens, W., Vanneuville, W., 2007a. Realisatie van een methode voor de berekening van schade bij geotechnisch falen van rivierdijken. Internal report Flanders Hydraulics Research, Belgium

Kellens, W., Vanneuville, W., 2007b. Opstellen van schadefuncties rekening houdend met de stroomsnelheid bij geotechnisch falen van zeeweringen. Internal report, Flanders Hydraulics Research

Kellens, W., Vanneuville, W., 2007c. Aanpassing van de schadefuncties bij golfoverslag op de zeewering. Internal report, Flanders Hydraulics Research

Kellens, W., Vanneuville, W., 2007d. Opstellen van slachtofferfuncties en factorengrids voor evacuatie. Internal report, Flanders Hydraulics Research

Kolen, B., Geerts, R., 2006. Als het tóch misgaat: Overstromingsscenario's voor rampenplannen, betooglijn, HKV Lijn in Water en AVIV in opdracht van Rijkswaterstaat RIZA, 91 p.

Oumeraci H., 2005, Integrated risk-based design and management of coastal flood defences, Die Küste 70, 151- 172.

Probabilitas, 1999, Statistische modellering van extreme hoogwaterstanden en het overeenkomstige zeeklimaat in relatief diep water, (Statistical modelling of extreme high water levels and the corresponding maritime climate in relatively deep water), improvement of the access to the port of Ostend), 2002, commissioned by Coastal Division, Ministry of Mobility and Public Works.

Swillens, M.F., 2002. Scheveningen: Badplaats of Bolwerk? Een studie naar de mogelijkheden om de stormvloedrisico's in badplaatsen te beheersen. Afstudeerrapport, TU Delft, subfaculteit der Civiele Techniek, 302 p.

Technum-IMDC-Alkyon, 2002, Hydrodynamische randvoorwaarden voor het ontwerp - waterstanden en golfklimaat (structureel herstel van de kustverdediging te Oostende en verbetering van de haventoegang naar de haven van Oostende), (Hydrodynamic boundary conditions for the water levels and wave climate (structural strengthening of the coastal defence in Ostend and improvement of the access to the port of Ostend), commissioned by Coastal Division, Ministry of Mobility and Public Works.

Van der Klis H., Baan P., Asselman N., Historische analyse van de gevolgen van overstromingen in Nederland - een globale schatting van de situatie rond 1950, 1975 en 2005 (Historical analysis of flooding in the Netherlands - an overall estimate of the situation in about 1950, 1975 and 2005) December 2005, WL Delft Hydraulics commissioned by DG Rijkswaterstaat, RIZA

Van Manen, S., 2001, Pilot Case Overstromingsrisico (PICASO) - Deel VI: Eindrapport, Ministerie van Verkeer en Waterstaat, Directoraat-Generaal Rijkswaterstaat, Bouwdienst.

Vanneuville, W., Maeghe, K., De Maeyer, Ph., Mostaert, F., Bogaert, P., 2002. Risicobenadering bij waterbeheersingsplannen, Methodologie en case-study Denderbekken, Universiteit Gent in opdracht van het Ministerie van de Vlaamse Overheid LIN-AWZ Afdeling Waterbouwkundig Laboratorium en hydrologisch onderzoek

Vanneuville, W., Maeghe, K., De Maeyer, Ph., Mostaert, F., 2003. Risicobenadering bij waterbeheersingsplannen, aanvulling 1: slachtoffers. Methodologie en case study Denderbekken, Universiteit Gent in opdracht van het Ministerie van de Vlaamse Overheid LIN-AWZ Afdeling Waterbouwkundig Laboratorium en hydrologisch onderzoek

Vanneuville, W., Maddens, R., Collard, Ch., Bogaert, P., De Maeyer, Ph., Antrop, M., 2006. Impact op mens en economie t.g.v. overstromingen bekeken in het licht van wijzigende hydraulische condities, omgevingsfactoren en klimatologische omstandigheden, studie uitgevoerd in opdracht van de Vlaamse Milieumaatschappij, MIRA, MIRA/2006/02, UGent

Verhaeghe, H., 2002. Toelaatbare golfoverslag over zeeweringen: literatuuroverzicht. Universiteit Gent, vakgroep Civilie Techniek, Afdeling Weg- en Waterbouwkunde, intern rapport, 23 p.

Verwaest T., 1999, Overschrijdingskromme extreme stormpeilen te Oostende - berekening volgens convolutie van astronomische componente en opzetcomponente, (Extrapolation curve for extreme storm levels in Ostend - calculation in accordance with the convolution of astronomical component and planned component), internal memorandum Coastal Division, Ministry of Mobility and Public Works.

Verwaest T., 2000, Kustverdediging, Watergebonden Veiligheid, proceedings of symposium by Flanders Hydraulics Research, Antwerpen, September 22.

Verwaest T. and Verstraeten J., 2005, Measurements of sea-level rise at Oostende (Belgium). In Baeteman C. (ed.), abstract book, Late Quaternary Coastal Changes: Sea Level, Sedimentary Forcing and Anthropogenic Impacts, a joint INQUA-IGCP Project 495 Conference, Dunkerque, June 28-July 2, 2005.

Viaene P., 2000. Effects of a possible climate change on sea level, river effluents and the high tide and storm frequencies: literature study [Effecten van een mogelijke klimaatverandering op het zeespiegelniveau, de rivierafvoer en de frequentie van hoogwaters en stormen: literatuurstudie]. WL Rapporten, 592. Flanders Hydraulics Research.

Visser, 2002. Breach growth in sand sikes, PhD, TUDelft, the Netherlands.

Vrisou Van Eck, N., Kok, M., Vrouwenvelder, A.C.W.M.,1999. Standaardmethode Schade & Slachtoffers als gevolg van overstromingen - deel 2: Achtergronden, HKV-Lijn in Water en TNO Bouw in opdracht van RWS-DWW, december 1999

Working group on updating the discount rate, advice January 2007, Dutch parliament document.

Ministry of Transport, Public Works and

Water Management VenW [NL]

National Institute for Coastal and Marine Management

Rijkswaterstaat RIKZ (project management)

PO Box 20907

2500 EX Den Haag

The Netherlands

Contact: Niels Roode

E-mail: niels.roode@rws.nl

Tel: +31 70 311 4368

Fax: +31 70 311 4600



Road and Hydraulic Engineering Division

Rijkswaterstaat DWW

PO Box 5044

2600 GA Delft

The Netherlands

Contact: Wout Snijders

E-mail: wout.snijders@rws.nl

Tel: +31 15 251 8428

Fax: +31 15 251 8555



Ministry of the Interior of the Land Schleswig-Holstein [D]

Emergency Planning & Disaster Management Division

PO Box 7125

D-24171 Kiel

Germany

Contact: Matthias Hamann

E-mail: matthias.hamann@im.landsh.de

Tel: +49 431988 3470

Fax: +49 431988 3480



Danish Coastal Authority [DK]

Højbovej 1

PO Box 100

DK-7620 Lemvig

Denmark

Contact: Thorsten Piontkowitz

E-mail: tpi@kyst.dk

Tel: +45 99 6363 63

Fax: +45 99 6363 99



Flemish Ministry of Transport and Public Works [B]

Agency for Maritime and Coastal Services

Coastal Division

Vrijhavenstraat 3

B-8400 Oostende

Belgium

Contact: Tina Mertens

E-mail: tina.mertens@mow.vlaanderen.be

Tel: +32 59 55 42 49

Fax: +32 59 50 70 37



Flanders Hydraulics Research

Berchemlei 115

B-2140 Antwerp

Belgium

Contact: Toon Verwaest

Email: toon.verwaest@mow.vlaanderen.be

Tel: +32 3 224 61 87

Fax: +32 3 224 60 36

Schleswig-Holstein State Ministry for Agriculture, Environment

and Rural Areas [D]

Coastal Defence Division

PO Box 7125

D-24171 Kiel

Germany

Contact: Jacobus Hofstede

E-mail: jacobus.hofstede@mlur.landsh.de

Tel: +49 431 988 4984

Fax: +49 431 988 66 4984

Lower Saxony Water Management, Coastal Defence and Nature Conservation Agency / NLWKN [D]

Division Norden - Norderney

Jahnstraße 1

DE-26506 Norden

Germany

Contact: Holger Blum

E-mail: holger.blum@nlwkn-nor.niedersachsen.de

Tel: +49 4931 947 158

Fax: +49 4931 947 125

Environment Agency [UK]

National Flood Risk Management Policy Team

79 Thorpe Road,

Norwich NR1 1EW

United Kingdom

Contact: Rodney Hicks

E-mail: rodney.hicks@environment-agency.gov.uk

Tel: +44 1473 706 521 (office)

Tel: +44 7900 678460 (mobile)

Interreg North Sea Region

ERDF